DEVELOPMENTAL EXPOSURE TO DIESEL EXHAUST CAUSES AUTISM-LIKE BEHAVIORAL, MOLECULAR, AND CORTICAL STRUCTURAL ALTERATIONS.

Yu-Chi Chang

A dissertation

submitted in partial fulfillment of the

requirements for the degree of

Doctor of Philosophy

University of Washington

2018

Reading Committee:

Lucio G. Costa, Chair

Thomas M. Burbacher

Toby B. Cole

Program Authorized to Offer Degree:

School of Public Health

Department of Environmental and Occupational Health Sciences

Abstract

DEVELOPMENTAL EXPOSURE TO DIESEL EXHAUST CAUSES AUTISM-LIKE BEHAVIORAL, MOLECULAR, AND CORTICAL STRUCTURAL ALTERATIONS.

Yu-Chi Chang

Chair of Supervisory Committee:

Professor Lucio G. Costa, PharmD

Department of Environmental and Occupational Health Sciences

Escalating prevalence of autism spectrum disorders (ASD) in recent decades has triggered increasing efforts in understanding the role played by environmental risk factors as a way to address this widespread public health concern. Several epidemiological studies show associations between developmental exposure to traffic-related air pollution and increased ASD risk. The purpose of this project was to elucidate the neurotoxic mechanisms of developmental exposure to traffic-related air pollution in mice. A series of experiments were performed to determine whether developmental diesel exhaust (DE) exposure induces ASD-related behaviors, and whether the neuroinflammatory pathway leading to dysregulation of reelin expression was affected. C57Bl/6J mice were exposed from GD0 to PND21 to 250-300 $\mu g/m^3$ DE or filtered air (FA) as control. DE-exposed mice exhibited deficits in all three of the hallmark categories of ASD behavior: disrupted social interaction in the reciprocal interaction test and social preference test, disrupted social olfactory and vocal communication, and increased repetitive behavior. In brains of DE-exposed mice, increased levels of interleukin-6, increased phosphorylation of STAT3, increased expression of DNMT1, and decreased expression of reelin were found. Furthermore, cortical lamina organization was examined with

immunohistochemistry staining, and subtle but significant differences in the distribution pattern of neurons expressing layer-specific markers were found. Additionally, increased PAX6, Tbr2, and Tbr1 mRNA levels were found in brains of neonatal DE- exposed mice, suggesting early promotion of the neurogenic pathway over preservation of neural progenitor cells' self-renewal ability, which is supported by our finding of decreased adult neurogenesis in the hippocampal dentate gyrus of PND60 DE- exposed mice. Overall, these studies show that developmental DE exposure, taken as a measure of traffic-related air pollution, causes behavioral, biochemical/molecular and structural changes that resemble those present in ASD.

TABLE OF CONTENTS

List of Figures

Glossary

AQI — Air Quality Index

ASD— Autism Spectrum Disorder

CALB — Calbindin

Creb1 — CAMP Responsive Element Binding Protein 1

CTIP2 — COUP-TF-Interacting Protein 2

CUX1 — CUT-Like Homeobox 1

DE — Diesel Exhaust

DG – Dentate Gyrus

DNMT— DNA Methyltransferase

E — Embryonic Day

ELISA— Enzyme-linked Immunosorbent Assay

FA —Filtered Air

GABA— Gamma-aminobutyric Acid

GAPDH— Glyceraldehyde 3-phosphate Dehydrogenase

IL17a— Interleukin 17a

IL6— Interleukin 6

JAK2— Janus Kinase 2

MIA —Maternal Immune Activation

PAX6— Paired Box 6

PM —Particulate Matter

PND —Postnatal Day

Poly (I:C)— polyinosinic-polycytidylic acid

PV – parvalbumin

qRT–PCR— real-time quantitative reverse transcription polymerase chain reaction

RELN— Reelin

Sp1 – specificity protein 1

STAT3— signal transducer and activator of transcription 3

Tbr1— T-Box, Brain 1

Tbr2— T-Box, Brain 2

TH17— T helper 17 Cell

TLR4 —Toll-like Receptor 4

TRAP— Traffic Related Air Pollution

UFP – Ultrafine Particles

USV —Ultrasonic Vocalization

Acknowledgments

First and for most I would like to thank my supervisory committee for investing time and provide helpful guidance in my project: Drs. Lucio G. Costa, Toby B. Cole, Thomas M. Burbacher, Stephen E. P. Smith, and Joel D. Kaufman. I would especially like to thank Dr. Lucio G. Costa for allowing me a lot of freedom to develop my dissertation project and supporting my ideas. I would also like to thank Dr. Stephen E. P. Smith for stepping in the role of my graduate school representative when my former GSR Dr. Michael T. Chin moved to another institution.

I have been fortunate to have a team of colleagues who are knowledgeable and caring in the Costa lab, the Roosevelt building, the Northlake Disease Facility, and in the Center on Human Development and Disability. I would like to especially thank Khoi Dao, Dr. Pam Roqué, and Jacqueline M Garrick for emotional support and stimulating discussions. A big “thank you” to Dr. Toby Cole, the person I go to for guidance in behavioral testing. I also like to express my appreciation to Jim Steward and Prof. Joel D. Kaufman, this project would not possible if not for their instrumental role in keeping the Northlake Disease Facility open. I would also like to thank our collaborator Dr. Robert F. Hevner and Ray A. M. Daza at the Seattle Children’s Research Institute for their generous help in the cortical histological assessment that is critical to my project.

I would like to thank the funding sources that ultimately allowed this work to be possible: R01ES028273, R01ES022949, P30ES07033, P42ES04696, U54HD083091, and funds from the Department of Environmental and Occupational Health Sciences, University of Washington.

I would like to thank my parents who made the sacrifice of using their retirement fund to help pay for my tuition before I was able to get on a training grant. I’d also like to thank my sister Dr. Ella Hsin-Wen Chang for offering constructive scientific criticisms over the years, from my

training grant and travel funding applications, to my thesis proposal.. Finally I would like to thank my husband Jon and cat Sherlock for they love and support.

Chapter 1

INTRODUCTION

1.1 Traffic Related Air Pollution

1.1.1 Traffic Related Air Pollution Exposure

Cities in Northeastern China, North India, and the Eastern Coast of the Arabian Peninsula have the highest recorded annual average PM2.5 concentrations in the world, according to aggregated data collected from 2008-2015 published on the World Health Organization (WHO) website (WHO, 2016). The same dataset also reported higher than 150 $\mu g/m^3$ annual average PM2.5 concentrations in urban areas in Iran, India and Saudi Arabia in 2012 and 2014, suggesting that residents in these areas faced prolonged exposure to high levels of air pollution. In addition, several studies have characterized seasonal effects on ambient PM2.5 concentrations in coastal cities in China and in Mexico City and found positive correlation, with higher ambient PM2.5 concentration in winter months with a dryer and colder climate (Feng et al., 2018; Liu et al., 2018; Morton-Bermea et al., 2018).

In urban areas where traffic-related air pollution is of major concern, a large portion of utility vehicles, including those used for commercial cargo transportation and public transportation, as well as some personal vehicles, are still operated on diesel fuel. For example, at least 1/3 of the total road transport fuel consumption in the United Kingdom between 2010 and 2012 was diesel fuel (Khan and Gregory, 2014). In addition, data collected in 2010 in Mexico City shows that diesel exhaust (DE) has been estimated to contribute >35% of ambient PM2.5 (Calderón-Garcidueñas et al., 2015). A 2010 report by the Health Effects Institute (HEI) also indicated that diesel vehicles contributed 32% of the PM2.5 mass in Los Angeles (Health Effects Institute, 2010). Indeed,

DEhas been ranked as the primary or secondary source of traffic-related air pollution (TRAP) based on analysis of fixed-site air quality measurements collected in Baltimore and Los Angeles, respectively (Riley et al., 2016; Tessum et al., 2018). In controlled laboratory exposure scenarios researchers are often limited to one fuel source. DE would therefore be ideal for building a relevant well controlled exposure model to study developmental health effects, considering that DE is a substantial source of ambient PM.

1.1.2 Health Effects Associated with Developmental Air Pollution Exposure

1.1.2.1 Effect of Air Pollution Exposure on Pregnancy Outcome, Pulmonary Risk, and Cardiovascular Risk

Air pollution exposure has been associated with adverse pregnancy outcomes including decreased fetal growth, preterm birth, stillbirth, and preeclampsia in epidemiological studies conducted in China, England, and the United States (DeFranco et al., 2016; Langrish et al., 2012; Smith et al., 2017; Wang et al., 2018). In the past decade, health impacts from developmental exposure to TRAP related to pulmonary and cardiovascular risk were extensively studied by many researchers. Positive associations between prenatal / early life outdoor air pollution exposure and asthma risk have been reported in populations in North America, Latin America, Caribbean, Asia, and Europe (Ding et al., 2017; Glad et al., 2012; Gleason et al., 2014; Hulst et al., 2014; Orellano et al., 2017; Pan et al., 2014; Yamazaki et al., 2015). In rodent models, prenatal exposure to PM2.5 induces injury and elevated levels of IL-1, IL-6 and TNF-α in lung of offspring (Tang et al., 2018). Exposure to ambient ultrafine particulates has been associated with increased cardiovascular pathologies in humans (Brook et al., 2010). In rodent models, prenatal and early life exposure to DE predisposes animals to later-onset cardiovascular disease (Liu et al., 2013; Weldy et al., 2013).

1.1.2.2 Effect of Air Pollution Exposure on the developing CNS

Developmental exposure to TRAP has also been associated with a number of behavioral disorders such as cognitive impairment, attention deficit disorders, and autism spectrum disorder (ASD) in many epidemiological studies (Calderón-Garcidueñas et al., 2013; Calderón-Garcidueñas et al., 2008; Guxens et al., 2016; Guxens et al., 2014; Kicinski et al., 2015; Yorifuji et al., 2016). In rodent models, exposure to air pollution during development has also been found to affect CNS development, leading to altered brain structure morphology such as enlarged lateral ventricles and decreased cortical volume (Allen et al., 2014; Bolton et al. , 2017; Calderón-Garcidueñas et al., 2012). Elevated levels of inflammatory cytokines and activated microglia morphology have been reported with developmental TRAP exposure in both *in vivo* and *in vitro* animal studies, as well as in epidemiological studies (Allen et al., 2016; Calderón-Garcidueñas et al., 2013; Calderón-Garcidueñas et al., 2016; Church et al., 2017; Roqué et al., 2016; Sunyer et al., 2015)

1.2 Autism Spectrum Disorder (ASD)

According to the fifth edition of the Diagnostic and Statistical Manual of Mental Disorders (DSM-5), autism spectrum disorders (ASD) represent a heterogeneous group of disorders characterized by three behavioral domains: difficulties in social interactions, issues with verbal and nonverbal communication, and repetitive behaviors (Autism Speaks Webpage, 2013).

1.2.2 Environmental Contribution to Autism Prevalence

According to a 2010 survey by the U.S. Centers for Disease Control and Prevention, autism prevalence has been reported to be 1 in 68 for children in the United States, indicating a ten-fold increase in the past 40 years. However, only a small subgroup of ASD cases can be attributed to genetics alone (Torre-Ubieta et al., 2016), and environmental factors are believed to contribute substantially to ASD etiology. Increased ASD risk has been associated with various environmental

exposures such as air pollution, heavy metals, organophosphorus insecticides, perinatal stress and infectious agents (Allen et al., 2014; Becerra et al., 2013; Boksa, 2010; Careaga et al., 2017; Costa et al., 2015; Kalkbrenner et al., 2014; Onore et al., 2014; Rossignol et al., 2014; Shelton et al., 2012; Volk et al., 2013; Weber-Stadlbauer, 2017). Increasing prevalence in recent years could be attributed to both broadening of diagnostic definition and increased exposure to environmental toxicants. An epidemiological study conducted in California estimated that 26.4% of the increased autism prevalence can be attributed to change in diagnostic practices between 1992 and 2005 (King and Bearman, 2009). Adding to the significance of environmental contribution to autism etiology, an epidemiological study by Hallmayer *et. al.* (2011), looking at ASD association in monozygotic and dizygotic twins, concluded that environmental components have a larger effect than genetic components in predicting ASD outcome.

1.2.3 Autism animal models

Several genetic and inducible animal models exhibiting ASD-like behavioral phenotypes are used in research.

1.2.3.1 Genetic Models of ASD

Two genetically homogenous inbred strains, BTBR T + tf/J and C58/J, are commonly used in studies focusing on the genetic basis of ASD-like behavioral phenotypes. The BTBR T + tf/J strain displays several ASD-like behavioral phenotypes, such as reduced sociability in adults, increased repetitive grooming, and an unusual pattern of ultrasonic vocalizations (Amodeo et al., 2012; Langley et al.,, 2014; Scattoni et al., 2011; Scattoni et al., 2013; Yang et al., 2012; Yang et al., 2007). In the C58/J mouse strain increased repetitive behavior and impaired social interaction were found (Blick et al., 2015; Moy et al., 2014). Mechanistic studies suggest that $GABA_B$ receptors seem to play an important role in modulating the ASD-like behavioral phenotype in both

BTBR T + tf/J and C58/J strains, since treatment with selective $GABA_B$ receptor agonists reverses the social deficits and repetitive behaviors (Silverman et al., 2015).

Many genetic polymorphisms associated with ASD have been identified in genome-wide association studies, and transgenic mouse models were created from findings of these studies. For example, many mutations in the SHANK3 genes have been identified in ASD patients (Monteiro and Feng, 2017). In rodent models, mutations in SHANK2 and SHANK3 genes both lead to increased repetitive behavior, abnormal social behavior, and decreased vocalization (Bozdagi et al., 2010; Lim et al., 2017; Won et al., 2012).

1.2.3.1 Maternal Immune Activation

Based on the observation that infection during pregnancy is associated with increased risk for ASD, rodent models were developed by exposing prevent dams to either poly(I:C) or lipopolysaccharide (LPS) to mimic viral or bacterial infection. In these animal models where the maternal immune response was activated, elevated levels of interleukin-6 (IL-6) and of interleukin-17α (IL-17α) have been shown to be sufficient in eliciting ASD-like behavior (Choi et al., 2016; Samuelsson et al., 2006; Shin Yim et al., 2017; Smith et al., 2007). Subsequent studies revealed that binding of IL-6 to its cognate receptor activates the kinase pathway involving Janus Kinase 2 (JAK2) and Signal Transducer and Activator of Transcription 3 (STAT3) (Chang et al., 2005; Erta et al., 2012; Hsiao and Patterson, 2011; Tsukada et al., 2015). In a recent study, prenatal maternal immune activation has been shown to activate neurons in the S1DZ region of the somatosensory cortex, leading to ASD-like behavioral changes in mice (Shin Yim et al., 2017), supporting the idea that structural changes in the somatosensory cortex could be involved in ASD-like behaviors. Additionally, prenatal LPS exposure has been shown to effect neurogenesis during neocortical development (Tronnes et al., 2015).

1.2.4 Air Pollution as an Environmental Risk Factor for ASD

Developmental exposure to traffic-related air pollution (TRAP) has been associated with increased ASD risk in many recent epidemiological studies conducted in North America and Europe (Becerra et al., 2013; Suades-González et al., 2015; Talbott et al., 2015; Volk et al., 2011; Volk et al., 2013), as well as in Asia (Jung et al., 2013). A study by Roberts *et al.* (Roberts et al., 2013) also reported increased ASD risk with diesel particulate exposure. Similarly, increased ASD risk with TRAP has been reported in populations in Taiwan and in Pennsylvania (Jung et al., 2013; Talbott et al., 2015). Studies by Volk *et al*. (Volk et al., 2013) in California, and by Raz *et al.* (Raz et al., 2014), as part of the Nurses' Health Study II Cohort, indicated that the third trimester seems to be the most susceptible period when examining the association between TRAP exposure and ASD outcomes.

The few available animal studies also suggest a connection between developmental exposure to air pollution and ASD. Mice exposed developmentally to high levels of DE particles exhibited altered behavioral phenotypes, including effects on locomotor activity and repetitive behaviors (Thirtamara et al., 2013). Mice exposed perinatally to ultrafine ambient particles exhibited repetitive and impulsive behaviors, as well as ventriculomegaly, a brain structural morphological change also reported in some ASD patients (Allen, et al., 2016; Allen et al., 2014). Additionally, prenatal exposure of mice to low levels of DE or DE particles have been shown to result in altered locomotor activity (Suzuki et al., 2010).

Our group has previously reported that acute DE exposure in adult mice causes neuroinflammation and oxidative stress (Cole et al., 2016), and that microglia activation is triggered by DE particles in a primary culture system (Roqué et al., 2016). Developmental DE exposure in rodents has been shown to increase levels of pro-inflammatory cytokines in placenta, fetal brain and fetal lung (Auten et al., 2012; Bolton et al., 2012; Li et al., 2017b; Weldy et al., 2013). Interestingly, IL-6, a cytokine identified as a key modulator of ASD-like behavior in rodent

studies (Choi et al., 2016; Samuelsson et al., 2006; Shin Yim et al., 2017; Smith et al., 2007), is among the list of elevated cytokines elicited by developmental DE exposure in the brain (Auten et al., 2012a; Bolton, et al., 2017; Bolton et al., 2012).

1.2.4 Reelin in ASD etiology

Reelin (RELN) is a secreted extracellular protein that has been known to modulate neuronal migration and dendrite formation during CNS development. In adult mice, RELN has been shown to play a role in synapse formation (D'Arcangelo, 2014; Levenson et al., 2008; Michetti et al., 2014). Several lines of evidence suggest the importance of RELN's role in the pathogenesis of ASD. First, decreased RELN levels have been reported in brains of ASD patients (D'Arcangelo, 2014). Second, mice haploid-deficient for RELN have been shown to exhibit some ASD-related behavioral phenotypes (Michetti et al., 2014). Third, cortical disorganization has been reported in both ASD patients and in RELN-deficient mice (Boyle et al., 2011; Stoner et al., 2014). Fourth, differences in DNA methylation patterns within the RELN promoter were reported in ASD patients (Grayson et al., 2006).

1.3 Developmental Preconditioning of Neurodegenerative Diseases

1.3.1 Evidence Associating Air Pollution Exposure with Increased Neurodegenerative Risk

Exposure to traffic-related air pollution has been shown to be associated with neurodegenerative diseases in many human and animal studies (Block & Calderón-Garcidueñas, 2009; Bolton et al., 2014; Calderón-Garcidueñas et al., 2016; Lilian Calderón-Garcidueñas et al., 2013; Costa et al., 2017; Lee et al., 2016; MohanKumar et al., 2008). A series of studies conducted by Calderón-Garcidueñas et al. in Mexico City reported oxidative stress and neuroinflammation, as well as neuropathological hallmarks of Alzheimer's and Parkinson's diseases, such as amyloid beta42 (Aβ42) plaques, tau hyperphosphorylation with pre-tangles, and α-synuclein accumulation in young adults exposed to TRAP during development (Calderón-Garcidueñas et al., 2012;

Calderón-Garcidueñas, 2013; Calderón-Garcidueñas et al., 2016; Calderón-Garcidueñas et al., 2015). Childhood air pollution exposure has also been associated with cognitive effects, according to studies conducted in Amsterdam and Boston (Suglia et al., 2008; van Kempen et al., 2012). Additionally, developmental air pollution exposure has been associated with altered brain structure; white-matter hyperintensities (WMHs) have been found in 56% of healthy exposed children compared to unexposed controls in a study conducted in Mexico City (Calderón-Garcidueñas et al., 2008). In a study in mice, prenatal exposure to DE has been shown to modulate expression levels of genes involved in neuronal differentiation and neurogenesis via epigenetic modification (Tachibana et al., 2015). Previously, our group reported decreased levels of adult neurogenesis in the hippocampal dentate gyrus (DG) of mice exposed to DE (Coburn et al. 2018); of particular relevance is that impaired adult neurogenesis, especially in the hippocampal region, has been implicated in Alzheimer's disease (Abrous et al., 2005; Fuster-Matanzo et al., 2012; Kent & Mistlberger, 2017; Maruszak et al., 2014; Toda & Gage, 2017; Zheng et al., 2016).

1.3.2 Importance of Temporal Balance between Neurogenesis and Progenitor Self-Renewal in the Pathogenesis of Neurodegenerative Diseases.

During CNS development, paired box 6 (PAX6), T-box brain 2 (Tbr2, also known as eomes), and T-box brain 1 (Tbr1) were found to be expressed sequentially by radial glia, intermediate progenitor cells, and postmitotic neurons, respectively (Englund et al., 2005). Adult neural progenitor cells (NPCs) have been identified to be derived from a slowly dividing subpopulation of embryonic NPCs, while the fast dividing NPCs are responsible for the peak of neurogenesis during CNS development (Furutachi et al., 2015; Singh & Solecki, 2015). These findings suggest that disrupted balance between self-renewal and differentiation of NSCs due to developmental exposure to environmental toxicants could affect progression of both neurodevelopmental and neurodegenerative disorders.

PAX6 has been shown to play an essential role in controlling the balance between neural stem cell self-renewal and neurogenesis in both *in vivo* and *in vitro* models (Gan et al., 2014; Sansom et al., 2009). In adult neurogenesis, similar progenitor cell types and temporal expression of the PAX6 ,Tbr2 and Tbr1 cascade are also observed in both the subventricular zone (SVZ) and the hippocampal subgranular zone (SGZ)(Brill et al., 2009; Hodge et al., 2008; Roybon et al., 2009a,b). In PAX77 mice, a transgenic mouse line over-expressing PAX6, Tbr2 and Tbr1, expression of these three genes was found to be positively regulated in fetal brain, and over-production of Tbr2-positive cells was observed at E12.5, followed by reports of microcephaly at E14.5 (Sansom et al., 2009). These findings indicated that over-expression of PAX6 in a transgenic model leads to increased neurogenesis, which compromises progenitor cell self-renewal potential early in development. Additionally, Tbr2 has been reported to play an essential role in regulating laminar fate during cortical genesis (Anca B Mihalas et al., 2016). In this thesis project, we investigated the effect of developmental DE exposure on the PAX6, Tbr2, and Tbr1 neurogenic pathway, as well as assessment of its potential consequences on cortical lamina organization and adult neurogenesis.

1.4 Hypothesis and Specific Aims

Hypothesis: Exposure to traffic-related air pollution during the critical window of CNS development contributes to both neurodevelopmental and neurodegenerative risks.

Aim 1: Assess behavioral endpoints relevant to ASD in mice developmentally exposed to DE compared to FA control.

Aim 2: Elucidate molecular mechanisms underlying the mode of toxicity of DE exposure in relation to its contribution to ASD etiology.

Aim 3: Examine changes in markers and histological effects associated with neurodegenerative pathogenesis due to developmental DE exposure.

Chapter 2

PRELIMINARY BEHAVIORAL TESTING OF MICE EXPOSED PRENATALLY TO DIESEL EXHAUST

2.1 Introduction

Autism spectrum disorder (ASD) represents a heterogeneous group of disorders characterized by difficulties in social interaction, verbal/ nonverbal communication, and repetitive behaviors. Epidemiological studies have shown that prenatal exposure to traffic related air pollution is associated with an increase in risk for autism. While current air quality regulations have not taken into consideration adverse CNS developmental effects, increasing prevalence and the chronic nature of ASD makes air pollution an important public health issue to be addressed. To investigate the effect of prenatal diesel exhaust exposure on behavior, a series of preliminary behavioral tests were performed on C57Bl/6J mice exposed to filtered air (FA) or diesel exhaust (DE) (250 $\mu g/m^3$) prenatally, from embryonic day 0 (E0) to E19. Maternal behavioral assessment and pre-weaning assessment of developmental milestones in the pups, including bodyweight gain, hair growth, pinna detachment, and development of the righting reflex were done to rule out potential confounder effects due to physical disability or lack of maternal care. Post-weaning behavioral assessments included tests of social novelty, elevated plus, rotarod, catwalk, grip strength, pre-pulse inhibition, and the Morris water maze. Overall, these preliminary results indicated a trend toward decreased sociability and inability to distinguish social novelty in DE males. No difference was detected in maternal care behaviors, grip strength, pre-pulse inhibition, nor pre-weaning assessment of developmental milestones.

2.2 Methods

2.2.1 Timed mating and Exposure

C57BL/6J females at the age of 12 to 15 weeks old were mated with similarly aged males for one night. Successfully mated females were identified the next morning by the presence of a vaginal plug. Plug-positive females were randomly housed in cages supplied with diesel exhaust (DE) or filtered air (FA) on E0. The exposure period started on E0 and ended on E18, and mice were exposed to DE for 6 hours a day and five days per week at the level of 250 $\mu g/m^3$ for particle concentration. E0 was designed to always start on a Monday to ensure consistent exposure. On E18, at the end of the daily exposures, all pregnant dams were transferred into clean FA cages until the pups reached weaning age (PND 21).

The exposure system connecting to the DE cages consisted of a Yanmar YDG5500 diesel generator (EPA certified) and air dilution system with dynamic feedback control; maintaining consistent exposure of 250 $\mu g/m^3$ in particle concentration (Fox et al., 2015). The UW Controlled Exposure Laboratory's Northlake Diesel Facility is described in more detail in Chapter 3, section 3.2.2.

2.2.2 Experimental Design

On PND3 two male and two female pups from each litter were tattoo marked and reserved for behavioral testing. The runts (weight >15% lighter than their littermates) from each litter were excluded from behavioral testing. One male and one female from each litter were then randomly assigned into test group 1 and test group 2. Maternal behavior was monitored from PND0 to PND3 for 30 minutes each day during the light cycle. Pre-weaning behavior assessment and body weights were recorded starting from PND4. Post weaning behavioral tests started when the mice were 3 weeks of age, in the following order:

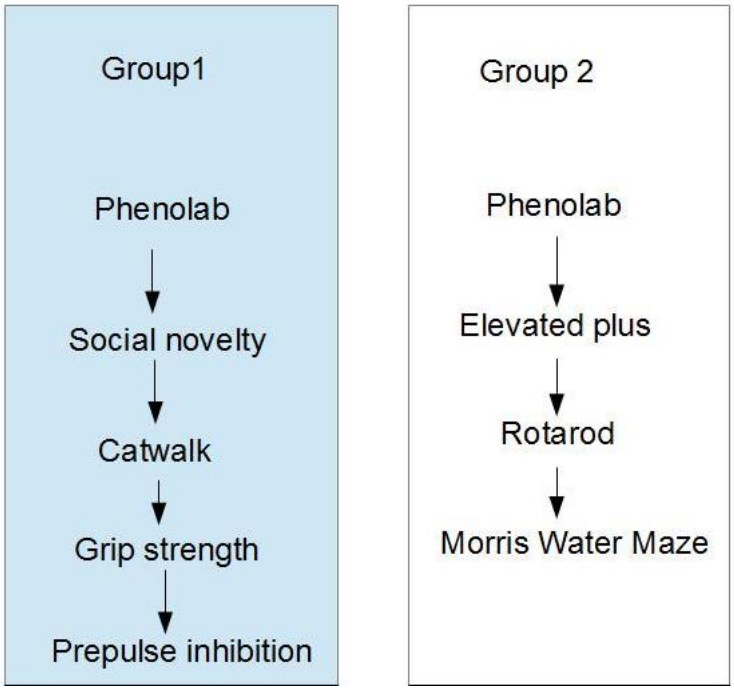

Fig. 2.1 Behavioral testing order

2.2.3 Maternal Behavior

Maternal behavior was scored twice a day (8-10 AM and 8-10 PM) for 30 minutes from PND0 to PND2. During each scoring session, behaviors such as eating, drinking, pup grooming, arch back feeding, blanket feeding, nest building, digging, and rearing were scored every minute. The maternal behaviors were then stratified into behaviors that were related to pup care (feeding, pup grooming, nest building) and behaviors that were not related to pup care (eating, drinking, self-grooming, rearing). Quality of pup care was quantified as the percentage of time the dam spent on activities relating to pup care during the 30-min scoring session.

2.2.4 Pre-weaning Tests

Righting reflex was measured every day from PND4 to PND9; the pups were flipped over belly side up and the time required to resume normal position (all four feet on the ground) was measured. Pup weight was measured on PND3, 4, 5, 6, 7, 8, 9, 12, 15, 18 and 21.

First appearance of external developmental milestones (pigmentation, pinna detachment, eye opening, back fur, and belly fur) were recorded on a daily basis.

2.2.5 Phenotyper Cage

Three-week-old mice were housed individually in PhenoTyper cages (Noldus Inc.) for 72 hours. Each PhenoTyper cage was lined with 1/8" corn cob bedding, and mice had free access to food and water. The top unit of the PhenoTyper cage was equipped with an IR camera, allowing tracking of the mouse in both light and dark cycle. Location, distance moved and velocity of the mouse were collected automatically by the Ethovision XT software (Noldus Inc.). During the first three hours, mouse activity was sorted into 10 minute bins and total distance moved and total duration spent in different parts of the Phenotyper cage (center, thigmotaxis, shelter) were plotted to show behavior in a novel environment. The rest of the 72-hr session was sorted into 3 hour bins, with light/ dark cycle denoted.

2.2.6 Elevated Plus Maze

The elevated-plus maze measures anxiety exploration and activity levels in mice by taking advantage of the innate tendency of mice to avoid open and elevated areas. The maze consisted of a central square (5 x 5 cm), from which radiate four arms (5 x 30 cm). Two of the arms had plexiglass walls (15 cm high) around the edge (closed arms), whereas the other two arms did not have walls (open arms) but did have a 0.25 cm-high edge to prevent the mice from falling from the maze. The maze was elevated 45 cm above the floor. Ethovision XT was used to track the mouse and measure entries and duration in the center, open arms, and closed arms. At the beginning of each trial mice were placed in the central square of the apparatus, facing an open

arm. Mice were allowed to explore the apparatus for 5 minutes while data were being collected. The apparatus was cleaned with 70% ETOH and allowed to be fully dried and ventilated before testing of the next mouse. Anxiety behavior was quantified as the amount of time a mouse spent in the closed arm compared to time spent in the open arm. Exploratory behavior was quantified as the number of entries a mouse made into different compartments of the maze, number of head dipping episodes, and number of times rearing.

2.2.7 Social novelty

Tests were performed as described by Moy SS et al. (2007) and Moy SS et al. (2004). These tests assess sociability, the tendency to spend time with another mouse, and preference for social novelty, including the ability to discriminate and choose between familiar and new mice. Driven by their exploratory drive, mice have natural preference for novel individuals. The social behavior apparatus is a rectangular, three-chambered plexiglass box with retractable doorways connecting the three compartments. The two compartments on the side each contain a holding cup. The cups are 11 cm high, composed of a solid 10.5 cm diameter bottom and stainless steel bars spaced at 1 cm intervals. The cups allowed non-aggressive tactile interaction and olfactory communication. The chambers of the apparatus were cleaned with water, then 70% ethanol, and dried with paper towels between each trial. The test was performed in a quiet room with light set to 100 lux.

The testing procedure consisted of three chronological phases: habituation, sociability, and social novelty. In the **habituation phase** the test mouse was first placed into the middle chamber and allowed to explore all three chambers freely for 10 minutes. During the habituation phase the holding cups in the two side chambers were empty. Ethovision XT was used to track the test mouse. At the end of the 10 min trial period, the test mouse was returned to its home cage. In the **sociability phase** an age and gender matched novel C57BL/6J mouse (raised in a different facility) was placed into one of the holding cups. The placement of the first novel mouse was randomized and equally distributed between the two holding cups. The test mouse was then

placed into the middle chamber and allowed to explore all three chambers freely for 10 minutes. Ethovision XT was used for tracking of the mice and data analysis. Sociability was quantified as the amount of time the test mice spent in proximity (i.e., inside the interaction zone within 5-cm radius of the holding cup) to the holding cup containing the first novel mouse versus the empty holding cup. In the **social novelty phase,** a second age and gender matched novel mouse was added into the holding cup that was empty during the sociability phase. The test mouse was then placed into the center chamber and allowed to explore all three chambers freely for 10 minutes. The test mouse's preference for social novelty was quantified by measuring time spent in the interaction zone near the second novel mouse versus time spent in the interaction zone near the familiar mouse.

2.2.8 Catwalk

CatWalk XT (Noldus Information Technology) was used to assess locomotion and gait. The CatWalk XT walkway consisted of a black tunnel with glass walkway on which a mouse traverses from one side of the glass plate to the other side. LED light is completely internally reflected inside of the glass runway, except in areas where the animal makes contact with the glass surface. A high speed camera mounted directly underneath the glass walkway recorded the walking pattern and sent the videorecording to a computer for analysis using CatWalk XT software. The experiment was performed in a quiet and darkened room, with red light. To eliminate interrupted runs due to excretion and vertical exploratory behaviors, runs that took more than three seconds to complete a total distance of 40 cm were ruled out. Three compliant runs were collected for each mouse. Mean and SEM of the regularity index value (% of total footsteps that fall into a pattern) were plotted for the four experimental groups.

2.2.9 Rotarod

Motor coordination was assessed using the rotarod test. The rotarod apparatus from Med Associates Inc. was composed of a rotating rod 3.2 cm in shaft diameter, 5.7 cm in lane width, with five lanes separated by dividers 24.8 cm in height. When the mouse falls off the rotating drum, it breaks a photobeam, installed at the bottom of each lane, to automatically record the amount of time spent on the drum. All subjects were trained for 1 minute at 4 RPM before the onset of testing. After the training session, the mice were returned back to their home cage to rest for 5 minutes. The rotarod was then set to accelerate from 3.5 to 35 RPM over a 5-min period for each trial. A total of five trials were collected for each mouse, with 5 minutes of rest between trials. Latency of falling from the rotarod was recorded. If the subject remained on the rotarod for the entire duration of the trial (5 minutes) the maximum cutoff time was recorded.

2.2.10 Grip Strength

Grip strength was measured with a digital force gauge (Chatillon & Sons) positioned horizontally with a metal grasping bar or mesh. The mouse was gently restrained by the tail, and allowed to grasp the bar with its four limbs, then was steadily pulled (~1 inch/sec) away from the grasping bar or mesh until the grip was broken. Three successive readings were taken for each mouse, with 2 minutes inter-trial interval.

2.2.11 Pre-Pulse Inhibition

To measure acoustic startle response and to assess how pre-pulse stimuli mitigate the startle response, the SR-Lab Prepulse system from San Diego Instruments was used.

The mouse was placed into a small cylindrical chamber (4 cm diameter, 10 cm length) that was small enough to restrict movement, but large enough that the animal could still turn around within it. The chamber was attached to a plexiglass platform that has a piezoelectric sensor mounted to the bottom. This sensor measures the startle response to stimulus and sends a signal out to a computer to record the data. This platform is placed in a soundproofed box with a 2” speaker

mounted 15 cm above the cylindrical animal enclosure. The speaker is attached to the computer, which is programmed to generate tones of varying volumes. Animals were placed into the enclosure and allowed to habituate for 5 minutes while a background noise of 70 dB was produced. Over the next 10-15 mm, 20-50 startling stimuli were presented through the speaker. These stimuli consisted of three types: 1) pulse alone: 40 ms at 120 dB; 2) prepulse: 40 ms of prepulse (2-lO dB over the background 70 dB) followed by a 40 ms pulse at 120 dB: and 3) no pulse: 40 ms of background sound (70 dB). These trials were presented in random order with 5-30 sec between pulses (average intertrial interval was 15 sec). Both magnitude and delay of the startle response were measured.

2.2.12 Morris Water Maze

This test evaluates spatial learning. The mouse was placed in a circular pool of water (120 cm diameter, 25 cm deep) maintained at room temperature and made opaque by the addition of white tempera paint. Visual cues (4A sized printouts of various shapes such as square, circle, star etc.) were posted on the wall around the pool. Throughout the training process mice learn to use the visual cues as reference for the location of submerged platform. In each trial the mouse was allowed 60 seconds to locate the submerged platform. Ten seconds after locating the platform, the mouse was removed, dried off and placed under a warm incandescent bulb. If the mouse did not locate the platform after 60 seconds, a researcher gently guided the mouse on to the platform for 10 seconds before removing and drying the mouse as described above. The latency to locate the platform, as well as videorecording of the mouse during the entire trial, was measured. Further analysis of video tracking results provided additional measurements, such as distance travelled before reaching platform, travel speed, and percentage of time (out of 60 seconds) spent in the quadrant containing the platform. For each test subject the trial was repeated 3 times per day with 30 minutes inter-trial period, for 6 days. On the 7^{th} day the platform was removed and the subjects were tested for retention 3 times, with a 30 min inter-trial period. To test for reversal learning, the

platform was then moved to the opposite side of the tank, and testing was carried out as described before, from day 8 to day 13. At the end of testing on day 13, the platform was made visible and mice were tested once again for delay to reach platform; this control trial allowed researchers to identify motivation issues which could confound the results.

2.3 Results

The findings from this pilot study focused on assessing baseline behavioral effects due to prenatal-only exposure (E0-E18) of DE at the level of 250-300 µg/m3 particulate concentration. Prenatal exposure at this level of DE did not have significant effects on locomotor activity, motor balance, anxiety, startle response, gait, spatial learning and memory, reversal learning, or muscle strength. Given that several epidemiological studies have indicated that the third trimester of pregnancy appears to be the most susceptible to the effects of TRAP, we decided to extend the exposure period in subsequent experiments from prenatal only exposure (E0 to E18) to prenatal and early life exposure (E0 to PND21), as in the mouse, brain development corresponding to the third trimester of pregnancy occurs early postnatally.In the following chapter behavioral findings from prenatal and early life exposure to DE are described.

2.3.1 Phenolab

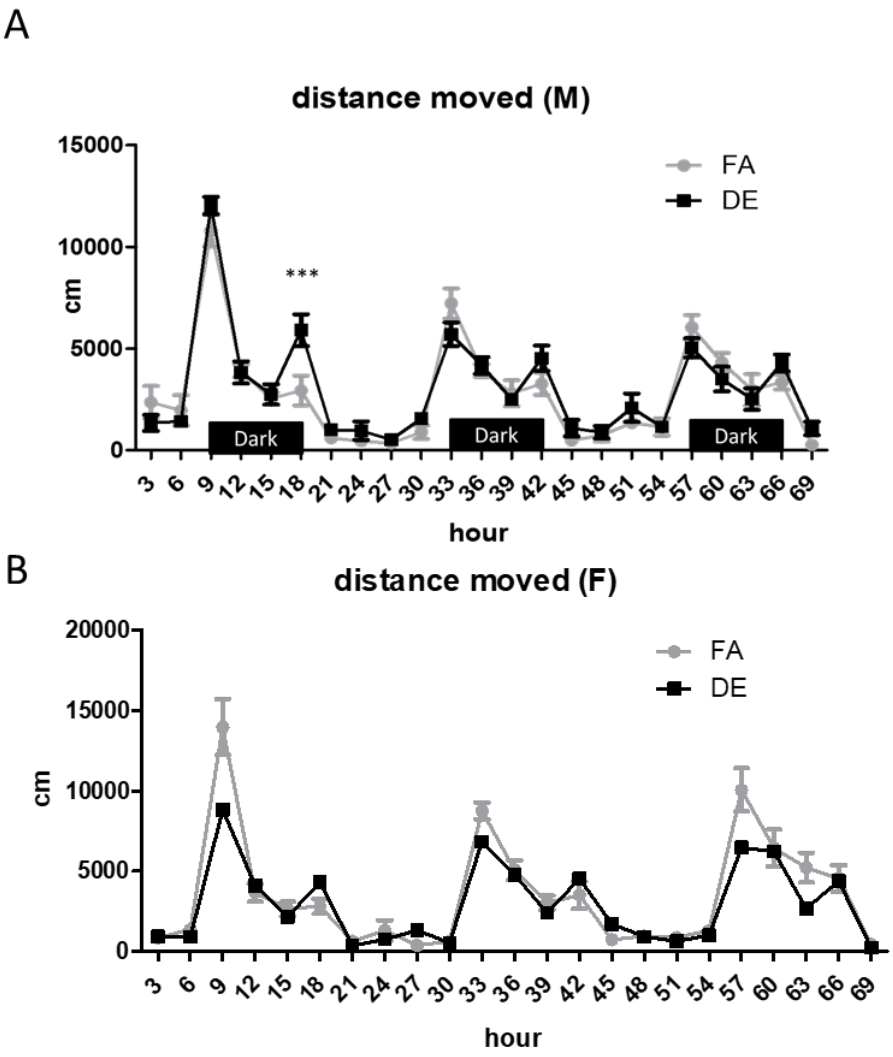

Fig. 2.2 Phenolab Results

A. Difference between FA and DE males in the first 3 hour was not significant. For the most part, there were no differences in activity between FA-treated males (FA M) and DE-treated males (DE M). However, right before the end of first dark cycle (18hr), DE Mshowed a significant increase in locomotor activity compared to FA M ($P<0.001$). Statistical method: 2 way-ANOVA matched by column (each row is a different time point) with Bonferroni posttest. B. No differences in activity level were found in females due to DE exposure. N= 5-6

2.3.2 Cat Walk

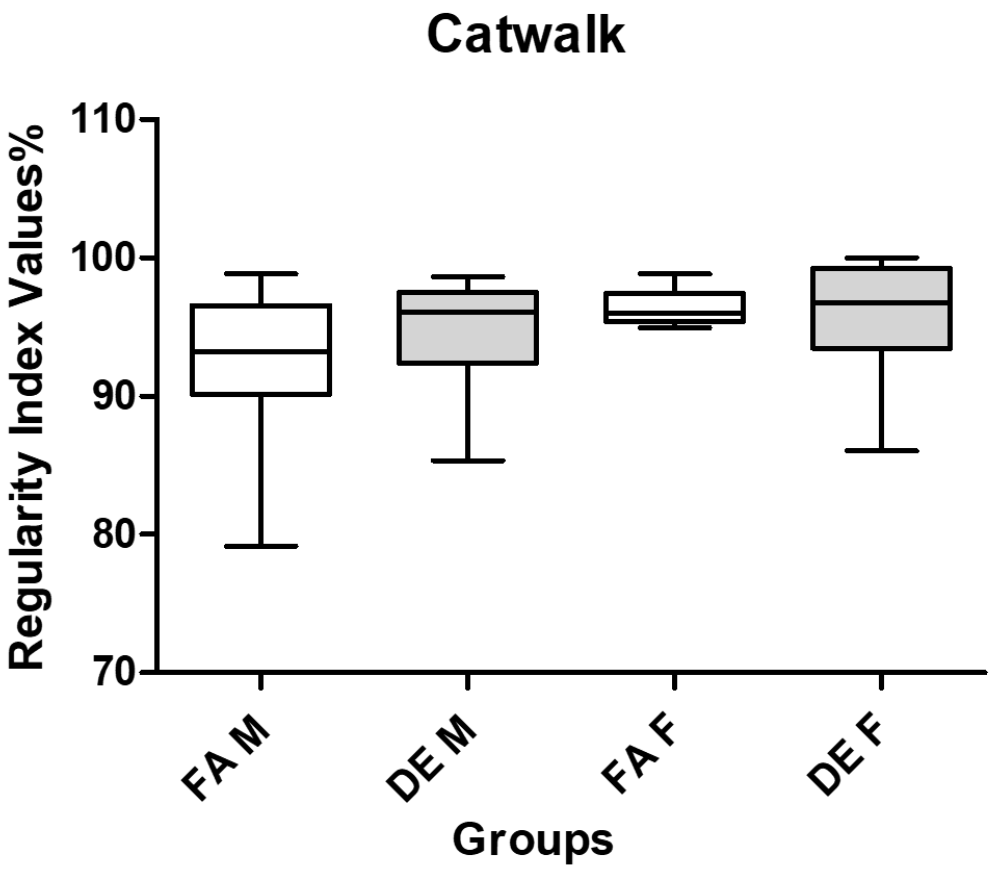

Fig. 2.3 Cat Walk

Mean and SEM of the regularity index value (% of total footsteps that fall into a pattern) were plotted for the four experimental groups: DE M (n=12), DE F (n=14), FA M (n=12), FA F (n=10). No significant differences were found due to DE exposure or sex of mice.

2.3.3 Elevated Plus Maze

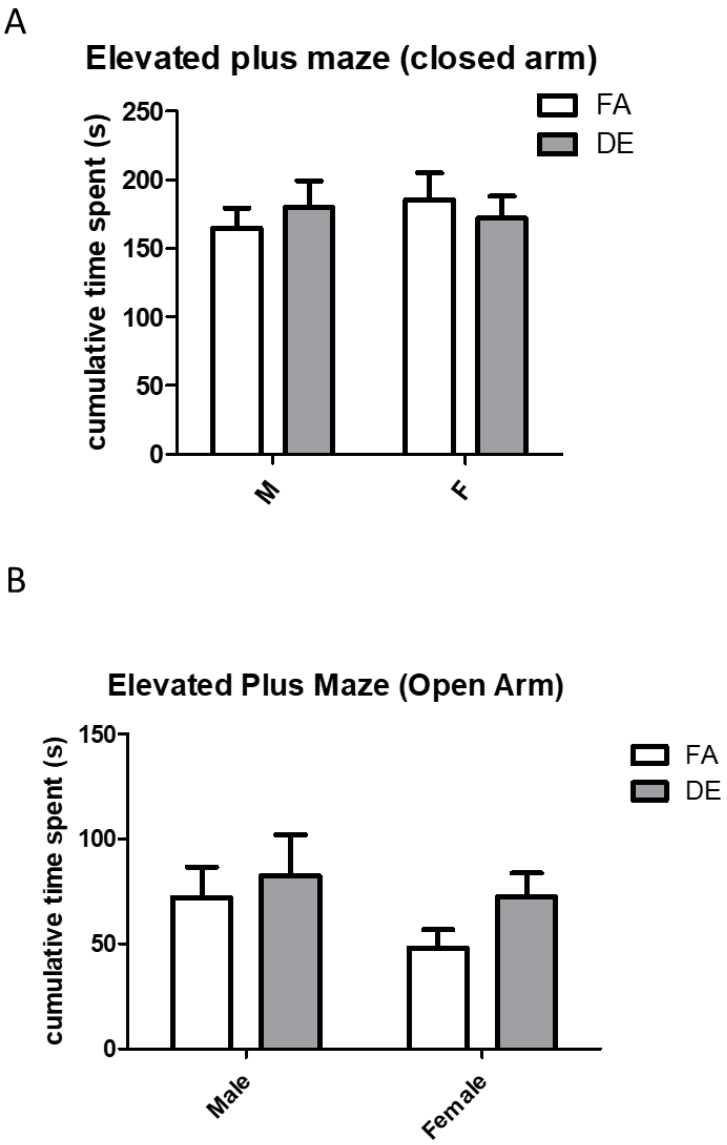

Fig. 2.4 Elevated Plus Maze

Subjects from all four experimental groups (DE M n=17, DE F n=16, FA M n=13, FA F n=11) were tested on Elevated Plus Maze for anxiety related behavior. Prenatal DE exposure did not have any significant effects on time spent in the open or closed arms.

2.3.4 Rotarod

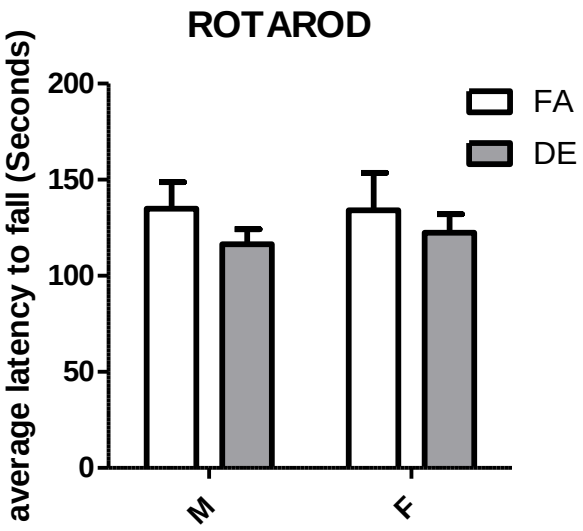

Fig 2.5 Rotarod

Subjects from all four experimental groups (DE M n=17, DE F n=16, FA M n=13, FA F n=11) were tested on the accelerating rotarod to test for gait coordination. Prenatal DE exposure did not have any significant effect on latency to fall from the rotating rod.

2.3.5 Grip Strength

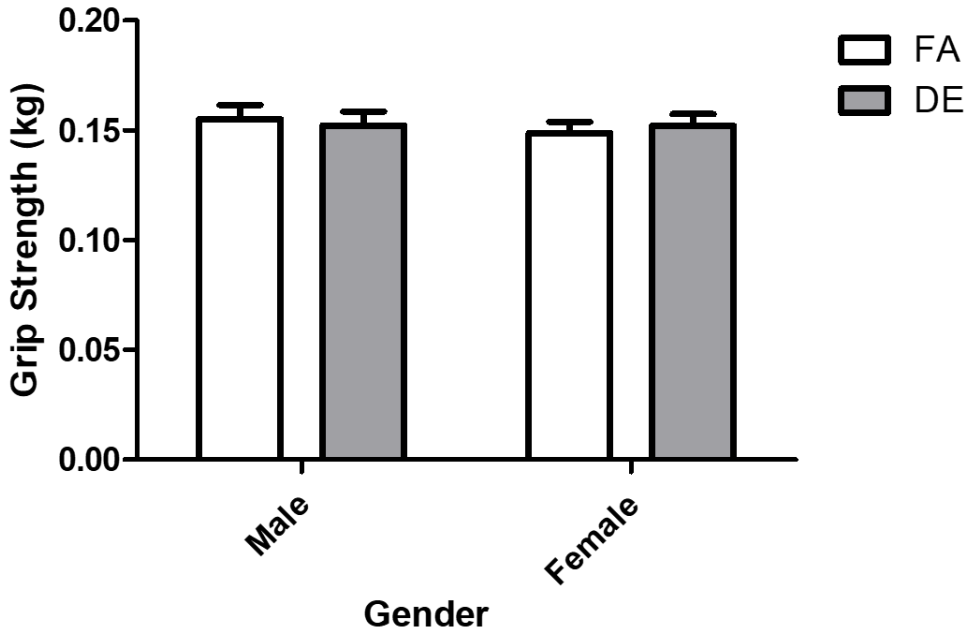

Fig 2.6. Grip Strength

Grip strength for all four paws was tested in all four experimental groups (DE M n=12, DE F n=12, FA M n=9, FA F n=9) and combined measurements are plotted as mean +/- SEM. DE exposure did not have any significant effects on grip strength.

2.3.6 Morris Water Maze

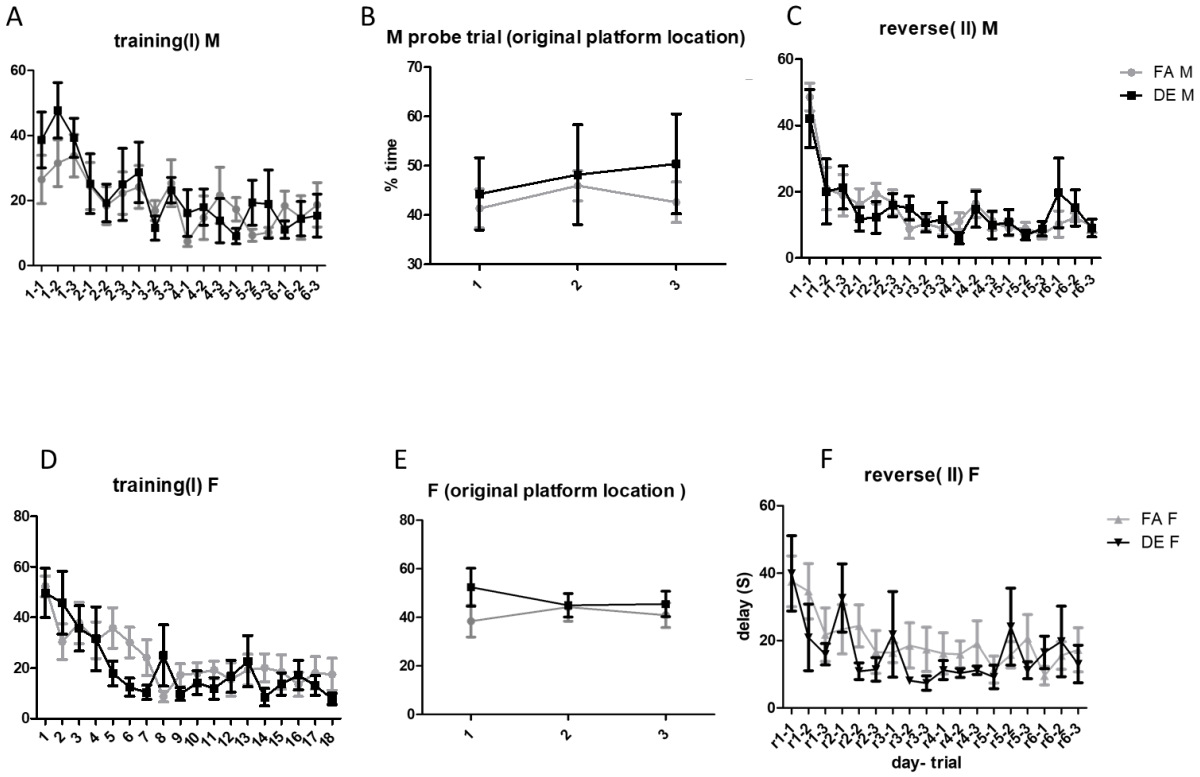

Fig 2.7 Morris Water Maze

Subjects in all four experimental groups (FA M n=8, DE M n=5, FA F n=8, DE F n=4) were subjected to the following training schedule: training phase (6 days) >> probe phase (1 day) >> reversal phase (6 days) in the Morris Water Maze, as a test for spatial learning and memory, as well as repetitive / persistent behaviors in the reversal phase. No statistically significant differences were found between DE and FA groups in time required to find the platform during training (D) or reversal (F) phases, or in retention of the original platform location (E).

2.3.7 Pre-Pulse Inhibition

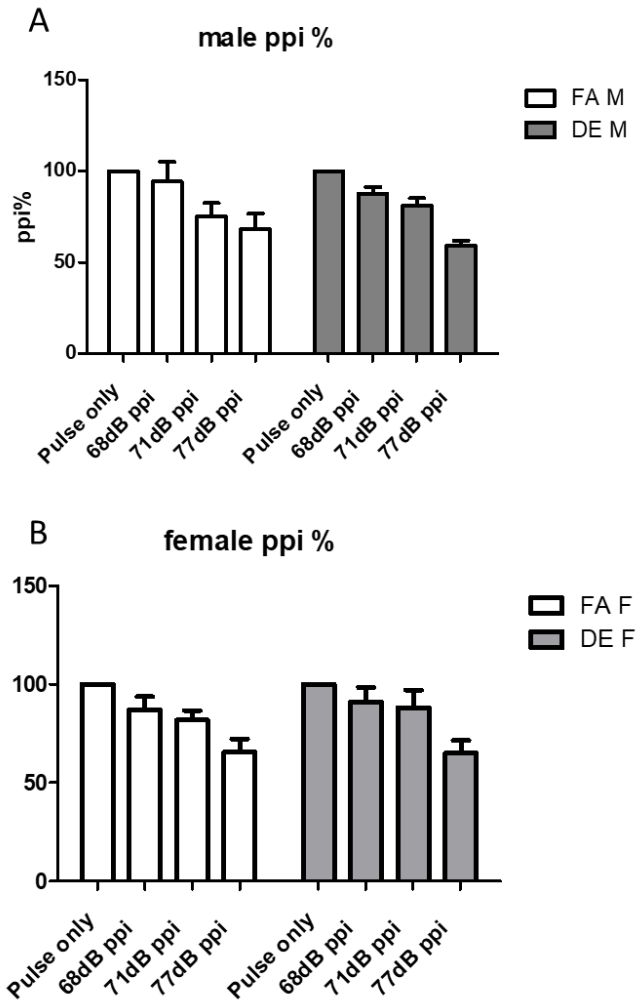

Fig 2.8 Pre-Pulse Inhibition

Startle response from all four experimental groups (FA M n=9, DE M n=11, FA F n=11, DE F n=10) following various pulse stimuli were plotted as % PPI (pulse alone versus pre-pulses at 68dB, 71dB or 77dB given shortly before presentation of pulse). DE exposure did not have any significant effects on startle amplitude, startle latency (not shown) or PPI.

2.3.8 Three Chambered Social Preference Test

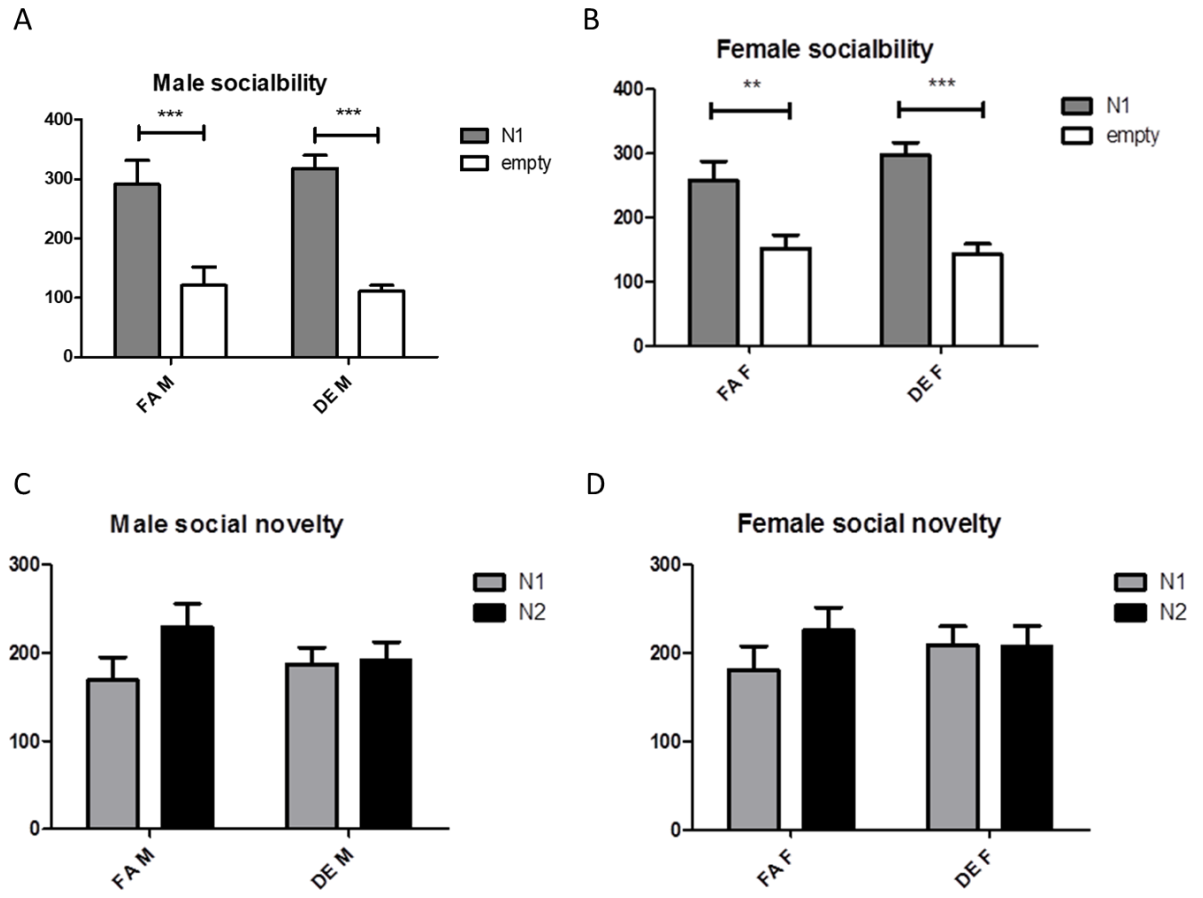

Fig 2.9 Three Chambered Social Preference Test

A. Male mice exposed to either diesel exhaust (DE; n=14) or filter air control (FA; n=8) from E0 to E18 spent significantly more time in the chamber containing age and gender matched novel mice compared to the chamber containing an empty wire cage (Two-way ANOVA with Bonferroni posttest $p<0.01$, $p<0.001$). There were no significant differences between the DE-exposed mice and the FA-exposed mice. **B.** Female mice exposed to DE or FA (DE; n=12, FA; n=10) spent significantly more time in chamber containing age and gender matched novel mice than in chamber containing empty wire cage (Two-way ANOVA with Bonferroni posttest $p<0.01$, $p<0.001$).

There were no significant differences between the DE-exposed mice and the FA-exposed mice. **C,D** No significant difference in ability to differentiate social novelty were found due to DE exposure in mice of either sex. Each column represents mean ± S.E.M.

Chapter 3

PRENATAL AND EARLY-LIFE DIESEL EXHAUST EXPOSURE CAUSES AUTISM-LIKE BEHAVIORAL CHANGES IN MICE

3.1 Introduction

Autism spectrum disorder (ASD) represent a heterogeneous group of disorders characterized by three behavioral domains: difficulties in social interactions, issues with verbal and nonverbal communication, and repetitive behaviors (Autism Speaks Webpage, 2013). According to a 2010 survey by the U.S. Centers for Disease Control and Prevention, autism prevalence has been reported to be 1 in 68 children in the United States, indicating a ten-fold increase in the past 40 years. Only a small subgroup of ASD cases can be attributed to genetics alone (Torre-Ubieta et al.,2016), and environmental factors are believed to contribute substantially to ASD etiology. Increased ASD risk has been associated with various environmental exposures such as air pollution, heavy metals, organophosphorus insecticides, perinatal stress and infectious agents (Allen et al., 2014; Becerra et al., 2013; Boksa, 2010; Careaga et al., 2017; Costa et al., 2015; Kalkbrenner et al., 2014; Onore et al., 2014; Rossignol et al., 2014; Shelton et al., 2012; Volk et al., 2013; Weber-Stadlbauer, 2017). Increasing prevalence in recent years could be attributed to both broadening of diagnostic definition and increased exposure to environmental toxicants. An epidemiological study conducted in California estimated that 26.4% of the increased autism

prevalence can be attributed to change in diagnostic practices between 1992 and 2005 (King and Bearman, 2009). Adding to the significance of environmental contribution to autism etiology, an epidemiological study by Hallmayer *et. al.* (Hallmayer et al., 2011), looking at ASD association in monozygotic and dizygotic twins, concluded that environmental components have a larger effect than genetic components in predicting ASD outcome.

Traffic-related air pollution (TRAP) is a widespread environmental concern, especially in densely populated areas such as Central America and South and East Asia (Pandis et al., 2014). High exposure levels of particulate matter (PM >100 $\mu g/m^3$) over extended periods have been commonly experienced by populations living in these areas (Brook et al., 2010). Air pollution is a mixture of several components, including gases, organic compounds, metals, and ambient PM. The sources of particulate air pollution, and hence its composition, can vary greatly from region to region, and diesel exhaust (DE) is an important, but not the only, component. In urban areas where traffic-related air pollution is of particular concern, a large proportion of utility vehicles operate on diesel fuel, including vehicles used for public transportation or transportation of commercial cargo, as well as many personal passenger vehicles. For example, at least 1/3 of the total road transport fuel consumption in the United Kingdom between 2010 and 2012 was due to consumption of diesel fuel (Khan and Gregory, 2014). In addition, data collected in 2010 in Mexico City showed that diesel exhaust (DE) has been estimated to contribute >35% of ambient PM2.5 (Calderón-Garcidueñas et al., 2015). It should be also mentioned that new filtration technologies which are being increasingly utilized, significantly reduce the release of PM. However, such measures may not be available or used in all parts of the world, leading to high PM2.5 levels from DE and other sources.

Developmental exposure to TRAP has been associated with increased ASD risk in many recent epidemiological studies conducted by research groups in North America and Europe (Becerra et

al., 2013; Guxens et al., 2016; Roberts et al., 2013; Suades-González et al., 2015; Volk et al., 2013, 2011). Two studies by Volk *et. al.* (Volk et al., 2013, 2011) reported that children exposed to higher levels of TRAP due to residential proximity to busy roadways are at a higher risk of developing ASD. Another study by Roberts *et al.* (Roberts et al., 2013) also reported increased ASD risk with diesel particulate exposure. Similarly, increased ASD risk with TRAP has also been reported in populations in Taiwan and in Pennsylvania (Jung et al., 2013; Talbott et al., 2015). Epidemiological studies conducted as part of the Nurses' Health Study II Cohort revealed the strongest association between ASD risk and TRAP when exposure occurred during late gestation and the neonatal period (Raz et al., 2014; Raz et al., 2017; Volk et al., 2013, 2011). The third trimester brain growth spurt has been identified as a particularly vulnerable period of brain development in studies focused on developmental neurotoxicity of alcohol. In rodent models hippocampal seizures, depression, and persistent cognition effects were found when ethanol exposure occurred during this peak period of brain growth (Bonthius et al., 2001; Xu et al., 2018). On a related note, air pollution exposure has been shown to cause a decrease in cortical thickness and lateral ventricular size in rodent models (Allen et al., 2014; Bolton et al., 2017), suggesting that this period of intense brain growth in the third trimester may be an important window of vulnerability for neurodevelopmental toxicity related to TRAP as well. In rodents, this window of particularly robust brain growth extends into the postnatal period (Ikonomidou, 2010; Semplea et al., 2013).

The few available animal studies also suggest a connection between developmental exposure to air pollution and ASD. Mice exposed developmentally to high levels of DE particles exhibited altered behavioral phenotypes, including effects on locomotor activity and repetitive behaviors (Thirtamara et al., 2013). Mice exposed perinatally to ultrafine ambient particles exhibited repetitive and impulsive behaviors, as well as ventriculomegaly, a brain structural morphological change also reported in some ASD patients (Allen et al., 2016, 2014). Additionally, prenatal

exposure of mice to low levels of DE or DE particles have been shown to result in altered locomotor activity (Suzuki et al., 2010). While epidemiological studies suggest an association between elevated air pollution and ASD, it is difficult to control for several potential confounders, and controlled-exposure animal studies have so far provided information only on a subset of autism related behavior phenotypes. The purpose of the present study was to conduct a more thorough evaluation of ASD-related behavioral endpoints, upon developmental exposure of mice to environmentally-relevant levels of DE under a controlled exposure setting.

3.2 Methods

3.2.1 Animals and Overall Study Design

All animal experiments were approved by the University of Washington Institutional Animal Care and Use Committee, and performed according to the National Research Council Guide for the Care and Use of Laboratory Animals, as adopted by the National Institutes of Health. C57BL/6J mice of both sexes (Jackson Laboratory, Bar Harbor, ME) were housed in University of Washington centralized vivaria under specific pathogen free (SPF) conditions, on a 12 hour light/dark cycle. Mice were housed in Allentown housing racks using 42cm (L) X 42cm (W) X 20cm (H) acrylic cages supplied with water bottles, food hoppers, cotton nestlets, and acrylic huts. Air (HEPA-filtered room air or diluted DE as described below) was provided to individual cages via the air circulation system in the Allentown racks. Before and during pregnancy and throughout the preweaning period, mice were provided with breeder chow (Picolab irradiated mouse diet 5085; Labdiet, St. Louis, MO). After weaning, mice were provided with standard rodent chow (Picolab irradiated rodent diet 5053; Labdiet, St. Louis, MO). Before the onset of the experiments, mice were acclimated for at least one week, with daily handling, to the vivarium at the UW Controlled Exposure Laboratory's Northlake Diesel Facility.

The overall study design, including the exposure and behavioral testing timelines is shown in Fig. 3.1. Pregnant dams and pups were exposed to DE (250-300 µg/m^3 PM concentration) for 6 hours per day and five days per week (Monday – Friday) from embryonic day 0 (E0) to postnatal day (PND) 21, as detailed below. The exposure period was based on epidemiological studies in humans showing that traffic-related air pollution exposure during all three trimesters of pregnancy and during the first 9 months of infants' life is associated with increased ASD risk (Guxens et al., 2016; Raz et al., 2017; Volk et al., 2011; Volk et al., 2013). The exposure duration was designed to cover key neurodevelopmental events happening during this window of susceptibility, which in mice equates to the period from E0 to PND21 (Semplea et al., 2013). For exposure of pregnant dams and pups, female mice (10-13 wk-old) were time-mated with males (3 females per breeding cage) on Sunday evenings, and vaginal plugs were checked the next morning before the Monday onset of the weekly exposures. Mice with confirmed vaginal plugs were removed from the breeding cage on E0 (on the morning of vaginal plug confirmation) and housed individually in cages in either the FA or DE housing racks for the duration of pregnancy, parturition, and until weaning of the litter. The use of Sunday timed mating ensured that E0 always occurred on a Monday, and that parturition (PND0) would occur on a Saturday or Sunday. This ensured the same developmental exposure periods for all mice (i.e., all dams were exposed on the same gestational days: E0-4, E7-11, & E14-18), and that DE exposure would not occur while mice were giving birth. On PND3, litters were culled to 5 pups, with two male and two female pups from each litter selected randomly for behavioral testing. Excess pups were euthanized by decapitation on PND3, and runts (weight >15% lighter than their litter mates) were excluded from the study. Mice for behavioral testing were tattoo-marked on their paw pads on PND3, and were weighed individually each day throughout the preweaning period. On PND21, after the last DE exposure, mice were weaned and transferred to standard Allentown housing racks (two same-sex mice per cage) for the duration of the post-weaning behavioral testing period.

3.2.2 Diesel Exhaust (DE) Exposures

DE exposures were carried out in the UW Controlled Exposure Laboratory's Northlake Diesel Facility (Fox et al., 2015; Gould et al., 2008). DE was generated from a single-cylinder Yanmar diesel generator engine (YDG5500), fueled with standard highway-grade number 2 diesel fuel obtained from local fuel distributors, and operated under ~70% electrical load. DE passed from the generator exhaust through a two-step dilution system, with continuous dynamic control of the fine particulate matter (PM2.5) concentration, allowing maintenance of a constant exposure level at 250-300 $\mu g/m^3$ PM monitored with an in-cage nephelometer. Diluted DE was delivered through a ductwork system to the air intake of an Allentown mouse housing rack, which distributed the diluted DE evenly to all of the cages in the rack. Control mice were exposed to filtered air (FA) in a separate Allentown housing rack located in the same facility, which supplied HEPA-filtered room air to the cages via its ventilation system. Chemical composition and particle size characterization of the DE generated in this facility has been described previously in detail (Fox et al., 2015; Weldy et al., 2013; Yin et al., 2013). Briefly, under identical conditions to those used in the current study, particle size characterization, as measured by gravimetric analysis using a micro orifice uniform deposit impactor (MOUDI) demonstrated a median diameter for in-cage particles of 77 nm, while the count median diameter was 87 nm, indicating a large portion of DE particles in the ultrafine size range (Yin et al., 2013). The mass fraction of particle-bound poly-cyclic aromatic hydrocarbons (PAH) was 20 ng/µg PM2.5, with a ratio of organic carbon to elemental carbon mass concentration of 0.10. Under these conditions, the concentrations of oxides of nitrogen in the DE were 1800 ppb NO_x and 60 ppb NO_2, carbon monoxide concentration was 2 ppm, and carbon dioxide concentration was 1000 ppm. Additional characterization of the elemental content of the DE is described in Fox et al. 2014, Weldy et al. 2013, and Yin et al. 2013 (Fox et al., 2015; Weldy et al., 2013; Yin et al., 2013). DE exposures for the current study were performed under identical conditions, and real-time particle concentrations were measured continuously using an in-cage nephelometer, with fine-tuning of the exposure level throughout each exposure by manual adjustment of the electrical load (2.0 – 2.5 Kw) and/or air flow.

3.2.3 Behavioral Testing

Behavioral tests were selected based on relevance to the three diagnostic domains of autism spectrum disorder (Chang et al., 2017). Deficit in social interaction was assessed by the social preference test and reciprocal interaction test. Vocal and olfactory communication deficits were assessed by neonatal ultrasonic vocalization (USV) recording, and by the olfactory habituation test. Persistent/repetitive behavior was assessed by the marble burying test and the T-maze spontaneous alternation test. To avoid interference associated with multiple testing, animals undergoing behavioral tests were separated into two testing groups as shown in Fig. 3.1: one male and one female from each litter were randomly assigned to each of the two behavioral testing groups, and subsequent tests performed on the same subjects were separated by at least one week. To assess pregnancy outcome, litter size, sex distribution and duration of pregnancy were recorded for each litter. Pre-weaning assessments, including righting reflex, neonatal USVs and body weights were recorded starting from PND4. Post-weaning behavioral testing was conducted beginning at 6 weeks of age, using the same animals tested during the pre-weaning period. At the conclusion of behavioral testing (10-wk), mice were euthanized by CO_2 asphyxiation followed by cervical dislocation.

Maternal behavior was scored from PND0 to PND2, once per day for 30-min, between 6:00 – 10:00 AM. During each scoring session, behaviors such as eating, drinking, pup grooming, arch-back feeding, blanket feeding, nest building, digging, and rearing were scored every minute. The maternal behavior was stratified into behaviors that were related to pup care (feeding, pup grooming, nest building) and behaviors that were not related to pup care (eating, drinking, self-grooming, rearing). Quality of pup care was quantified as the percentage of time the dam spent on activities relating to pup care during the 30 min scoring session.

Righting reflex was measured on PND4-9 and PND12; the pups were placed on a flat clean paper towel dorsal side down, and latency to resume righting position (all four paws on the ground) was measured. Each trial was allowed a maximum of 30 sec to complete. Mice acquiring the reflex were retested on all subsequent days.

Open field test. Each mouse was placed into a clean 42cm (L) X 42cm (W) X 20cm (H) acrylic cage with no bedding for 30 min and was video-recorded (Microsoft LifeCam HD-6000). Locations of subjects were tracked with Ethovision XT 11 (Noldus Information Technology, Leesburg, VA - USA) to assess anxiety response in a novel environment. Time spent in the periphery area (thigmotaxis) versus center area (20 X 20 cm) was measured automatically by the Ethovision software.

Social preference test. The social preference test was conducted using a three chambered social approach apparatus, a clear acrylic box consisting of three same-sized chambers (20 cm × 40 cm × 22 cm) with small openings in the dividing walls that allowed the subject to access all three chambers without restriction. A metal-wire holding cup for the novel and familiar mice was placed in each of the side chambers. The testing procedure consisted of three chronological phases: habituation, sociability, and social novelty (Chang et al., 2017). Supplemental Fig. 3.1 illustrates the arena setup for the sociability and social novelty phases. In the habituation phase the test mouse was placed into the middle chamber and allowed to explore all three chambers freely for 10 min. In the sociability phase, an age- and gender-matched novel C57BL/6J mouse was placed into one of the holding cups. Sociability was quantified as the amount of time the test mouse spent in proximity (inside of the interaction zone, within a 5 cm radius from the holding cup) to the holding cup containing the first novel mouse versus the time spent in proximity to the empty holding cup. In the social novelty phase, a second age- and gender-matched novel mouse was added into the holding cup that had been empty during the sociability phase. The preference of the test mouse

for social novelty was quantified by measuring time spent in the interaction zone near the second novel mouse versus time spent in the interaction zone near the now-familiar mouse.

Reciprocal Interaction between the test subject and an age- and sex-matched socially naïve C57BL/6J stimulus partner was assessed (Chang et al., 2017). Test and naïve mice were individually housed for an hour before being introduced to each other in a clean standard housing cage for 10 min. A Microsoft LifeCam HD-6000 camera was used for video recording. Total social contact, including sniffing (nose–nose, anogenital, body), push–play behavior, following, rearing, and huddling was scored manually by a researcher blinded to the experimental groups.

Olfactory habituation to social odors. For olfactory communication, sniffing response toward different olfactory cues with and without social valence was assessed (Chang et al., 2017). Mice were housed individually for an hour before testing began. Olfactory cues were prepared in the following concentrations: distilled water, almond extract (McCormick, Hunt Valley, MD; 1:100 dilution), banana flavoring (McCormick, Hunt Valley, MD; 1:100 dilution), pooled male urine (from age-matched C57BL/6J mice at 1:100 dilution), and pooled female urine (from age-matched C57BL/6J mice at 1:100 dilution). For presentation, 10 µl of olfactory stimuli were applied onto filter paper taped inside of polystyrene weigh boats (VWR, Radnor, PA; 4.1 x 4.1 x 0.8 cm) and placed on top of the wire cage-top for 2 min before replacing with the next olfactory stimulus. During each 2 min presentation period, test-mouse behavior was video-recorded (Microsoft, LifeCam HD-6000). Number of sniffs and duration of sniffs were scored manually from the video-recording by two different researchers who were blinded to the treatment groups.

Neonatal isolation-induced ultrasonic vocalization. To assess neonatal vocal communication, ultrasonic vocalizations (USV) were recorded for 5 min from PND6 mice isolated from their dam and littermates inside of a 250 ml glass beaker and surrounded by a sound-attenuating box, with an electrical heating pad (Sunbeam 731-500) maintaining temperature at 22-25ºC. USVs were recorded with the UltraVox system from Noldus Information Technology (Leesburg, VA, USA).

Frequency and duration of calls were quantified in ten call categories: 1) complex, 2) two-components, 3) upward, 4) downward, 5) chevron, 6) short, 7) composite, 8) frequency-steps, 9) flat, and 10) unstructured calls, as shown in Supplemental Fig. 3.3, using the UltraVox software provided by Noldus inc. (Leesburg, VA, USA). Characteristic criteria for each call category are described in Scattoni et al., 2009 (Scattoni et al., 2009).

Marble burying test. Repetitive digging was assessed by placing the mouse into a clean standard sized housing cage (484 sq. cm) filled with shaved aspen bedding 5 cm in depth then topped with 12 marbles (1.58 cm in diameter) evenly spaced in a 3 X 4 grid. A clear acrylic ceiling with ventilation holes was used to prevent mice from climbing out of the cage during testing. Digging activity was video-recorded for 30 min (Microsoft, LifeCam HD-6000); number of buried marbles (>2/3rd covered) were scored every 5 min from video footage by a researcher blinded to exposure (Chang et al., 2017). The cage and acrylic ceiling were cleaned with 70% ethanol then refilled with new bedding material; marbles were washed with soap, rinsed with water and 70% ethanol and dried for subsequent trials.

T maze spontaneous alternation test. To assess repetitive behaviors and/or working memory, each subject was placed into a T-shaped maze (consisting of three black plexiglass 30 X10 cm arms joined by a 10 X 10 cm center) with the nose pointing away from the center, and was allowed to choose between right and left goal arms throughout a 15-trial session. Once a mouse entered a particular goal arm, it was restricted in that goal arm for 30 sec before being returned back to the starting position for the next trial of testing. Subjects that failed to enter a goal arm within 2 min were disqualified from testing. The whole testing procedure was video recorded (Microsoft, LifeCam HD-6000) and scored manually. Spontaneous alternation rate was calculated as the ratio between the alternating choices and total number of choices (Chang et al., 2017).

3.2.4 Statistical Analysis

Statistical analyses were performed using GraphPad Prism software (GraphPad Software Inc., La Jolla, CA). For most measures, statistical significance was determined by two-way ANOVA using exposure and sex as independent variables, with the Bonferroni correction for multiple comparisons. For the marble burying test, statistical significance was determined by two-way ANOVA with repeated measures, using the Bonferroni correction. For the olfactory habituation test, differences in the initial responses to odor presentation were analyzed by two-way ANOVA with Bonferroni correction, whereas habituation (i.e., the decrease in response with repeated presentation of the olfactory cue) was determined for each of the four groups (DE male, FA male, DE female, FA female) by one-way ANOVA with repeated measures, using Dunn's test for multiple comparisons. For the three chambered social preference test, time spent in the 'N1' versus 'empty' chambers (for the social approach phase) or 'N1' versus 'N2' chambers (for the social novelty phase) were compared within each of the four groups by one-way ANOVA with the Bonferroni correction. Values of $p<0.05$ were considered statistically significant. Results are expressed as the mean ± SEM.

3.3 Results

3.3.1 The effect of diesel exhaust on pregnancy outcome and pre-weaning behaviors

For this study 13 FA- and 14 DE-exposed litters were generated over 12 overlapping exposure cohorts. Both DE- and FA- exposed pups were born in similar litter size and sex ratio (Fig. 3.2A). There were no significant differences in pup weights (Fig. 3.2B), and the appearance of the righting reflex was the same for both DE- and FA-exposed pups (Fig. 3.2C, 3.2D). Monitoring maternal behavior at PND0-2 revealed no significant differences in time spent on pup-care activities such as grooming, nursing, and nest building between dams exposed to DE or FA (Fig.

3.3). In the open field test (Supplemental Fig. 3.2A, 3.2B), no significant differences were found in locomotor activity or thigmotaxis, a possible indicator of anxiety and/or exploratory drive.

3.3.2 The effect of diesel exhaust on social behavior

In the social preference test, sociability and the ability to detect and remember social novelty were assessed using a three-chambered social approach apparatus. In the sociability phase, DE- and FA-exposed mice of both sexes demonstrated a significant preference for spending time in the chamber containing the novel mouse, compared to the empty chamber (Fig. 3.4A). The ability to differentiate social novelty was assessed by measuring time spent in the chamber containing a second novel mouse (N2) vs. time spent in the chamber containing the now-familiar mouse (N1). DE-exposed female mice showed no preference between the novel and familiar mice, whereas DE-exposed males and FA-exposed mice of both sexes demonstrated a clear preference for the novel mouse compared to the familiar mouse (Fig. 3.4B).

The reciprocal interaction test allows assessment of intrinsic social behavior with an age- and sex-matched social partner in an unrestricted setting. During the 10-min interaction period, DE-exposed males spent significantly less time on interactive sniffing with the novel social partner, as compared to FA-exposed males (Fig. 3.5). No differences were found in interactive sniffing between DE-exposed and FA-exposed females; there was a tendency towards decreased interactive sniffing in the DE-exposed females, but the difference was not statistically significant.

3.3.3 The effect of diesel exhaust on communication

Vocal communication was assessed by recording isolation-induced neonatal ultrasonic vocalizations (USV) at PND6. DE-exposed males emitted significantly fewer USV calls compared to FA-exposed males (Fig. 3.6A). DE-exposed females also tended to emit fewer USV calls than FA-exposed females, but the difference was not statistically significant (Fig. 3.6A). USVs were

also categorized into nine USV categories as described by Scattoni et. al. (Scattoni et al., 2008) (see Supplemental Fig. 3.3 for examples of each call category from the current study). Since the number of calls in specific USV categories could be confounded by inter-individual differences in the total number of calls, the number of calls from each USV category was normalized to the total number of calls emitted by the same subject (number of calls emitted by each pup in specific USV category/total number of USV calls). DE-exposed mice of both sexes emitted significantly fewer 'frequency-step' calls compared to the FA-exposed mice (Fig. 3.6B). DE-exposed males and females also emitted significantly more 'unstructured' calls compared to the FA-exposed mice (Fig. 3.6C). Increased emission of unstructured USV calls has also been reported in genetic mouse models of autism (Ey et al., 2013; Scattoni et al., 2011).

In the olfactory habituation test (Fig. 3.7A, 3.7B), olfactory communication was assessed by quantifying sniffing responses elicited by repeated presentations of two non-social olfactory cues (almond and banana) and a social olfactory cue (sex-matched urine). During the first presentation of same-sex urine, DE-exposed female mice (Fig. 3.7B), but not males (Fig. 3.7A), showed a significant decrease in sniffing response compared to the FA-exposed animals. A habituation response in the olfactory test was reflected as a decreasing level of interest in subsequent repeated presentations of the same odor. Repeated presentation of non-social olfactory cues elicited a significant habituation response in all experimental groups, as expected, indicating unaffected olfactory function in the DE-exposed mice (Fig. 3.7A, B). DE-exposed mice of both sexes failed to habituate to the repeated presentation of same-sex urine, whereas FA-exposed males and females showed a significant habituation response (Fig. 3.7A, B).

3.3.4 The effect of diesel exhaust on repetitive behavior

In the T-maze spontaneous alternation test (Fig. 3.8), the number of repeated entries into the same goal arm by each mouse was scored as a measurement of repetitive behavior over 15 trials.

DE-exposed mice of both sexes exhibited a significant increase in the number of repeated entries compared to FA-exposed mice of the same sex (Fig. 3.8). Mice that failed to choose a goal arm within the 2-min trial period were retested at a later time, and were removed from the test if they failed to choose a goal arm on the subsequent trial. A total of 6 mice (1 FA male, 2 FA females, and 3 DE females) were excluded using this criterion.

The marble burying test (Fig. 3.9A, 3.9B) also demonstrated increased repetitive behavior associated with developmental DE exposure. For this test, the number of buried marbles was counted over a 5-min period as a proxy measurement for repetitive digging. In both sexes, DE-exposed mice buried more marbles than FA-exposed control mice of the same sex (Fig. 3.9A, 3.9B).

3.4 Discussion

To our knowledge, this is the first detailed and comprehensive assessment of behavioral phenotypes relevant to all three characteristic domains of autism (difficulties in social interaction, communication deficiency, and increased repetitive behaviors) in mice exposed developmentally to an environmentally relevant level of DE (250-300 $\mu g/m^3$).The level of DE exposure used in the current study falls into the "very unhealthy" and "hazardous" air quality index (AQI) categories (U.S. Environmental Protection Agency, 2015). These levels are not uncommon in cities such as Beijing, New Delhi, and Mexico City. Based on air quality data collected between April 2008 and March 2014 from a monitor installed at the U.S. Embassy in Beijing, air quality fell within the range of our exposure level about 20% of the total 2,028 days surveyed (Ma, Wayne and Chen, 2014). Satellite monitoring data revealed that populations in some cities in South and Southeast Asia have been receiving prolonged exposure of >100 $\mu g/m^3$ of PM2.5 (Shi et al., 2018; van Donkelaar et al., 2014).

Quality of maternal care has been known to have long-lasting effects on pup behavior; specifically, maternal neglect has been shown to lead to increased anxiety and hyperactivity behaviors (George et al., 2010). The interpretation of behavioral testing results could be confounded by differences in locomotor activity, anxiety response, and other factors that may arise from these or other developmental defects. To assess the effects of DE exposure on maternal care behavior and subsequent consequence on pup anxiety, maternal care behavior and pup behavior in the open field test were assessed. No differences were observed in quality of maternal care or pup anxiety in the open field. Litter size, sex distribution, and pup weights did not differ between DE- and FA-exposed mice. Righting reflex also showed no differences between DE-exposed and FA-exposed animals. Altogether, these findings suggest that locomotor activity, anxiety / exploratory drive, and developmental deficits due to the maternal care environment played a minimal role, if any, in confounding the interpretation of behavioral testing results.

To assess the sociability domain, the three-chambered social preference test and the reciprocal interaction test were conducted. Exposure to DE did not affect sociability in the three chambered social preference test, as indicated by the preference of both DE-exposed mice and FA-exposed mice for the novel mouse over the empty chamber. However, in the social novelty phase, DE-exposed females showed no preference when presented with a choice between the novel and familiar mice, suggesting inability to differentiate social novelty. Inability in differentiating social novelty has also been reported in C3H/HeJ, AKR/J, A/J, and 129S1/SvImJ mouse strains, which have been reported to exhibit autism-like behavioral traits (Kim et al., 2017; Moy et al., 2007). Related to the fact that autism is a spectrum of disorders with a wide range of variation in severity and type of behavioral traits, we suspect that the inability to differentiate social novelty but not social preference, as shown in DE- exposed females represents a more subtle but specific type of social deficit with recognizable functional implications. In the reciprocal interaction test, DE-exposed males exhibited significantly decreased social sniffing behaviors compared to FA-

exposed males, and females showed a similar trend, though it was not statistically significant. Decreased male–male social sniffing has also been reported in the BTBR mouse strain and in Shank3+/- transgenic mice, which are considered good mouse models of ASD (Bozdagi et al., 2010; Scattoni et al., 2013). Our results with these two tests suggest the presence of sex differences in the effect of DE on specific types of social behavior. While DE-exposed females exhibited a deficit in social novelty in the three-chambered social preference test, DE-exposed males exhibited a more robust phenotype in the reciprocal interaction test, where they showed a deficit in interactive sniffing episodes with same-sex mice. This difference in responding to social contexts provided by the two tests can likely be attributed to innate behavioral differences between male and female C57BL/6J mice.

For the communication domain, neonatal isolation-induced USVs and olfactory habituation were used to assess vocal and olfactory communication, respectively. Mouse pups emit USVs with frequency ranges from 30 to 90 kHz (Branchi et al., 2006). Neonatal vocal repertoires similar to those observed in DE-exposed mice in the current study have also been detected in the reelin+/- and the BTBR T+tf/J mouse models of ASD during the early developmental period (De Felice et al., 2015; Ju et al., 2014; Kirsten et al., 2012; Romano et al., 2013; Scattoni et al., 2009, 2008). DE-exposed male pups showed a significant decrease in the total number of emitted USV calls, compared to FA males, and DE-exposed females showed a similar but not statistically-significant trend. A decreased number of USV calls has also been reported in the maternal immune activation (lipopolysaccharide treated) autism mouse model (Kirsten et al., 2012). Sonographic patterns have been commonly analyzed in rodent models for detailed assessment of the types of calls emitted (Brudzynski et al., 1999; Chang et al., 2017; Michetti et al., 2014; Scattoni et al., 2009, 2008, 2011). Nine call categories have been identified as the typical vocalization repertoire (Brudzynski et al., 1999; Chang et al., 2017; De Felice et al., 2015; Michetti et al., 2014; Romano et al., 2013; Scattoni et al., 2009, 2008, 2011; Wöhra et al., 2013)(See also Supplemental Fig.

3.3); DE-exposed males and females emitted fewer calls of the frequency-step call category compared to FA-exposed mice. A similar shift in call-category preference has been reported in genetic autism models, such as the BTBR T+tf/J and reelin mutant mouse (Michetti et al., 2014; Scattoni et al., 2011), as well as mice exposed developmentally to chlorpyrifos (De Felice et al., 2015). In the current study, there were also a greatly increased number of unstructured USV calls in DE-exposed males and females. Unstructured calls are broken/deformed calls within the mouse pup's frequency range, but which could not be recognized to fall in any of the nine call categories. Unstructured calls have also been reported in the BTBR T+tf/J mouse autism model (Scattoni et al., 2011). While a large portion of the calls emitted by the DE-exposed mice in our study were unstructured calls, a few FA-exposed mice also produced unstructured calls, though they were very rare (1-2 unstructured calls in the 5 min recording session), and not all FA-exposed mice emitted them. Since naïve B6 females have also been reported to produce small numbers of unstructured calls (Scattoni et al., 2011), unstructured calls in other published studies may have been present but overlooked, due to their rarity in control animals. In future studies, measuring unstructured USV calls could be a robust tool for assessing vocal communication deficits; however, additional research is needed to confirm that unstructured calls reflect a true communication deficit, as opposed to their representing an additional category of USV that is used for a specific type of communication.

In the olfactory habituation test, olfactory responses toward repeated presentations of social and non-social olfactory cues were measured; under typical situations, naïve mice would show decreasing interest with repeated presentations of the same scent, indicating habituation. The olfactory habituation test is also commonly used to assess olfactory communication in various autism mouse models (Bozdagi et al., 2010; Silverman et al., 2011; Silverman et al., 2010; Yang et al., 2012). In our experiments, while mice from all experimental groups habituated to the repeated presentation of the two non-social odors (banana, almond); only FA-exposed mice were

able to habituate toward social odors (sex- and age-matched pooled urine). These findings provide evidence that the inability of DE-exposed male and female mice to habituate to social odors is not due to loss of olfactory function, since DE-exposed animals of both sexes were able to habituate to non-social odors.

To assess the repetitive domain, the T-maze spontaneous alternation test and marble burying test were conducted. The T-maze has been used frequently to assess hippocampal dependent spatial memory under a variety of testing protocols (Crawley, 2012; Deacon and Rawlins, 2006; Lainiola et al., 2014). In the T-maze spontaneous alternation protocol used in the current study, mice were allowed to explore freely within the T-maze and repetitive behavior was assessed by measuring repeated entries into the same goal arm in subsequent trials (Deacon and Rawlins, 2006; Favre et al., 2015; Kirsten et al., 2012; Wrenn et al., 2003). Our data showed significant increases in the number of repeated entries by DE-exposed mice of both sexes, comparing to FA-exposed control mice; this result is consistent with findings reported in the maternal immune activation model and valproic acid-exposed model of autism (Favre et al., 2015; Kirsten et al., 2012). Repeated arm entries in the T-maze might be interpreted as a deficit in spatial working memory. However, our finding that repetitive behavior was also increased in the marble-burying test suggests that the T-maze results are best interpreted as an increase in repetitive behavior. The marble buying test has been used to assess repetitive behavior in rodent models of autism as well as in models of obsessive-compulsive disorder (Amodeo et al., 2012; Angoa-Pérez et al., 2013; Deacon, 2006; Moy et al., 2014; Reiner et al., 2016; Wurzman et al., 2015). In the marble buying test, evenly spaced marbles serve as a proxy measurement for repetitive digging behavior; with increased repetitive digging more marbles will be buried. Our results show that DE-exposed males and females buried marbles more quickly and buried more marbles in the 30 min testing period, compared to FA-exposed control mice. As increased repetitive behavior in male and

female DE-exposed mice were found in both of these independent tests, it is likely that developmental DE exposure affects repetitive behavior.

Association between ASD related behavioral phenotypes and developmental ambient particulates exposure have also been recently assessed in different rodent models. A study recent conducted by Li et. al. (Li et al., 2017b) in Sprague-Dawley rats exposed by intranasal instillation to ambient PM2.5 (2 or 20 mg/kg body weight) from PND 8 to 22, revealed decreased number of neonatal USV calls and inability to differentiate social novelty in exposed rats, in agreement with our findings. However, this study did not find deficits in social olfactory communication and increased repetitive behaviors, at difference with what we found. While highlighting the importance of critical windows of susceptibility during development, the differences between our findings and those of Li et al.(2017b) suggest that exposure to a complex mixture of air pollution (such as DE) rather than solely to ambient particulates, may represent a most relevant variable. Indeed, while several studies have shown that particles may have neurotoxic properties (Hartz et al., 2008; Larner et al., 2017; MohanKumar et al., 2008; Win-Shwe and Fujimaki, 2011), other components of DE may contribute to its developmental neurotoxicity. Another recent study by Church et. al. (Church et al., 2017) in B6C3F1 mice exposed to ambient PM2.5 (135.8 mg/m^3) during the whole gestational period and up to PND10 found a behavioral phenotype similar to what reported in the present study, e.g. a decreased interactive sniffing response, and increased repetitive grooming behavior.

In recent years several large-scale epidemiological studies have shown associations between exposure to TRAP and increased risk of ASD (Costa et al., 2017; Roberts et al., 2013; Suades-González et al., 2015; Volk et al., 2011). As mentioned in the introduction, exposure to concentrated ambient ultrafine particles (UFP) during development causes lateral ventricle dilation, a predictor of poor neurodevelopmental outcome that has been associated with autism and schizophrenia (Allen et al., 2014, 2016). Prenatal DE exposure also causes motor

coordination, impulsive behavior and monoaminergic systems in various brain regions in mouse models (Suzuki et al., 2010; Yokota et al., 2013).

In the present study, DE exposure was conducted throughout gestation and the pre-weaning period. This exposure period was chosen based on epidemiological studies in humans showing that traffic-related air pollution exposure during all three trimesters of pregnancy and during the first 9 months of infants' life is associated with increased ASD risk (Guxens et al., 2016; Raz et al., 2017; Volk et al., 2013, 2011). The exposure period was designed to cover key neurodevelopmental events happening during this window of susceptibility, which in mice equates to E0 to PND21 (Semplea et al., 2013). The current study does not address the relative importance of DE exposure during the gestational versus postnatal periods for producing effects on ASD-related behaviors. It would be of great interest to better define windows of DE susceptibility during development, and to ascertain mechanisms of specific CNS effects that occur during specific developmental events. Of some relevance to this are our unpublished findings from a preliminary pilot study that mice exposed only during the gestational period tended not to show effects on social behavior, repetitive behavior in the Morris Water Maze reversal task, or various other neurobehavioral measures.

It is not clear whether the neurobehavioral consequences of DE exposure were due to direct effects on the CNS, e.g., by translocation to the olfactory bulb, or to indirect effects arising from ingestion of DE particles or from peripheral inflammation, e.g., of the lungs. In the current study, the route of exposure to DE clearly changed once the pups were born, as they began to breathe on their own and to inhale the DE directly. Indeed, developmental DE exposure of rodents has been shown to increase levels of pro-inflammatory cytokines in placenta, fetal brain and fetal lung, including studies done in the same facility and under the same conditions used in the current study (Fox et al., 2014; Cole et al., 2016; Weldy et al., 2013; Roqué et al., 2016). Our group

previously reported that acute DE exposure in adult mice causes neuroinflammation and oxidative stress in multiple brain regions (Roqué et al., 2016; Coburm et al., 2018) . DE particles, a primary component of TRAP, have also been reported to activate microglia both *in vitro* and *in vivo* Further, developmental exposure to DE particles has been shown to increase inflammatory cytokines and alter microglia morphology in a toll-like receptor 4 (TLR4) dependent manner (Bolton et al., 2017). TLR4 has been shown to play a critical role in the maternal immune activation mouse model of autism, in which prenatal infection-induced activation of TLR4, and subsequent elevation of the key inflammatory cytokines IL6 and IL17α, are responsible for autistic-like behavior observed in pups (Hsiao et al.,2011, 2013; Smith et al., 2007). These findings suggest that DE exposure during perinatal development may activate pathways involved in maternal immune activation. The heterogeneous nature and escalating prevalence of ASD presents a complex and pressing public health challenge that warrants further mechanistic studies.

3.5 Figures

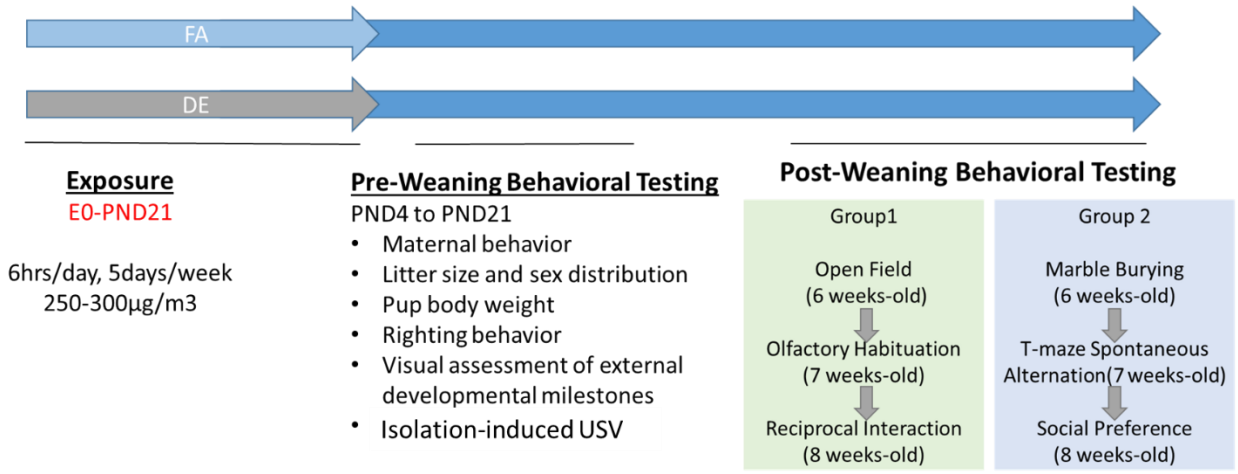

Fig. 3.1. Experimental Design

C57/BL6J mice were timed mated and exposed to 250-300 µg/m^3 of DE or FA from E0 to PND21 for 6/day and 5 days/week. Pre-weaning developmental assessment started on PND3. Behavioral assessment focusing on three characteristic domains of ASD started when the mice were 6 weeks old.

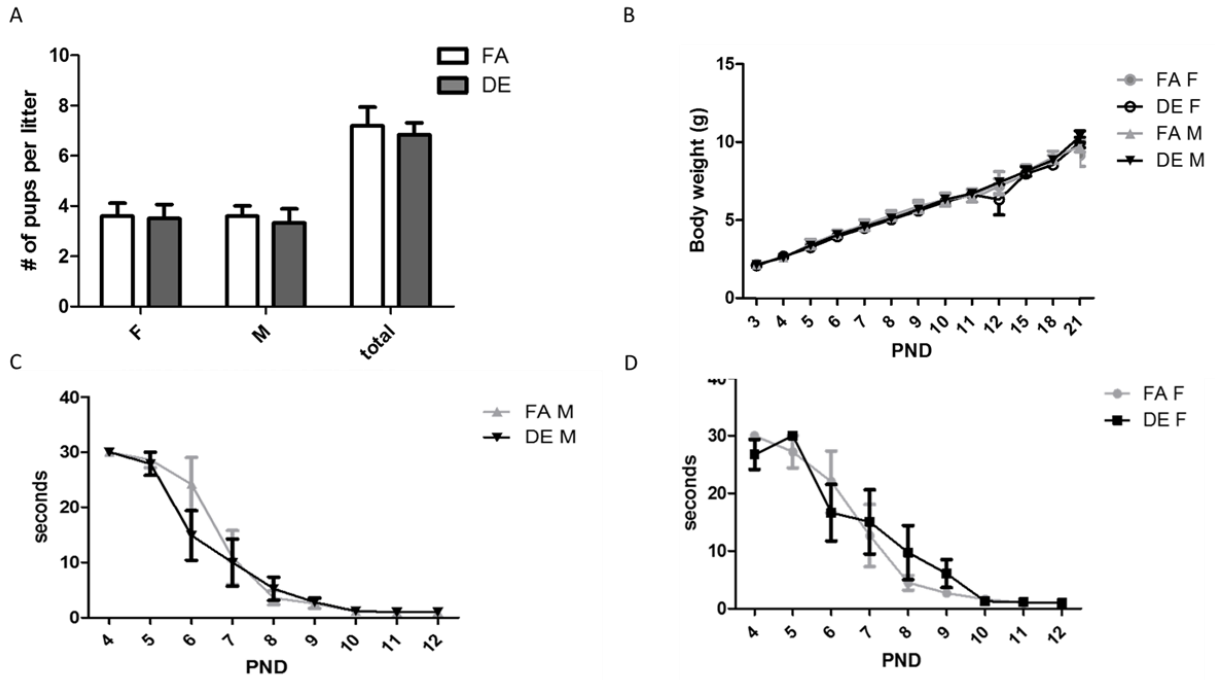

Fig. 3.2. Pre-weaning Developmental Assessment

(A) Number of male, female, and total pups from each litter. No significant differences in sex distribution or number of pups per litter were found between FA and DE groups (B) Pup weight (averaged weights of the 2 same-sex pups from each litter) measured from PND3 to PND21. No significant differences in pup weight between different experimental groups were found. Righting reflex response was measured in males (C) and females (D) from PND4-12. No significant difference in righting response time (sec) between DE exposed and FA control mice were found in either sex (Two-way ANOVA with Bonferroni correction). FA M n=13, DE M n=14, FA F n=12, DE F n=13.

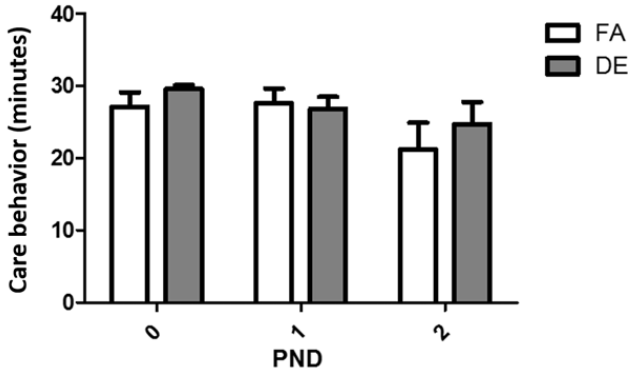

Fig. 3.3. Maternal Care Behavior

Amount of time spent by dams on behaviors related to caring for pups (pup grooming, nursing, nest building, sitting with pups) were recorded in 1 min intervals for 30 min each day during the first three days of pups' life. No differences were found between FA and DE dams (Two-way ANOVA with Bonferroni correction). FA N= 13, DE N=14.

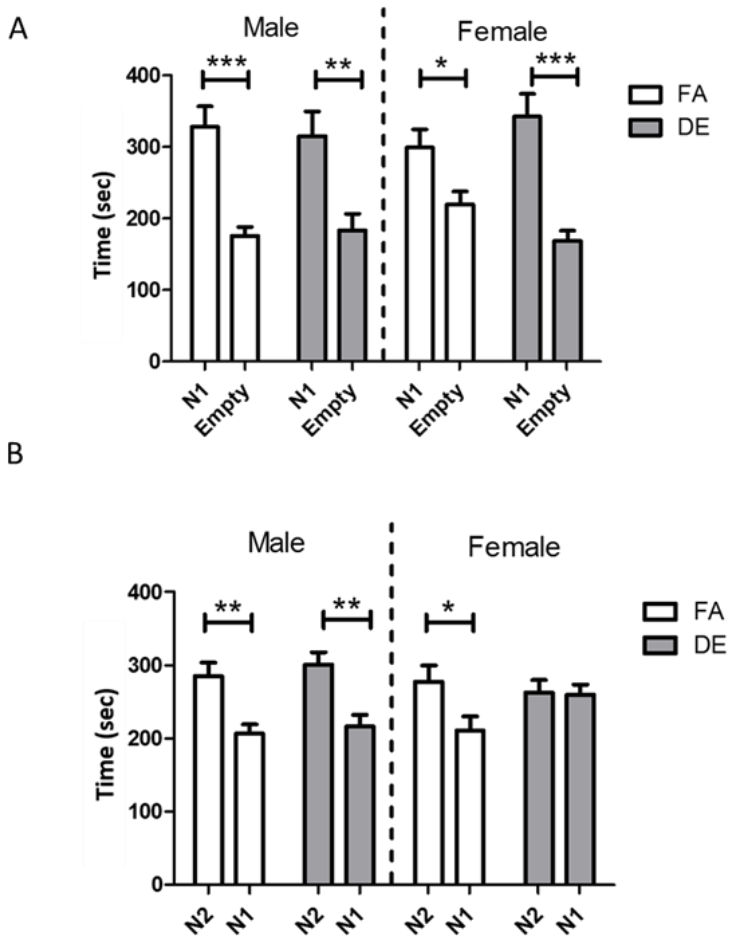

Fig. 3.4. Three Chambered Social Preference Test

In the sociability phase of three chambered social preference test (A), sociability was assessed by measuring cumulative time spent by test mice in chamber containing novel mice (N1) vs. empty chamber. There were no differences between FA-exposed and DE-exposed mice; both FA and DE-exposed mice of both sexes exhibited preference toward novel mice over empty setup (**p*<0.05, **p<0.01, ****p*<0.001; One-way ANOVA with Bonferroni correction). In the social novelty phase (B); cumulative time spent by test mice in the chamber containing the novel mouse (N2) vs. familiar mouse (N1) was measured. DE-exposed female mice showed no preference between novel vs. familiar mice, while FA-exposed mice of both sex and DE-exposed males preferred the novel mouse over the familiar mouse (**p*<0.05, **p<0.01; One-way ANOVA with Bonferroni correction). FA M n=14, DE M n=13, FA F n=13, DE F n=13.

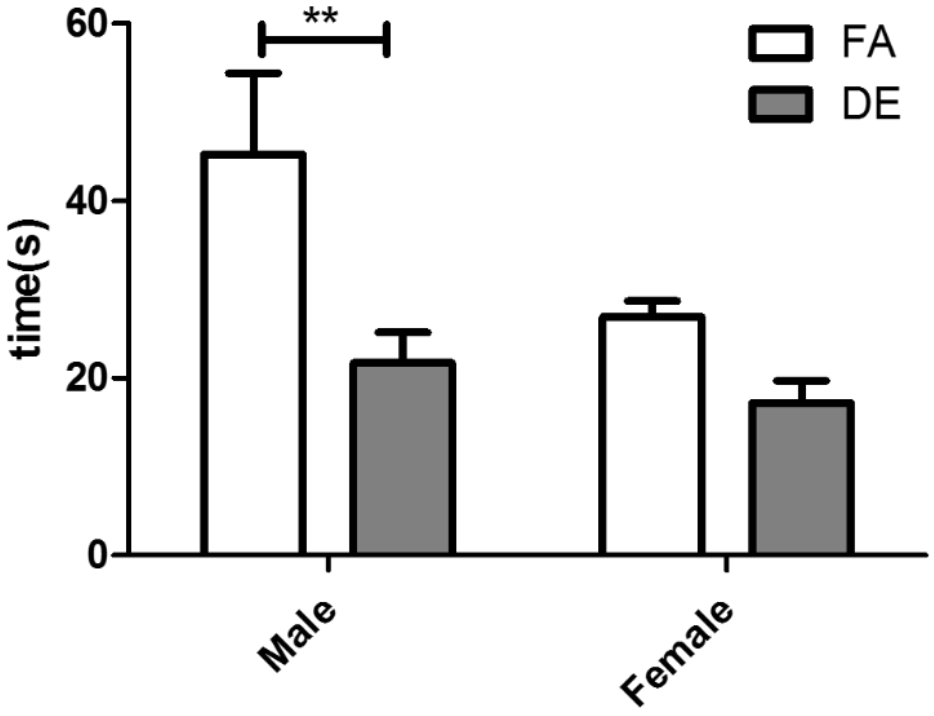

Fig. 3.5. Reciprocal Interaction Test

Interactive sniffing duration during reciprocal interaction was plotted in as mean ± SEM. Males exposed to DE exhibited less interactive sniffing compared to FA-exposed control males (**p<0.01; Two-way ANOVA with Bonferroni correction). DE-exposed female mice also showed a trend of decreased interactive sniffing that was not statistically significant. FA M n=11, DE M =13, FA F n=10, DE F n=13

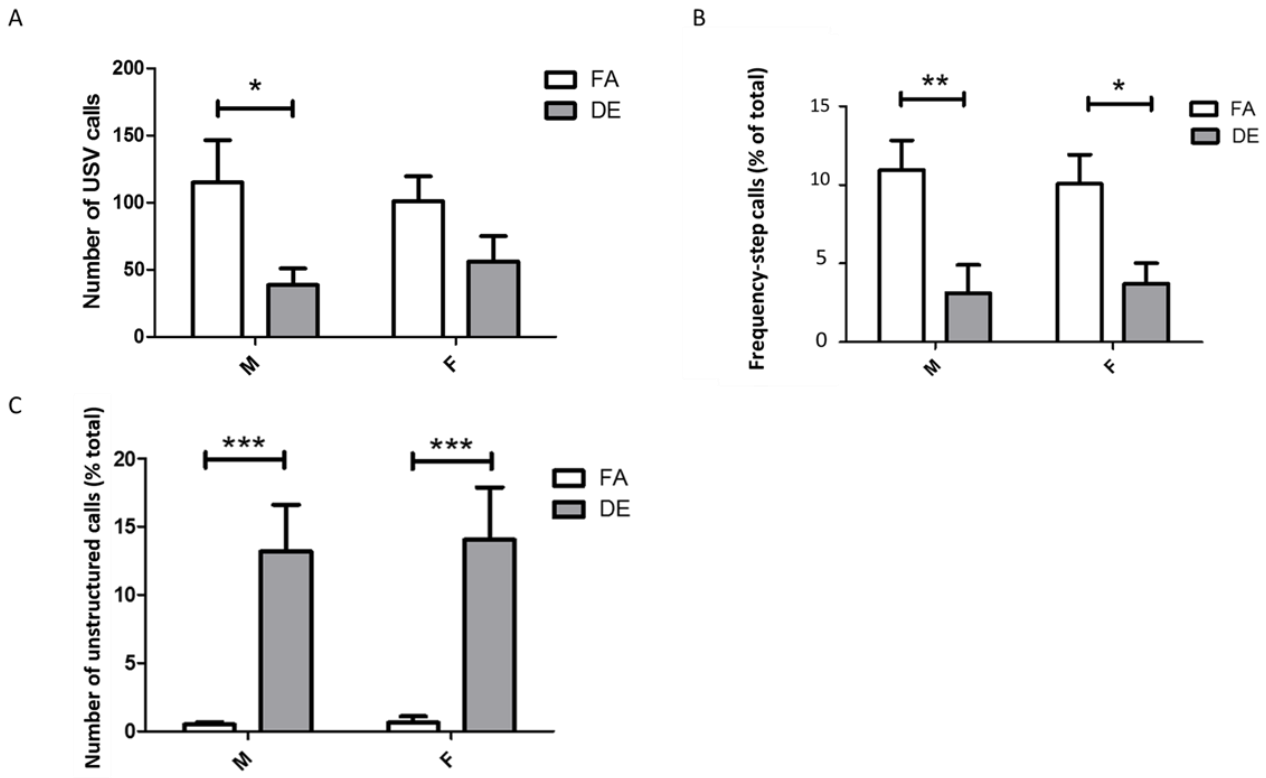

Fig. 3.6. Neonatal USV Calls

Neonatal ultrasonic vocalizations (USV) on PND6. Total number of calls (A) emitted during the 5-min isolation period. Males exposed to DE emitted fewer USV calls compared to FA-exposed control males (*p<0.05; Two-way ANOVA with Bonferroni correction). (B) Frequency-step calls normalized to total number of calls by the same pup). DE-exposed mice of both sex produced fewer frequency-step calls compared to same-sex FA-exposed controls. (Male: **p<0.01; Female: *p<0.05; Two-way ANOVA with Bonferroni correction) (C) Unstructured calls normalized to total number of calls by the same pup. DE-exposed mice of both sex emitted far more unstructured USV calls compared to same sex FA-exposed controls. (***p<0.001; Two-way ANOVA with Bonferroni correction) FA M n=16, DE M n=12, FA F n=16, DE F n=12. (See Supplemental Fig. 3 for examples of each type of USV call).

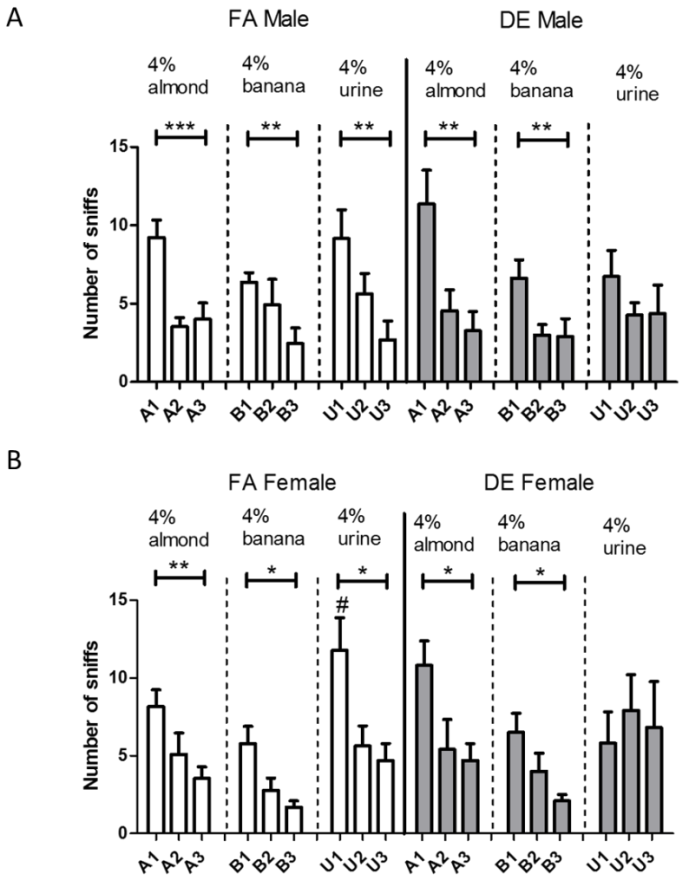

Fig. 3.7. Olfactory Habituation test

In the olfactory habituation test, sniffing responses elicited by repeated presentations of non-social odors (almond and banana) or social odor (same sex urine) were analyzed in males (A) and females (B). For the initial presentation of same-sex urine (U1), FA-exposed female mice showed a significantly higher number of sniffing bouts, nearly twice the number of bouts seen in the DE-exposed females (# $p<0.05$; Two-way repeated-measures ANOVA, with Bonferroni correction). Habituation response was measured as a decreasing number of sniffing responses with repeated presentations of the same odor. DE-exposed mice of both sexes were unable to habituate to repeated presentation of same-sex urine, a social odor, while FA-exposed control mice of both sexes showed significant habituation toward same-sex urine. (*$p<0.05$; **$p<0.01$; ***$p<0.001$; One-way repeated-measures ANOVA, with Dunn's multiple comparison test). Graph plotted as mean ± SEM; FA M n=9, DE M n=10, FA F n=8, DE F n=7.

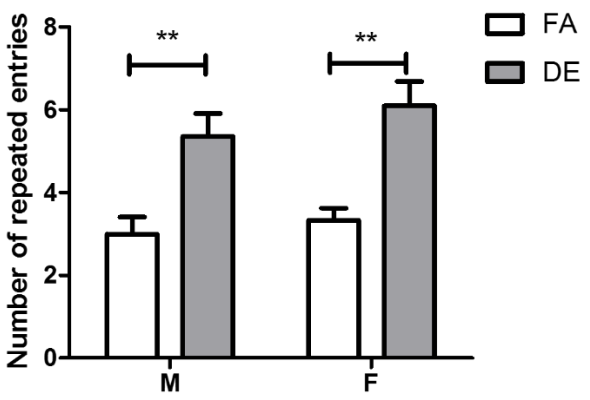

Fig. 3.8. Repetitive Entries in T-maze spontaneous alternation test

Repeated entries in the T-maze spontaneous alternation test (mean ± SEM; n = 9–14). DE-exposed mice of both sex made significantly more repeated entries than FA-exposed mice of the same gender (**p<0.01; Two-way ANOVA with Bonferroni correction).

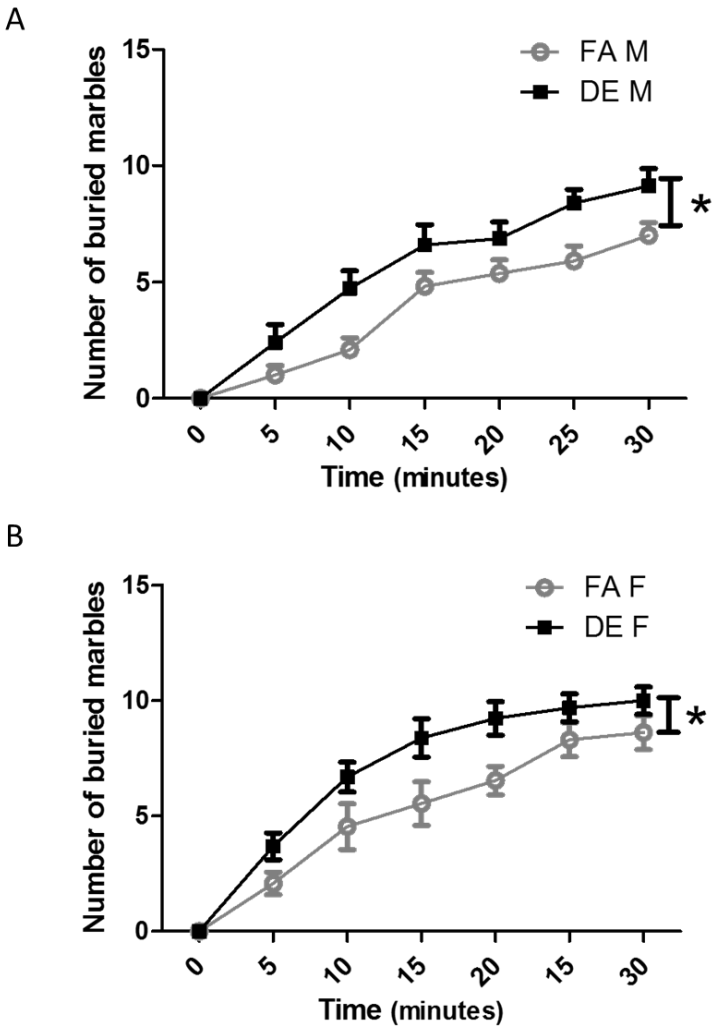

Fig. 3.9. Marble Burying Test

For the marble burying test, the number of buried marbles was scored in five minutes intervals and plotted as mean ± SEM (n = 11–15). Number of marbles buried by males (A) and females (B) were plotted separately. DE-exposed mice of both sexes buried more marbles than FA-exposed control mice (Female *p= 0.0250; Male *p=0.0263; Two-way repeated-measures ANOVA with Bonferroni correction).

3.6 Appendix

3.6.1 Supplemental Information

A

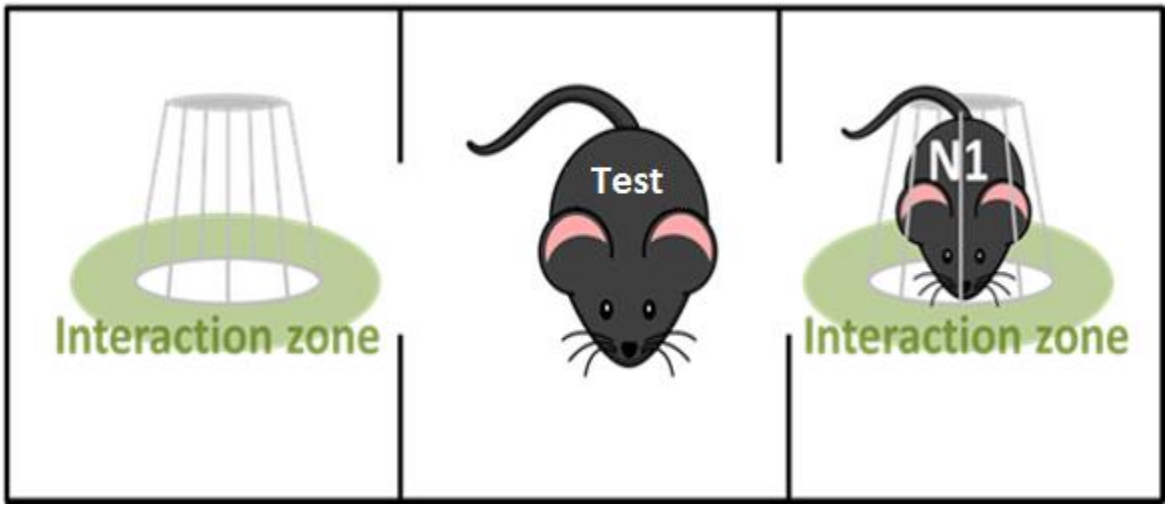

2b

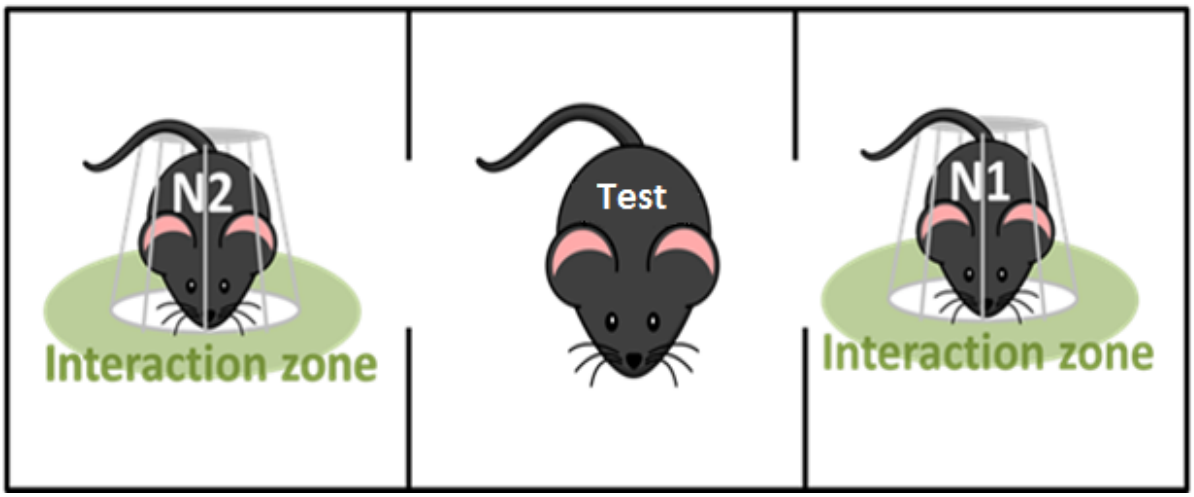

Supplemental Figure 3.1 Three chambered social preference test set up

A. Sociability phase set-up: to test for sociability, one sex and age matched novel mouse (N1) was randomly placed into a metal holding cup while the test mouse was allowed to explore all three chambers freely. **B.** Social-novelty phase set-up: after the sociability phase an additional sex and age matched novel mouse (N2) was placed in the empty metal holding cup while the test mouse was allowed to explore all three chambers freely.

A

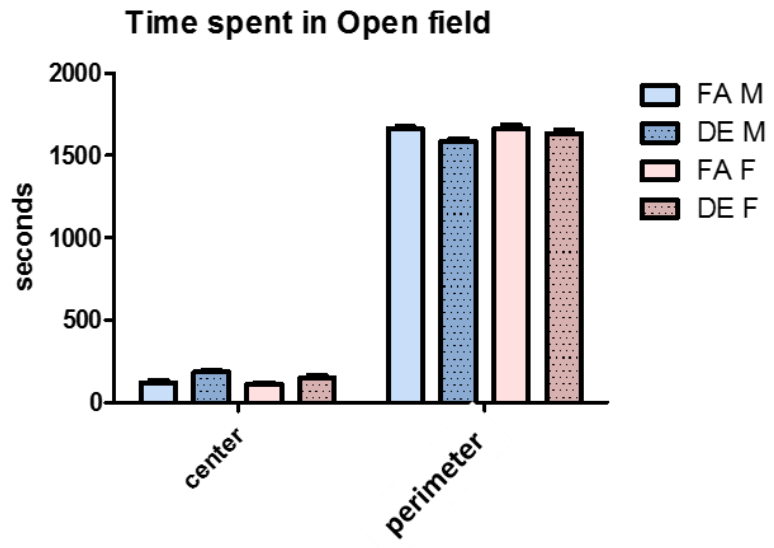

B

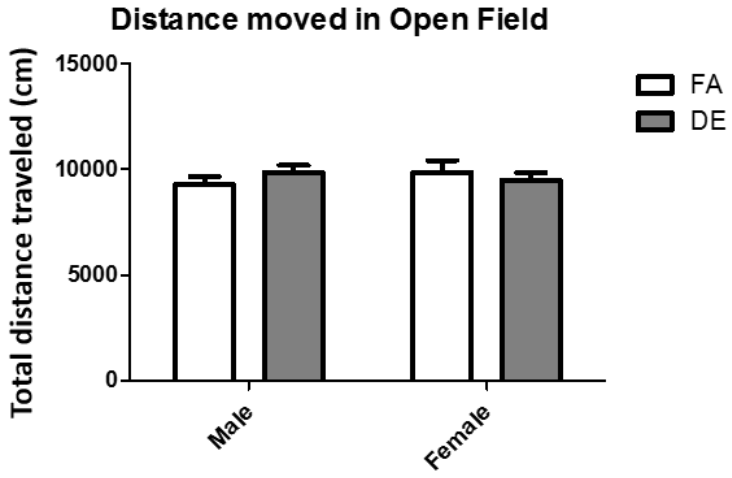

Supplemental Figure 3.2 Open Field Test

In the open field test, anxiety response was assessed by time spent in center vs. perimeter of the open field (2a). Locomotor activity was measured by total distance traveled during the open field test (2b). No significant differences were found in both assessments. FA M n=13, DE M n=14, FA F n=12, DE F n=13

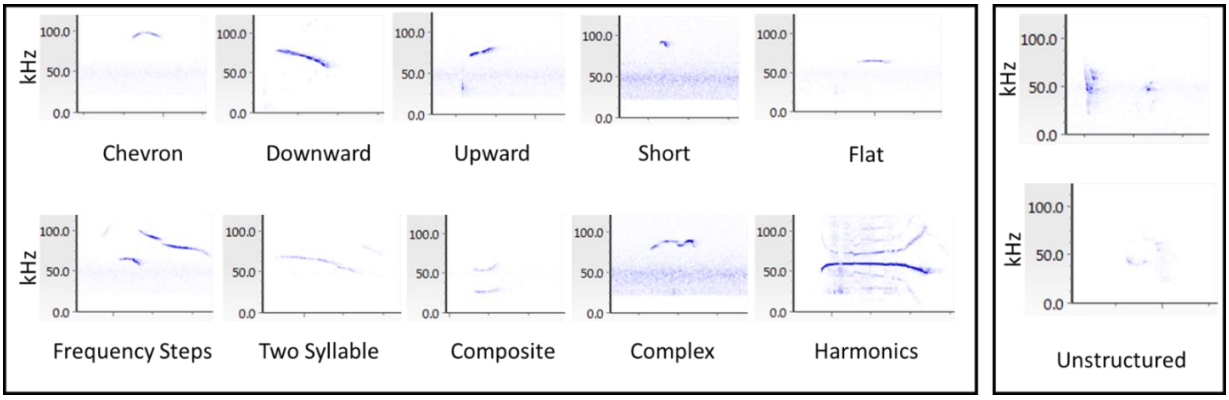

Supplemental Figure 3.3 Pup USV call categories

Representative call patterns of all nine call categories are depicted in supplemental figure 3. In the left panel two examples of unstructured calls emitted by DE exposed pups are provided. All USV calls depicted here were emitted by PND6 pups.

Chapter 4

PRENATAL AND EARLY LIFE DIESEL EXHAUST EXPOSURE DISRUPTS CORTICAL LAMINA ORGANIZATION: EVIDENCE FOR A REELIN-RELATED PATHOGENIC PATHWAY INDUCED BY INTERLEUKIN-6

4.1. Introduction

The escalating prevalence of autism spectrum disorder (ASD) in recent years has prompted research in understanding the role played by environmental risk factors in the etiology of the disease. The most recent prevalence rate for ASD in the United States has been reported to be 1 in 68, indicating a ten-fold increase in the past 40 years (Christensen et al., 2016). Although increasing prevalence may be attributed to broadening of diagnostic definition, the contribution of environmental risk factors cannot be discounted. Indeed, an epidemiological study conducted in California estimated that 26.4% of the increased autism prevalence can be attributed to change in diagnostic practices between 1992 and 2005 (King and Bearman, 2009). However, in support of the significance of environmental contributions to autism etiology, an epidemiological study looking at ASD association in monozygotic and dizygotic twins concluded that environmental components have an even larger effect than genetic components in predicting ASD outcome (Hallmayer et al., 2011).

Of all the environmental risk factors associated with ASD, air pollution exposure is the most ubiquitous, affecting a large number of individuals, especially in densely populated areas in Central America and in South and East Asia (Pandis et al., 2016; van Donkelaar et al., 2014).

High exposure levels of particulate matter (PM >100 μg/m^3) over extended periods have been commonly experienced by populations living in these areas (Brook et al., 2010). Developmental exposure to traffic-related air pollution (TRAP) has been associated with increased ASD risk in many recent epidemiological studies conducted in North America and Europe (Becerra et al., 2013; Suades-González et al., 2015; Talbott et al., 2015; Volk et al., 2011; Volk et al., 2013), as well as in Asia (Jung et al., 2013). Two epidemiological studies conducted as part of the Nurses' Health Study II Cohort indicated that exposure to TRAP during the third trimester resulted in the strongest association of ASD outcome comparing to earlier trimesters (Raz et al., 2015; Volk et al., 2013), while another study found robust association with early-life exposure (Raz et al., 2017). Converging evidence from animal studies (reviewed in Costa et al. 2017) support the hypothesis that TRAP may represent an important contributor to ASD etiology.

PM, a component of diesel exhaust (DE), is known for its ability to cross cellular membranes and cause oxidative damage Our group has previously reported that acute DE exposure in adult mice causes neuroinflammation and oxidative stress (Cole et al., 2016) as well as provided evidence for microglia activation triggered by DEP treatment in a primary culture system (Roqué et al., 2016). Developmental DE exposure in rodents has been shown to increase levels of pro-inflammatory cytokines in placenta, fetal brain and fetal lung (Auten et al., 2012; Bolton et al., 2012; Li et al., 2017b; Weldy et al., 2013). Elevated levels of interleukin-6 (IL-6) and of interleukin-17α (IL-17α) have been shown to be sufficient in eliciting ASD-like behavior in offspring from maternal immune activated (MIA) dams, subjected to lipopolysaccharide or poly (I:C) treatment to mimic bacterial or viral infection during pregnancy (Choi et al., 2016; Samuelsson et al., 2006; Shin Yim et al., 2017; Smith et al., 2007). Binding of IL-6 to its cognate receptor activates the kinase pathway involving Janus kinase 2 (JAK2) and Signal Transducer and Activator of Transcription 3 (STAT3) (Chang et al., 2005; Erta et al., 2012; Hsiao and Patterson, 2011; Tsukada et al., 2015). Activated STAT3 forms homodimers that translocate into the nucleus,

where they bind to DNA and act as transcription factors (Hsiao and Patterson, 2011; Parker-Athill and Tan, 2010; Tsukada et al., 2015). The expression of DNA methyltransferase 1 (DNMT1) has been shown to be modulated by STAT3 (MuhChyi et al., 2013; Zhang et al., 2005). DNMT1 is abundantly expressed in both developing and adult mammalian brains (Inano et al., 2000; Robertson et al., 1999; Veldic et al., 2004), and is responsible for both *de novo* methylation and maintenance of DNA methylation patterns. DNMT1 has been shown to bind directly to, and to exert epigenetic alterations at the reelin (RELN) promoter region (Kundakovic et al., 2009). Indeed, treatment with a DNMT inhibitor results in a dose-dependent increase of reelin expression in an *in vitro* model (Kundakovic et al., 2007). In brains of individuals with other neurodevelopmental disorders (e.g. schizophrenia or bipolar disorder), over-expression of DNMT1 and increased binding of DNMT1 to the RELN promoter have been observed (Dong et al., 2015). Also, in temporal cortex of ASD patients, methylation sequencing of the RELN gene promoter revealed opposite methylation patterns compared to non-ASD individuals (Lintas et al., 2016).

RELN is a secreted extracellular protein that has been known to modulate neuronal migration and dendrite formation during CNS development. In adult mice, RELN has been shown to play a role in synapse formation (D'Arcangelo, 2014; Levenson et al., 2008; Michetti et al., 2014). Several lines of evidence suggest the importance of RELN's role in the pathogenesis of ASD. First, decreased RELN levels have been reported in brains of ASD patients (D'Arcangelo, 2014). Second, mice haploid-deficient in RELN have been shown to exhibit some ASD-related behavioral phenotypes (Michetti et al., 2014). Third, cortical disorganization has been reported in both ASD patients and in RELN-deficient mice (Boyle et al., 2011; Stoner et al., 2014). Fourth, differences in DNA methylation patterns within the RELN promoter were reported in ASD patients (Grayson et al., 2006). Given RELN's involvement in organizing cortical structural architecture (Boyle et al., 2011), we decided to investigate cortical laminar organization in the somatosensory cortex using

the cortical layer-specific markers RELN and calretinin. In the adult cortex, RELN is expressed mostly by Cajal–Retzius cells in cortical layer I and also by some GABAergic interneurons in layers II through VI (Impagnatiello et al., 1998; Pesold et al., 1998). Calretinin is a calcium-binding signaling protein, expressed in a subpopulation of GABAergic interneurons in layers II/III and IV (Gonchar, 2008). A recent study showed that activation of neurons in the S1DZ region of the somatosensory cortex leads to ASD-like behavioral changes in mice (Shin Yim et al., 2017), supporting the idea that structural changes in the somatosensory cortex could be involved in ASD-like behaviors.

We have reported previously that developmental DE exposure caused deficits in all three of the hallmark categories of ASD behavior, i.e. social interaction in the reciprocal interaction and social preference tests, social olfactory and vocal communication, and repetitive behavior (Chang et al. 2018). While other studies have also reported subsets of ASD-like behavior changes, such as repetitive/ impulsive behavior and social deficits upon developmental exposure to air-pollution or PM (Allen et al., 2016; Church et al., 2017; Li et al., 2017; Thirtamara et al., 2013), the environmentally relevant level of DE exposure (250-300 μg/m^3) used in our study appeared to produce a more robust behavioral phenotype (Chang et al. 2018). Given that developmental DE exposure has been shown to cause ASD-like behavioral changes (Thirtamara et al. 2013; Chang et al. 2018), and an increase in neuroinflammation (Bolton et al., 2017; Bolton et al., 2012), in this study we investigated a potential mechanistic pathway which would link DE exposure to a neuroinflammatory response, sequentially leading to dysregulation of RELN expression, resulting in disorganization of cortical lamina.

4.2 Methods

4.2.1. Animals and Exposure

Two month-old male and female C57BL/6J mice were obtained from the Jackson Laboratory (Bar Harbor, ME) and housed in the University of Washington Northlake Diesel Exposure Facility under specific pathogen free conditions on a 12-hour light/dark cycle in an Allentown caging system (Allenton, NJ, USA) supplied with filtered air, and free access to water and food. The overall study design is shown in Fig. 4.1. Following one week of acclimation, each male was paired with two females for timed mating. Evidence of a vaginal plug served as confirmation of successful mating, and mated females were considered to be at embryonic day (E)0 upon identification of vaginal plug and were randomly selected to be individually housed in cages supplied with either diluted DE or filtered air (FA) from gestational day 0 (GD0) to postnatal day 21 (PND21). DE exposure was carried out for six h/day and five days/week at the level of 250-300 $\mu g/m^3$ of PM2.5 concentration, corresponding to a time weighted hourly average of 35.71- 44.64 $\mu g/m^3$. DE was generated on site from a Yanmar YDG5500 diesel generator fueled with standard highway-grade number two diesel fuel obtained from local fuel distributors and operated under load. Generated DE then passed through a two-step dilution system with dynamic control of fine particulate matter (PM2.5), maintaining constant exposure level at 250-300 $\mu g/m^3$. Chemical composition and particle size characterization of the diesel exhaust have been previously described in detail (Fox et al., 2015; Gould et al., 2008). During the exposure period, mice in both groups (DE or FA) were housed in the same room under identical conditions, subjected to the same noise level and light cycle. All animal experiments were consistent with the National Research Council Guide for the Care and Use of Laboratory Animals, as adopted by the National Institutes of Health, and were approved by the University of Washington Institutional Animal Care and Use Committee.

4.2.2. Tissue Collection

Five pregnant dams from each exposure group were euthanized with CO_2 at E16.5. Placenta and matching fetal tails were snap-frozen in liquid nitrogen and stored at -80°C for cytokine evaluation by ELISA and sex genotyping, respectively. At PND3, PND21, and PND60, pups born to DE- and

FA- exposed dams were euthanized by CO_2 narcosis followed by cervical dislocation. At PND3 whole brain samples were rapidly dissected and snap-frozen in liquid nitrogen, then stored at -80 ˚C for quantitative real-time PCR (qRT–PCR) and Western-blot analysis. At PND21 and PND60, the cerebral cortex was rapidly dissected and snap-frozen in liquid nitrogen then stored at -80°C. Additionally, five animals/group/sex were euthanized by CO_2 narcosis followed by cervical dislocation at PND60, and transcardially perfused with 10 ml of phosphate buffered saline (PBS) followed by 10 ml of 4% paraformaldehyde. Brains were then carefully removed from the skull, placed into 4% paraformaldehyde at 4°C overnight for additional fixing, then cryoprotected in 30% sucrose at 4°C until the brains sank to the bottom of the tube. After cryoprotection, brains were hemisected and embedded in Tissue-Tek* CRYO-OCT cutting compound (Fisher Scientific, Pittsburgh, PA) with midline facing the bottom of the standard size Cryomold® (25 x 20 x 5 mm, Sakura Finetek, Netherlands) to ensure a consistent sectioning angle. The embedded brains were stored at -80˚C for later immunohistochemical analysis.

4.2.3. Quantitative Real-time qPCR

Levels of mRNA of IL6, DNMT1, DNMT3a, DNMT3b, DNMT3l, and RELN were measured by qRT-PCR after normalization to the housekeeping gene GAPDH (encoding glyceraldehyde-3-phosphate dehydrogenase) in whole brain samples from DE- or FA- exposed PND3 pups. RELN levels were also measured in cortical samples from PND21 and PND60 mice. RNA was extracted by blending frozen brain samples in TRIzol reagent (Thermo Fisher Scientific, Rockford, IL) with a tissue homogenizer followed by chloroform extraction and washing with 70% ethanol according to standard procedures. RNA was further purified with the GeneJET RNA purification kit (Thermo Fisher Scientific Inc., Rockford, IL) according to the RNA clean-up protocol provided in the kit. Quality and concentration of RNA isolates were confirmed by NanoDrop (Thermo Fisher Scientific

Inc., Rockford, IL) measurements (260/280 ratio >1.8, 260/230 ratio between 2.0 -2.2). Reverse transcription was done using the iScript cDNA Synthesis kit (Biorad; Hercules, CA) with 1 µg of RNA per 20 µl reaction. The iTaq™ Universal SYBR® Green One-Step Kit (Biorad; Hercules, CA was used for signal detection during real-time quantitative PCR on a Bio-Rad CFX384 Real-Time PCR Detection System (Biorad; Hercules, CA) with IL6, DNMT1, DNMT3a, DNMT3b, DNMR3l, RELN, and GAPDH primers adapted from the primer data base (Wanget. al., 2012), as shown in Supplemental Table 1. Relative mRNA expression of target genes was normalized to the housekeeping gene GAPDH, relative expression (ddCq) was calculated according to Haimes & Kelley (2010), and expression in DE exposed animals was compared with control animals of the same sex. GAPDH expression was not affected by DE treatment.

4.2.4. Measurement of IL-6 levels by ELISA

IL-6 protein levels were measured in E16.5 placentas using the MDS V-PLEX Plus ELISA kit (MesoScale Discovery, Gaithersburg, MD, USA). Briefly, tissue was quickly homogenized and sonicated on ice in Cell Lysis buffer (10 mM HEPES; 150 mM NaCl; 1 mM CaCl2; 0.5 mM MgCl2; 10 µg/ml leupeptin; 10 µg/ml aprotinin; 1 mM PMSF; 50 mM NaF) supplemented with complete mini protease inhibitor cocktail tablets (Sigma-Aldrich; St. Louis, MO) according to the manufacturer's directions. Total protein content was measured using the Pierce BCA Protein Assay Kit (Thermo Fisher Scientific, Rockford, IL), and protein concentrations in all samples were adjusted to 10 µg/µl with cell lysis buffer. 25 µl of homogenate of equal protein concentration/well was loaded and run in triplicate according to the manufacturer's instructions. The electro-chemiluminescent signal was visualized using SECTOR S 600 (MesoScale Discovery, Gaithersburg, MD, USA).

4.2.5 Measurement of phosphorylated STAT3 (Tyr705) and total STAT3 by Western Blot

In brief, frozen brain tissue was homogenized on ice in RIPA buffer (10 mM Tris, pH 7.4, 100 mM NaCl, 1 mM EDTA, 1 mM EGTA, 1% Triton X-100, 10% glycerol, 0.1% SDS, 0.5% deoxycholate) supplemented with complete mini protease inhibitor cocktail tablets and PhosSTOP phosphatase inhibitor cocktail tablets (both from Sigma-Aldrich; St. Louis, MO) using a glass Potter-Elvehjem homogenizer. The protein content of each sample was determined using the Pierce BCA Protein Assay Kit (Thermo Fisher Scientific, Rockford, IL). 35 µg of protein were loaded into pre-cast gels (10% Bis-Tris gels) and electro-transferred onto a polyvinylidene difluoride (PVDF) immunoblot membrane (0.45 µm). After transfer, membranes were cut to isolate the 86kDa bands for STAT3 and p-STAT3 from the 43kDa bands for β-actin. The membranes were blocked with 5% (w/v) non-fat milk for 1 h. The top portion of the membranes were incubated with a rabbit anti-Phospho-Stat3 (Tyr705) antibody (1:500; Catalog #9145; Cell Signaling Technology, Danvers, MA) and horseradish peroxidase-conjugated anti-rabbit secondary antibody (1:1000; Catalog No.7074; Cell Signaling Technology, Danvers, MA). The bottom portion of the membranes were incubated with a mouse anti-β-actin antibody (1:1000 ; Catalog No. 554022; BD Pharmingen, San Jose, CA) and a horseradish peroxidase-conjugated anti-mouse polyclonal secondary antibody (1:1000; Catalog No. 554002; BD Biosciences, San Jose, CA). The membranes were developed with a chemiluminescent substrate (ECL kit from Thermo Scientific, Waltham, MA). The top portion of the membranes were stripped with Restore™ Western Blot Stripping Buffer and re-blocked with 5% non-fat milk before incubating with a rabbit anti-Stat3 antibody (1:2000; Catalog #12640 ; Cell Signaling Technology, Danvers, MA) followed by a horseradish peroxidase-conjugated anti-rabbit secondary antibody (1:1000; Catalog #7074; Cell Signaling Technology, Danvers, MA), then were developed as described above. Band intensity was measured by densitometry using ImageJ (provided by the National Institutes of Health), and the intensity of the bands was normalized to β-actin content.

4.2.6 Immunohistochemical Analysis of Cortical Lamina Organization

Brains from PND60 mice embedded in optimum cutting temperature (OCT) compound (Sakura Finetek USA ; Torrance, CA) were cut sagittally at 10-12 µm starting 2000 µm away from midline, and the somatosensory cortex region was sampled at 200µm intervals for five serial sets. The sections were direct-mounted on glass slides and air dried before being stored at -80°C. Immunohistochemistry was performed as previously described (Englund et al., 2005). The following primary antibodies were utilized at the indicated dilutions: mouse anti-RELN (1:1000; EMD Millipore, MAB5364); rabbit anti-Calretinin (1:2000; Swant, CR 7697); Alexa Fluor 488-conjugated or 568-conjugated goat anti-mouse or rabbit IgG (Thermo Fisher Scientific, 1:600). The nuclear counterstain DAPI (4',6-diamidino-2-phenylindole) (Sigma, St. Louis, MO) was used to label DNA following the manufacturer's instructions, after incubation with primary and secondary antibodies. Brains from five animals in each experimental group were processed and analyzed, and 3-5 sections/brain were collected. Digital immunofluorescence images were obtained on a Zeiss Axio Imager Z1. In each image, the cortical depth (distance between ventricle and pia mater), was divided into 10 evenly-spaced bins, with bin 1 positioned nearest to the pia mater. Fluorescent-labeled cells were counted in each of the 10 bins and the area of each bin was measured using Adobe Photoshop, with the researcher blinded to the experimental groups. Cell density in each bin was calculated by dividing the total area of the bin by the total number of cells.

4.2.7 Statistical analyses

Statistical analyses were performed using GraphPad Prism 6 (GraphPad Software, Inc.; San Diego, CA, USA). Differences in IL-6 levels in placenta between DE- and FA- exposed groups were determined by Student's T- Test. mRNA levels of gene of interest (IL-6, DNMTs, reelin) and STAT3-phosphorylation measured in PND3 were analyzed by two-way ANOVA followed by Bonferroni post hoc comparison to test the effect of exposure and potential sex differences. For

immunohistochemistry, the two-tailed Student's T- Test was used to assess differences in cell density between FA and DE brains of the same sex in each bin.

4.3. Results

4.3.1 Developmental DE exposure increases IL-6 expression

Elevated levels of the pro-inflammatory cytokine IL-6 were found in neonatal (PND3) pup brains and in placentas (E16.5) from mice exposed to DE. Neonatal brains from DE-exposed PND3 pups of both sexes showed significantly increased levels of IL-6 mRNA compared to FA-exposed mice of the same sex and age (Fig. 4.2A), when normalized to the housekeeping gene GAPDH ($p<0.05$; two-way ANOVA with Bonferroni posttest). There were no differences in GAPDH expression between DE- and FA-exposed animals (not shown). In E16.5 placenta IL-6 protein levels, measured by ELISA, were significantly increased by DE exposure (Fig. 4.2B) ($p<0.05$; two tailed T-test with Welch's correction).

4.3.2 Developmental DE exposure activates STAT3 through phosphorylation at Tyr705

STAT3 and phospho-STAT3 (Tyr705) were measured by Western blot analysis in whole brain lysates from PND3 pups to assess the extent of STAT3 activation. After normalizing to β-actin, phospho-STAT3 (Tyr705) immuno-blotting revealed increased band intensity for phospho-STAT3 in DE- exposed mice compared to FA control animals of the same sex (Fig. 4.3A), while no differences were found in total STAT3 levels (Fig 4.3B). This finding indicates increased STAT3 activation by phosphorylation at residue Tyr705 at PND3, during the early postnatal period of developmental DE- exposure.

4.3.3 Developmental DE exposure is associated with increased DNMT1 expression

To assess the expression of DNMTs [known to be modulated by STAT3 (Huang et al., 2016; Zhang et al., 2005)], qPCR analysis was conducted with RNA samples isolated from PND3 whole

brains. Relative expression of the target genes DNMT1, DNMT3a, DNMT3b, DNMT3l were normalized to the housekeeping gene GAPDH. Expression of DNMT1 increased significantly in brains of DE- exposed mice (Fig. 4.4A). Other DNMTs, i.e. DNMT3a, DNMT 3b, DNMT 3l, also showed trends of increasing expression due to DE exposure when compared to same-sex control animals, but of these three, only DNMT3b expression levels in males showed a statistically significant increase (Fig. 4.4C). There were no differences in GAPDH expression between DE- and FA-exposed animals (not shown).

4.3.4 Developmental DE exposure is associated with long-lasting decreased RELN expression in brain

Since DNMT1 has been shown to down-regulate RELN expression (Kundakovic et al., 2009; Noh et al., 2005), the increased DNMT1 expression in DE-exposed mice may decrease levels of RELN mRNA. At PND3, a significant decrease in RELN mRNA levels was found in whole brain samples of DE-exposed mice compared to same-sex control mice (Fig. 4.5A). Similarly, in cerebral cortex of PND21 (Fig. 4.5B) and PND60 (Fig. 4.5C) mice, RELN mRNA levels showed a decreasing trend with DE exposure, which was statistically significant in PND60 males (Fig. 4.5C).

4.3.5. Developmental DE exposure is associated with disorganization of cortical lamina

RELN is known as a critical player in guiding the process of neuronal migration during cortical development (D'Arcangelo, 2014; Franco et al., 2011; Jossin & Cooper, 2011; Reiner et al., 2015), and disrupted cortical organization has been reported in RELN deficient "reeler" mice (Boyle et al., 2011). Immunohistochemical analysis was performed with the lamina-specific markers RELN and calretinin to examine cortical organization in PND60 brains of mice exposed to either DE or FA during development. Significant differences were seen in the cortical distribution of both RELN- and calretinitin-positive cells. The distribution of RELN-positive cells revealed ectopic

clusters of cells in deeper layers of the cortex in both DE- exposed males (clusters located in bin 4, 6, 7 and 8; Fig. 4.6C) and females (clusters located in bin 5, 6, 7, and 9; Fig. 4.6D), with the cell clusters located outside of the marker's normal destined distribution, as seen in FA control animals of the same sex (e.g., for males, compare Fig. 4.6A,B). When comparing cell density in all sampled areas (all 10 bins combined) no significant difference in RELN+ cell density was found between DE- and FA- exposed mice, indicating that the average density of RELN+ cells across all cortical layers was not affected by DE exposure.

The distribution of calretinin-positive cells in DE-exposed mice also showed higher cell density clusters in deeper layers of cortex in both DE- exposed males (clusters located in bin 5 and 7; Fig. 4.7C) and females (clusters located in bin 7 and 9; Fig 4.7D), as compared to FA control animals of the same sex. Again, when comparing cell density across all sampled areas (all 10 bins combined) no significant difference in calretinin+ cell density was found between DE- and FA-exposed mice. Thus, immunohistochemistry analysis revealed statistically-significant cortical disorganization in DE- exposed males and females, with both markers presenting clusters of cells in deeper layers within the somatosensory cortex, suggesting neurons were under-migrated during corticogenesis in the DE-exposed mice.

4.4 Discussion

Positive associations between developmental TRAP exposure and increased risk for ASD have been reported by several epidemiological studies (Becerra et al., 2013; Suades-González et al., 2015; Talbott et al., 2015; Volk et al., 2011; Volk et al., 2013). Various animal studies have also reported ASD-like behavioral changes due to air-pollution exposure during development (Church et al., 2017; Li et al., 2017; Thirtamara et al., 2013; Chang et al., 2018). We have previously found that developmental exposure to DE (from GD0 to PND21) causes behavioral changes in all three characteristic domains of ASD, i.e. an increase in repetitive behavior, disrupted verbal and olfactory communication, and social behavior deficits (Chang et al., 2018). However, possible

mechanisms underlying the developmental effects of air pollution and their potential roles in ASD are still unknown. Exposure to ambient ultra-fine particles (UFP) has been reported to induce inflammation and microglial activation leading to ventriculomegaly and excitatory/inhibitory imbalance (Allen et al., 2016). Prenatal DE exposure has been shown to cause toll-like receptor 4-dependent microglial activation, as well as astrocyte activation in mice (Bolton et al., 2017; Li et al., 2017). In the present study, we hypothesized a possible pathway that may lead from neuroinflammation to cortical laminar disorganization, a morphological alteration observed in brains of autistic patients as well as in the MIA mouse model of autism (Choi et al., 2016; Stoner et al., 2014).

The proposed pathway (Fig. 4.8) supported by our data involves DE exposure inducing an inflammatory response and increasing IL-6 levels (Allen et al., 2016; Bolton et al., 2017; Li et al., 2017), leading to activation of the JAK2/ STAT3 pathway and upregulation of DNMT1 (Hsiao and Patterson, 2011; Parker-Athill and Tan, 2010; Tsukada et al., 2015). Since increased levels of DNMT1 have been shown to promote DNA methylation, causing downregulation of RELN expression (Kundakovic et al., 2007; Kundakovic et al., 2009), we hypothesized that RELN expression would be reduced, and this in turn would cause disruption of the process of neuronal migration leading to long-lasting cortical laminar disorganization (Boyle et al., 2011). This mechanistic hypothesis was tested systematically in the present study. As expected, we observed an increase of IL-6 protein levels in E16.5 placenta (Fig 4.2B), and of IL-6 mRNA expression in PND3 neonatal whole brain (Fig 4.2A). Other studies have also reported increased levels of IL-6 in placenta and fetal brain caused by developmental DE exposure in mice (Auten et al., 2012; Bolton et al., 2012; Fujimoto et al., 2005), although the latter studies utilized higher concentration of DE particles. A recent study reported significant up-regulation of IL-17α in serum and in mononuclear cells isolated from placenta after induction of inflammatory response with Poly (I:C) injection (a MIA model) (Choi et al. 2016). The same study also showed that the increase in IL-

17α was IL-6 dependent, as IL-6 is a key factor for TH17 cell differentiation (Choi et al., 2016). We attempted measuring protein levels of IL-17α in E16.5 placenta samples by ELISA, but the results were inconclusive, as most samples were under the detection limit (data not shown). Since IL-17α is produced by a small population of differentiated TH17 cell, in future studies measuring expression levels of IL-17 α receptor subunit A (IL-17Ra) may be a more robust and reliable approach in characterizing the inflammatory response associated with ASD-like behavioral phenotypes.

In agreement with our hypothesis, we found that developmental DE exposure induced STAT3 activation as evidenced by the increased levels of phosphorylation at residue tyrosine 705, a phosphorylation site known to be activated by JAK2 (Chang et al., 2005), while levels of total STAT3 were unaffected (Fig. 4.3A, 4.3B). Downstream of JAK2/STAT3 we found upregulation of DNMT1 (Fig. 4.4A), which is known to be modulated by STAT3 (MuhChyi et al., 2013; Zhang et al., 2005). We also found significant increases of DNMT3b expression in DE-exposed males (Fig. 4.4C), and non-significant trends of increased expression levels of other DNMTs (4a, 4l) in response to DE exposure. Increased expression of DNMT1 has been reported in lungs of C57BL/6 mice exposed to concentrated ambient PM2.5 at a level of $5.5X10^5$ particle/ cm^2 (Soberanes et al., 2012). In mice prenatally exposed to 73.61 $\mu g/m^3$ of ambient PM2.5 for 5 h/day, increased expression of DNMT1, DNMT3a, and DNMT3b were detected in adult heart samples (Tanwar et al., 2017). The finding of an increased expression of DNMT1 in the brain suggested potential alterations of DNA methylation in DE-exposed neonatal pups. In particular, DNMT1 has been shown to modulate the expression of RELN, an important neurodevelopmental signaling molecule, by directly binding and modifying DNA methylation status at the RELN promoter region (Kundakovic et al., 2007; MuhChyi et al., 2013; Zhang et al., 2005). As expected, RELN mRNA levels in brains of PND3 pups were significantly decreased upon developmental DE exposure (Fig. 4.5A). Since epigenetic modifications often result in long-lasting effects on gene expression,

we also measured RELN mRNA levels at two later ages (PND21 and PND60) and found that decreased RELN expression was sustained into adulthood (Fig. 4.5C). Decreased RELN expression (D'Arcangelo, 2014) and differential DNA methylation patterns within the RELN promoter (Grayson et al., 2006) have both been found in ASD patients compared to control individuals.

To investigate whether developmental DE exposure may induce structural abnormalities in the cerebral cortex as observed in ASD (Stoner et al., 2014a), we carried out an immunohistochemical analysis of cortical laminar organization in somatosensory cortex of PND60 mice. Specifically, we determined the distribution of cells expressing cortical lamina-specific markers RELN and calretinin in different cortical layers. Structural abnormalities in the S1DZ region of the somatosensory cortex have been found to play an important role in modulating autism-like behavior (Shin Yim et al., 2017). In cerebral cortex of control mice, RELN is mostly localized in layer I and more sparsely in layers II through VI (Impagnatiello et al., 1998; Pesold et al., 1998). We found a larger proportion of RELN positive cells concentrated within layers IV and V in brains of both male and female mice developmentally exposed to DE, while the total number of RELN+ cells in FA- or DE- exposed animals was not statistically different. In contrast, calretinin is typically expressed in GABAergic interneurons localizing in layers II/III and IV (Gonchar, 2008), and this was confirmed by our findings in cerebral cortex of FA-exposed mice (Fig. 4.7). Developmental DE exposure caused changes in the distribution of calretinin-positive cells, which were localized in layers V and VI at significantly higher cell density compared to control mice of the same sex (Fig. 4.7). Although the level of cortical disorganization found in DE- exposed mice is mild compared to findings in mouse models of ASD (Boyle et al., 2011; Choi et al., 2016), our results parallel reports of small patches of disorganization found in prefrontal cortex of adolescent ASD patients (Stoner et al., 2014b). Considering that disruption of developmental events elicited

by a pervasive environmental toxicant such as air pollution would have long-lasting effects in organizational structure of the brain, the public health implication suggested by our finding is rather striking. Two possible scenarios can be considered that could result in dislocalized RELN+ and calretinin+ cells: disruption in neuronal migration, and/ or disruption in the fate of neuronal differentiation. Further histological assessment with markers involving neurogenesis and differentiation (e.g. PAX6, Tbr2, and Tbr1) (Englund et al., 2005; Mihalas and Hevner, 2017) would be helpful to distinguish between the two possibilities.

The association between air pollution and increased ASD risk has been reported by many epidemiological studies and by a number of animal studies, yet mechanistic studies supporting these findings are just starting to emerge. We have found that developmental exposure to DE elicited neuroinflammation, triggering JAK2/ STAT3 pathway activation, resulting in decreased expression of RELN which leads to long-term changes in cortical lamina organization. The biochemical and histological changes observed in developmentally DE exposed mice parallel findings in ASD patients. Future studies are much warranted not only to gain further understanding in how gene-environment interaction modulates ASD, to improve protection for vulnerable populations, and for exploring other potential mechanisms.

4.5 Figures

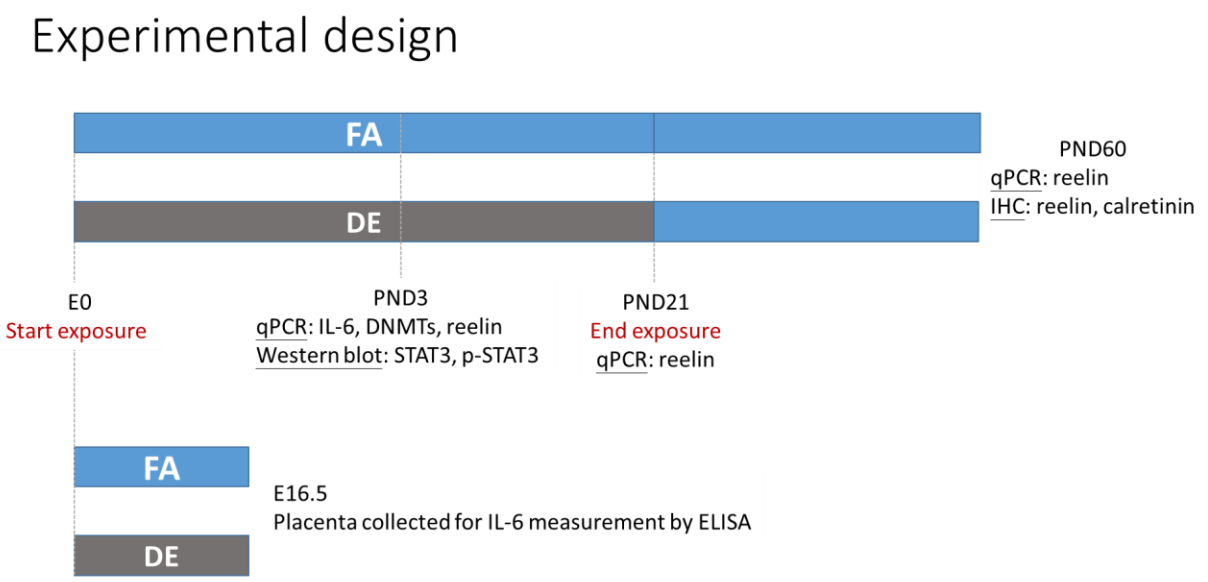

Fig. 4.1 Experimental design for mechanistic study

Exposure started at the beginning of pregnancy upon confirmation of copulation plug (E0) and ended at weaning (PND21). Exposure to DE was conducted for 6 h/day, 5 days/week at the level of 250 to 300 μg/m^3 in PM concentration. At E16.5 a subset of pregnant dams exposed to either DE or FA were sacrificed, and placenta were collected for evaluation of inflammatory cytokine IL-6 levels by ELISA. At PND3, brains were collected for qPCR and Western blot assays. At PND21 cortical samples were collected for qPCR, and at PND60 cortical samples were collected for qPCR and perfusion-fixed cryo-protected brains were collected for immunohistochemistry.

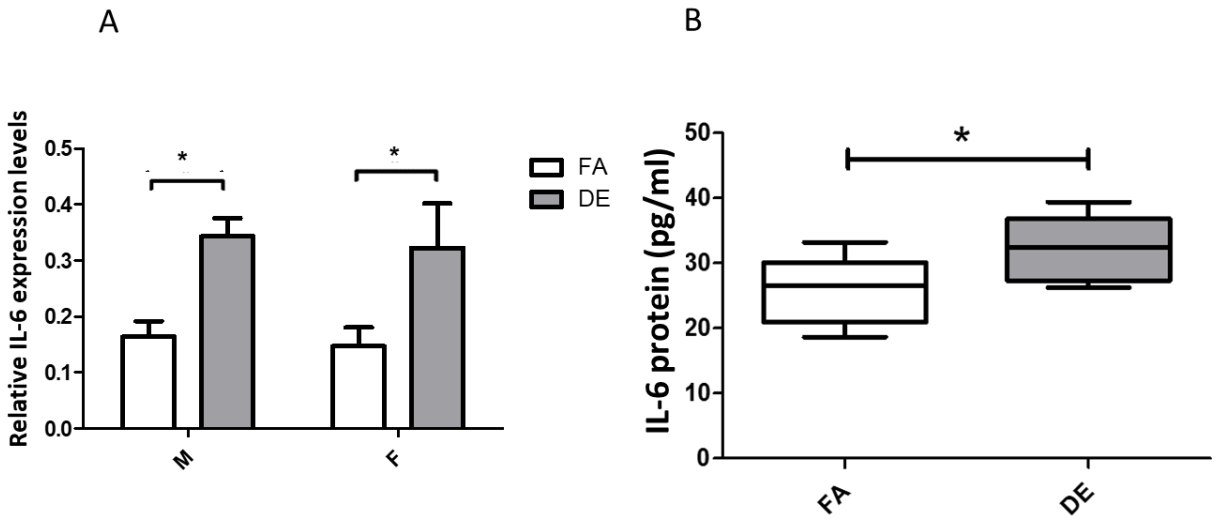

Fig. 4.2 Developmental DE exposure increases IL-6 expression

(A) IL-6 mRNA levels in whole brain lysate from PND3 pups exposed to filtered air (FA) or diesel exhaust (DE) from GD0 to PND3. After normalizing to the house keeping gene GAPDH, significantly increased IL-6 expression levels, plotted as mean (± SE), were found in DE-exposed males and females compared to FA controls of the same sex. (*$p<0.05$; two-way ANOVA with Bonferroni posttest; n=5). (B) IL-6 protein levels in E16.5 placenta were measured by enzyme-linked immunosorbent assay (ELISA). Increased IL-6 protein levels, plotted as mean (± SE), were found in E16.5 placenta from dams exposed to DE compared to control dams (*$p<0.05$; two tailed T-test with Welch's correction; n=10).

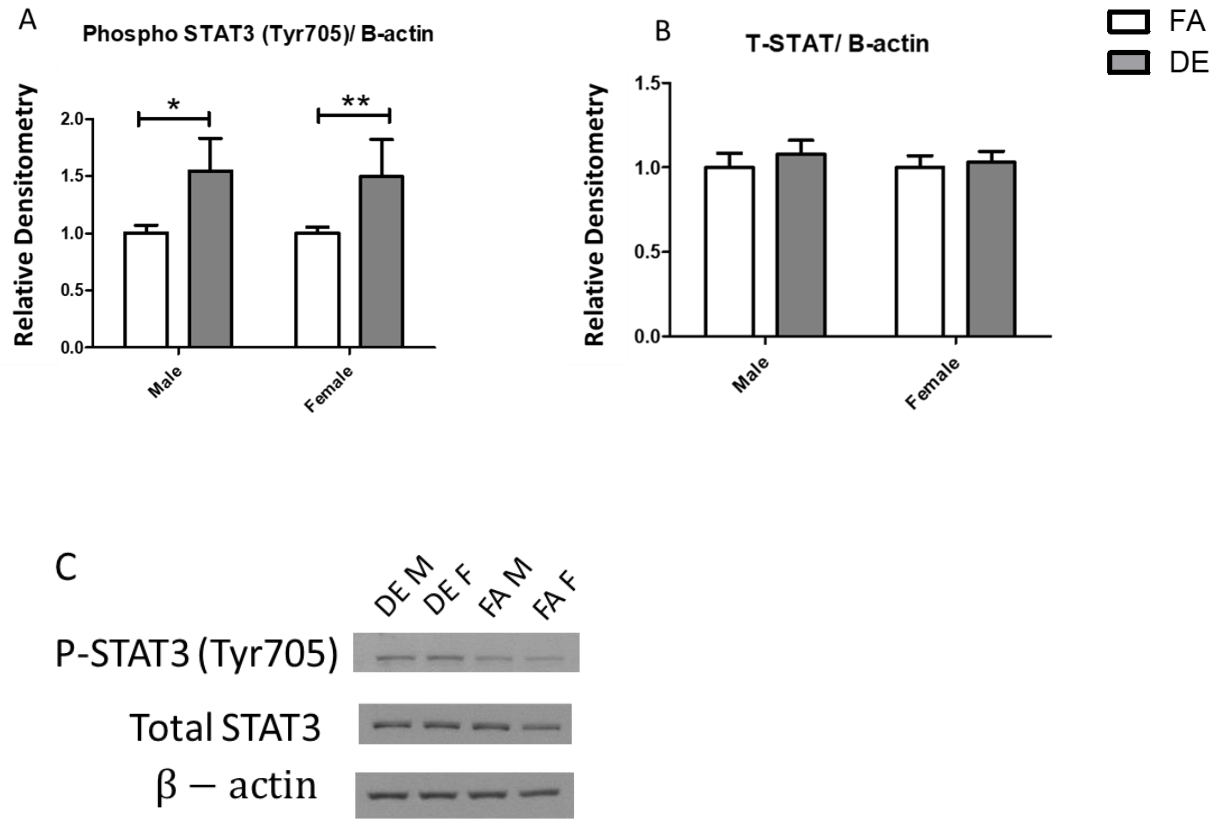

Fig. 4.3 STAT3 phosphorylation in brains from PND3 mice.

STAT3 phosphorylation at residue tyrosine 705 (Tyr705) was measured by Western blot in whole brain lysate from PND3 mice. Increased levels of phosphorylated STAT3 (Tyr705) were found in DE-exposed males and females compared to FA-exposed controls of the same sex (A). There were no differences in total STAT3 protein levels associated with DE exposure (B). Both phosphorylated STAT3 (Tyr705) and total STAT3 levels were normalized to the loading control beta-actin. Results represent the mean (± SE) of 5 pups from different litters for each experimental group (*$p<0.05$, **$p<0.01$; two-way ANOVA with Bonferroni posttest; n=5). (C) Representative Western blot image.

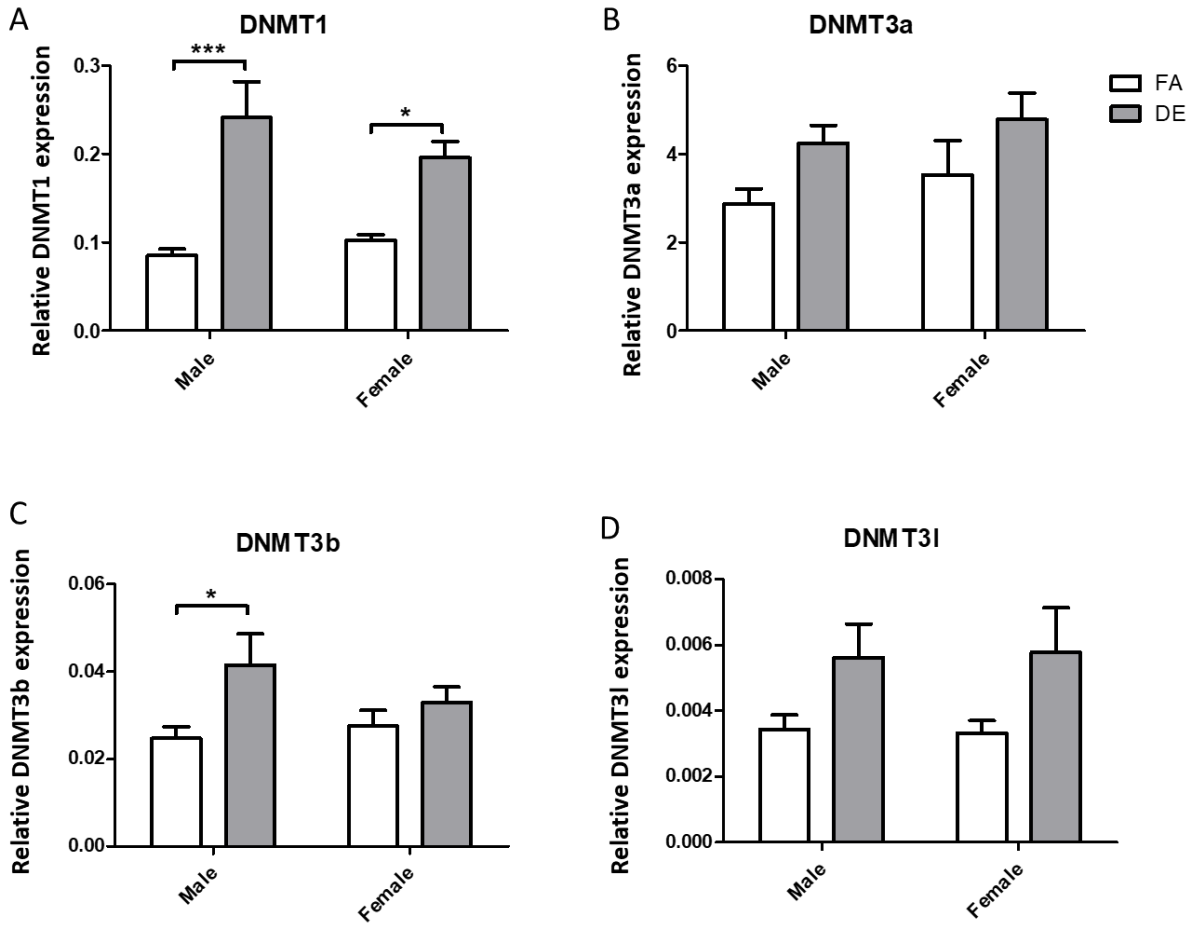

Fig. 4.4 mRNA expression of DNMTs in brains of PND3 mice

mRNA Levels of DNMTs (1, 3a, 3b, 3l) were measured in brains of male and female PND3 mice exposed to FA or DE. Expression of DNMT1 increased in DE-exposed males and females compared to FA-exposed control mice of the same sex (A). Expression levels of other DNMTs (3a, 3b,3l) did not show statistically significant differences between treatments, except for DNMT3b expression in DE-exposed males (B, C, D). Relative mRNA expression of DNMTs were normalized to the house keeping gene GAPDH. Results represent the mean (± SE) of five pups from different litters for each experimental group (*$p<0.05$, ***$p<0.001$, two-way ANOVA with Bonferroni posttest).

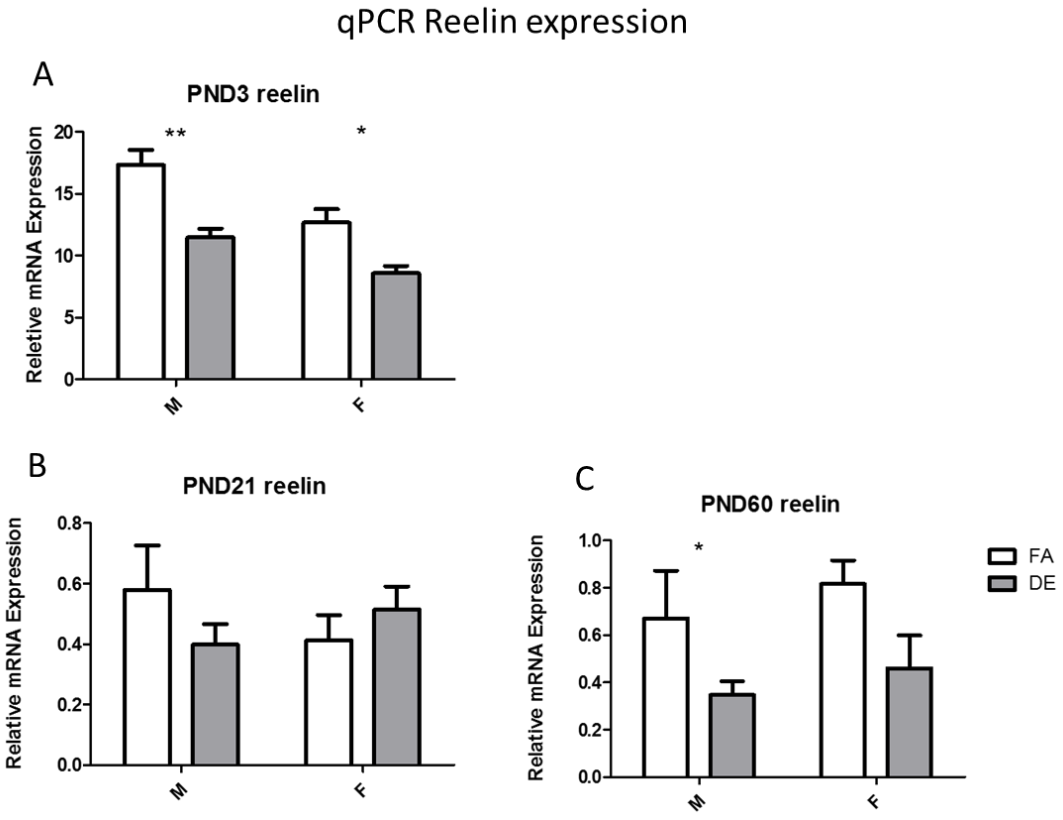

Fig. 4.5 Developmental DE exposure decreases RELN expression in brain

Reelin mRNA levels in brain were measured at three developmental time points (PND3, PND21, and PND60). (A) At PND3 expression of RELN in whole brain samples were significantly lower in DE-exposed mice of both sexes compared to FA control mice of the same sex. (B) RELN expression in the cerebral cortex of PND21 mice showed no significant change due to DE exposure in either male and female mice. (C) RELN expression in cerebral cortex of PND60 mice was significantly decreased in DE-exposed male mice. DE exposed females also showed a trend towards decreased RELN expression, but the difference was not statistically significant. RELN expression levels were normalized to the house keeping gene GAPDH. Results represent the mean (± SE) of 4-5 pups from different litters for each experimental group (*$p<0.05$, **$p<0.001$; two-way ANOVA with Bonferroni post-test).

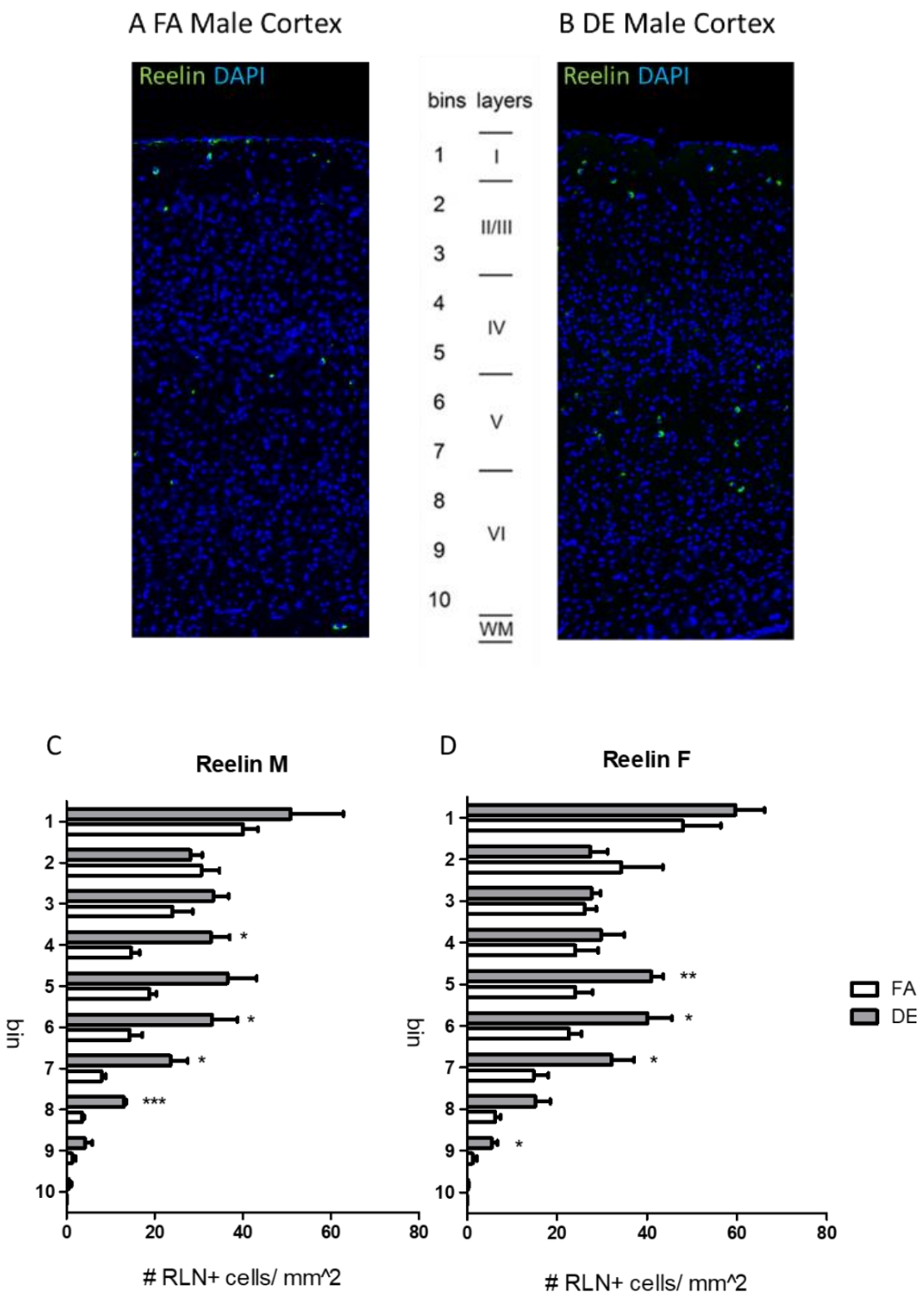

Fig. 4.6 RELN positive cells in somatosensory cortex of PND60 mice.

In cortex of control mice, RELN is mostly localized in layer I and more sparsely in layers II through VI (Impagnatiello et al., 1998; Pesold et al., 1998). (A, B) Representative image of RELN+ cells (green) with nuclei counterstain DAPI (blue) from FA- and DE- exposed males. Distribution of RELN-positive cells revealed ectopic clusters in deeper layers of cortex; in males increased RELN+ cell density was found in bins 4, 6, 7, and 8 (C), and in females RELN+ cell density increased in bins 5, 6, 7, and 9 as a consequence of DE-exposure (D). No significant difference was found in the total number of RELN+ cells per sampled area due to DE exposure. Results represent the mean (± SE) of 5 mice from different litters for each experimental group; 3-5 sections/ mouse were examined (*$p<0.05$, **$p<0.01$, ***$p<0.001$; unpaired T-test with Welch's correction)

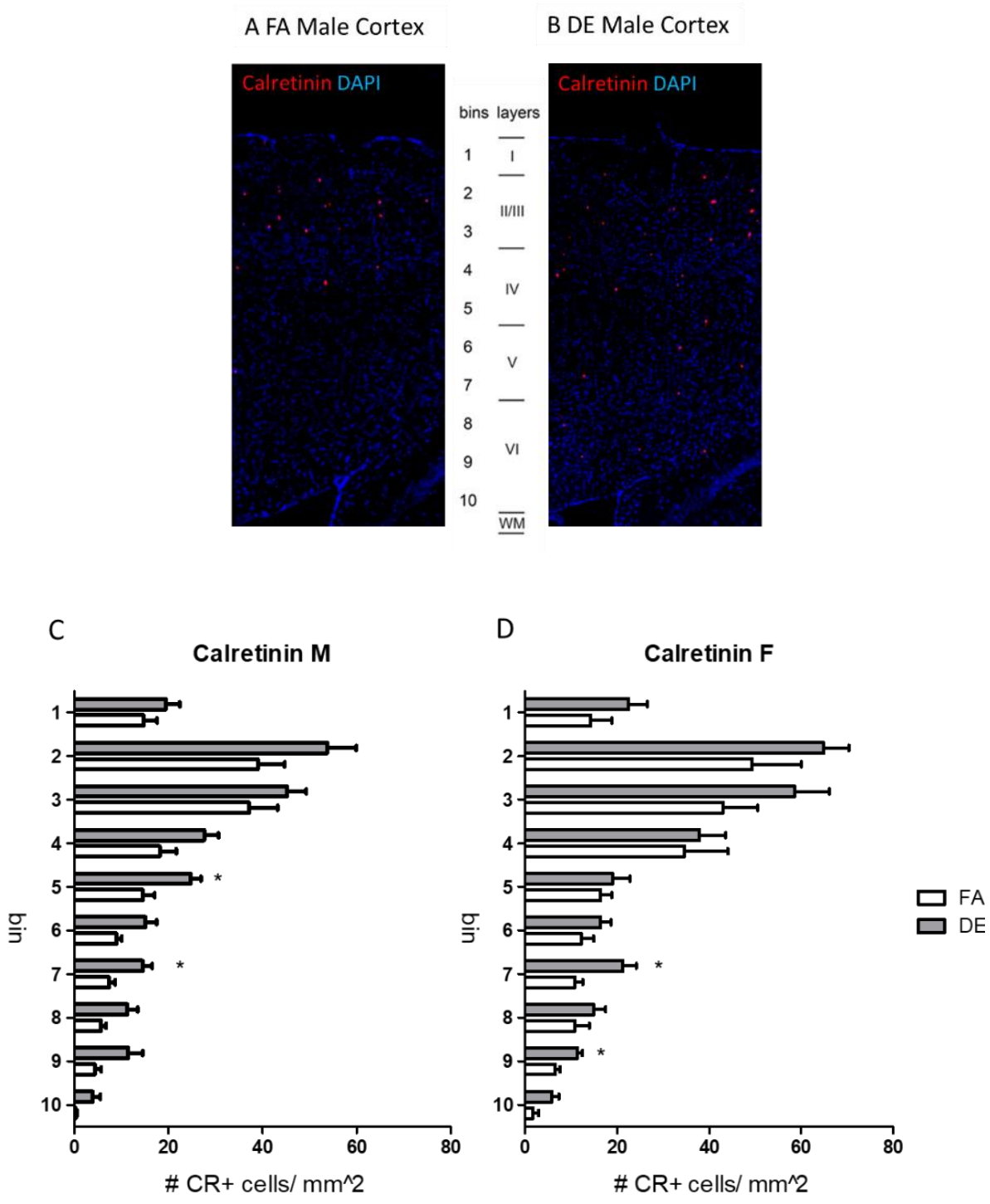

Fig. 4.7 Calretinin positive cells in somatosensory cortex of PND60 mice.

In cortex of control mice, calretinin is typically expressed in GABAergic interneurons localizing in layers II/III and IV (Gonchar, 2008). (A, B) Representative image of calretinin+ cells (red) with nuclei counterstain DAPI (blue) from FA- and DE- exposed males. Distribution of calretinin+ cells revealed ectopic clusters in deeper layers of cortex; in males increased calretinin+ cell density was found with DE exposure in bins 5 and 7 (C) and in females calretinin+ cells formed ectopic clusters in bins 7 and 9 due to DE exposure (D). No significant difference was found in number of calretinin+ cells per sampled area due to DE exposure. Results represent the mean (± SE) of 5 mice from different litters for each experimental group; 3-5 sections/ mouse were examined (*$p<0.05$; unpaired T-test with Welch's correction).

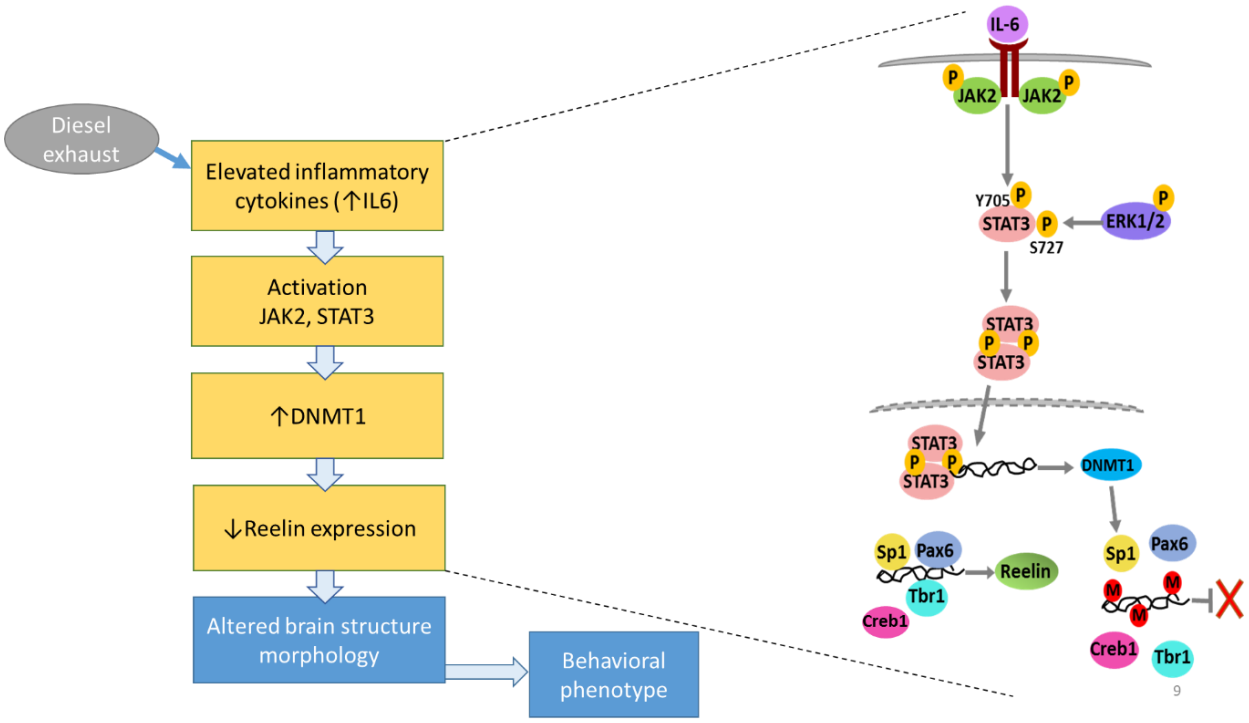

Figure 4.8 Proposed mechanism for developmental DE exposure-induced cortical disruption.

Developmental exposure to DE causes neuroinflammation, evidenced by elevated levels of IL-6. This in turn leads to activation of the JAK2/STAT3 pathway; activated STAT3 acts as a transcription factor and up-regulates DNMT1 expression, which modulates RELN expression via DNA methylation. Known for its critical role in guiding the process of neuronal migration during development, decreased expression of RELN during critical developmental periods would lead to altered cortical structure as observed in ASD (Stoner et al., 2014b). Of note is that with the same period and level of developmental DE exposure we previously found significant alterations in all three characteristic behavioral domains of ASD (communication, repetitive behavior, social interactions) (Chang et al. 2018).

4.6 Appendix

Supplemental Table 4.1 Sequences of primers for qRT-PCR

	Forward Primer Sequence (5' -> 3')	Reverse primer Sequence (5' -> 3')
IL-6	TAGTCCTTCCTACCCCAATTTCC	TTGGTCCTTAGCCACTCCTTC
DNMT1	AAGAATGGTGTTGTCTACCGAC	CATCCAGGTTGCTCCCCTTG
DNMT3a	GGCCGAATTGTGTCTTGGTG	CCATCTCCGAACCACATGAC
DNMT3b	CTGTCCGAACCCGACATAGC	CCGGAAACTCCACAGGGTA
DNMT3l	CACCCCTTGTTTGAGGGAGG	ATGGTGCAGTAACTCTGGTGT
RELN	TTACTCGCACCTTGCTGAAAT	CAGTTGCTGGTAGGAGTCAAAG
GAPDH	TGACCTCAACTACATGGTCTACA	CTTCCCATTCTCGGCCTTG

Sequences of primer sets used in the present study are shown; both forward and reverse primers are listed from 5’ to 3’.

Chapter 5

DEVELOPMENTAL DIESEL EXHAUST EXPOSURE DISRUPTS PAX6 CONTROLLED BALANCE BETWEEN NEUROGENESIS AND PROGENITOR CELL SELF-RENEWAL

5.1. Introduction

Exposure to traffic-related air pollution (TRAP) has been associated with neurodevelopmental diseases such as autism spectrum disorder (ASD), attention-deficit/hyperactivity disorder, and obsessive-compulsive disorder(Becerra et al., 2013; Costa, et al., 2017; Fuertes et al., 2016; Min & Min, 2017; Suades-González et al., 2015; Volk et al, 2011, 2013), as well as neurodegenerative diseases such as Alzheimer's disease (AD) and Parkinson's disease (PD) (Block & Calderón-Garcidueñas, 2009; Calderón-Garcidueñas et al., 2015; Costa et al., 2014, 2015, 2017; Guxens et al., 2014; Tanner et al., 2014) in many human studies. We have previously reported autism-like behavioral changes and cortical lamina disorganization, a structural phenotype found in brains of children with ASD (Stoner et al., 2014a), in mice developmentally exposed to diesel exhaust (DE)(Chang et al., 2018a; Chang et al.,2018b). Other animal studies also reported behavioral effects in repetitive/ impulsive behavior and social deficits (Allen et al., 2016; Church et al., 2017; Li et al., 2017; Thirtamara et al., 2013) as well as increased neuroinflammation coupled with activation of microglia via toll-like receptor 4 activation (Bolton et al., 2017; Bolton et al., 2012) caused by developmental exposure to air pollution. In adult mice, we have also reported that acute DE exposure causes neuroinflammation and oxidative stress (Cole et al., 2016) as well as providing evidence for microglia activation triggered by DEP treatment in a primary culture system (Roqué et al., 2016). These results are in agreement with studies conducted by other researchers linking air pollution exposure and neuroinflammation to neurodevelopmental diseases (Block and

Calderón-Garcidueñas, 2009; Calderón-Garcidueñas et al., 2013a; Lee et al., 2016; Liu et al., 2015).

In addition, perinatal exposure to air pollution has been associated with AD and PD in epidemiological studies (Calderón-Garcidueñas et al., 2013, 2015, 2016). In mice prenatally exposed to DE, differential DNA methylation was reported in promoter regions of genes involved in neuronal differentiation and neurogenesis pathways (Tachibana et al., 2015). Previously, wereported decreased levels of adult neurogenesis in the dentate gyrus (DG) of mice acutely exposed to DE (Coburn et al., 2018). Impaired adult neurogenesis, especially in the hippocampal region, has been suggested to contribute to risk of AD (Abrous et al., 2005; Fuster-Matanzo et al., 2012; Kent & Mistlberger, 2017; Maruszak et al., 2014; Toda & Gage, 2017; Zheng et al., 2016). Adult neural progenitor cells (NPCs) have been identified to be derived from a slowly dividing subpopulation of embryonic NPCs, while the fast dividing NPCs are responsible for the peak of neurogenesis during CNS development (Furutachi et al., 2015; Singh & Solecki, 2015). These findings suggest that disrupted balance between self-renewal and differentiation of NSCs due to developmental exposure to environmental toxicants could affect progression of both neurodevelopmental and neurodegenerative disorders.

Paired box 6 (PAX6), T-box brain 2 (Tbr2 also known as eomes), and T-box brain 1 (Tbr1) are expressed sequentially by radial glia, intermediate progenitor cells, and postmitotic neurons, respectively, during CNS development (Englund et al., 2005). In adult neurogenesis, similar progenitor cell types and temporal expression of the PAX6 Tbr2 and Tbr1 cascade are also observed in both subventricular zone (SVZ) and subgranular zone (SGZ)(Brill et al., 2009; Hodge et al., 2008; Roybon et al., 2009a,b). PAX6 has been shown to play an essential role in controlling the balance between neural stem cell self-renewal and neurogenesis in both *in vivo* and *in vitro* models (Gan et al., 2014; Sansom et al., 2009). In PAX77 mice, a transgenic mouse strain over-expressing PAX6, Tbr2 and Tbr1, expression of these genes was found to be positively regulated

in fetal brain, and over-production of Tbr2-positive cells was observed at E12.5 followed by microcephaly at E14.5 (Sansom et al., 2009). These findings indicated that over-expression of PAX6 in a transgenic model leads to increased neurogenesis which compromises progenitor cell self-renewal potential early in development. Additionally, Tbr2 has been reported to play an essential role in regulating laminar fate during cortical genesis (Mihalas et al., 2016). In the present study we investigated the effects of developmental DE exposure on the PAX6/ Tbr2/ Tbr1 neurogenic pathway and assessed potential consequences in cortical lamina organization and adult neurogenesis.

5.2. Material/ Method

5.2.1 Animals and Exposure

Nine-week old male and female C57BL/6J mice were obtained from the Jackson Laboratory (Bar Harbor, ME) and housed in the University of Washington Northlake Diesel Exposure Facility under specific pathogen-free conditions, on a 12-hour light/dark cycle in an Allenton caging system (Allenton, NJ, USA) connected to filtered air supply with unrestricted access to food and water. Following one week of acclimation period, each male was time-mated with two females overnight, and evidence of a vaginal plug, confirmation of successful mating, was checked the next morning before 8:30 am. Females with identified vaginal plug were then considered to be at embryonic day (E0). The plug-positive females were randomly assigned to be housed individually in cage racks designated for either diesel exhaust (DE) or filtered air (FA) exposure. Animals were housed individually in these cages throughout the entire duration of pregnancy and during the pre-weaning period of their pups (E0- Postnatal day PND21). Mice housed in DE rack were exposed for 6 hours a day and five days per week (Monday through Friday) at the level of 250-300 $\mu g/m^3$ of PM2.5 concentration, equivalent to a time weighted hourly average of 35.71-44.64 $\mu g/m^3$.

Between each day's exposure mice housed in DE rack were supplied with FA. Mice housed in the FA rack were supplied with FA at all times. In order to keep exposure schedule consistent on the same developmental days in different cohorts, mating pairs were always set-up on Sundays to allow first day of exposure to fall on E0.

DE was generated on site from a Yanmar YDG5500 diesel generator fueled with standard highway-grade number 2 diesel fuel obtained from local fuel distributors and operated under load. Generated DE passed through a two-step dilution system with dynamic control of fine particulate matter (PM2.5), maintaining constant exposure levels at 250-300 $\mu g/m^3$. Chemical composition and particle size characterization of the DE have been previously described in detail (Fox et al., 2014; Gould et al., 2008; Weldy et al., 2013). During the exposure period, mice in both exposure groups were housed in the same room under identical conditions, subjected to the same noise level and light cycle. All animal experiments were approved by the University of Washington Institutional Animal Care and Use Committee.

5.2.2 Tissue Collection

At PND3, pups born to DE- and FA- exposed dams were euthanized by decapitation and whole brains were rapidly removed and snap-frozen in liquid nitrogen then stored at -80°C for later quantitative real-time PCR (qRT–PCR) analysis. At PND60, mice were euthanized with CO2 narcosis followed by cervical dislocation, and transcardially perfused with 10 ml of phosphate buffered saline (PBS) followed by 10 ml of 4% paraformaldehyde at the rate of 2 ml/ minute. Brains were then carefully removed from the skull, placed into 4% paraformaldehyde at 4°C overnight for additional fixing, then cryoprotected in 30% sucrose at 4°C until the brains sank. After cryoprotection, brains were hemisected at midline and imbedded in Tissue-Tek* CRYO-OCT cutting matrix (Fischer Scientific, Pittsburgh, PA) with midline facing the bottom of standard size Cryomold® (25 x 20 x 5 mm, Sakura Finetek, Netherlands) to ensure consistent sectioning angle.

The embedded brains were stored in -80°C in moisture trapping resealable zip bags for later immunohistochemistry analysis.

5.2.3 Real-time qPCR

mRNA levels of PAX6, Tbr1, Tbr2, Sp1, and Creb1 were measured by qRT-PCR in whole brain samples from DE- and FA- exposed PND3 mice. Expression levels were normalized to the housekeeping gene, GAPDH (encoding Glyceraldehyde-3-Phosphate Dehydrogenase). In brief,

RNA was extracted by homogenizing frozen brain samples in TRIzol reagent (Thermo Fisher Scientific, Rockford, IL) with a tissue homogenizer, followed by standard chloroform extraction and ethanol precipitation procedures. RNA was further purified with the GeneJET RNA purification kit (Thermo Fisher Scientific Inc., Rockford, IL) according to the RNA clean-up protocol provided by the manufacturer. Quality and concentration of RNA isolates were confirmed by NanoDrop (Thermo Fisher Scientific Inc., Rockford, IL) measurements. For qRT-PCR analysis only samples with 260/280 ratio >1.8 and 260/230 ratio between 2.0 -2.2 were used. Reverse transcription was done using iScript cDNA Synthesis kit (Biorad; Hercules, CA) with 1µg of RNA per 20ul reaction. iTaq™ Universal SYBR® Green One-Step Kit (Biorad; Hercules, CA) was used for signal detection during real-time quantitative PCR on a Bio-Rad CFX384 Real-Time PCR Detection System (Biorad; Hercules, CA) with primers shown in Supplemental Table1. Relative mRNA expression of target genes was normalized to thehousekeeping gene GAPDH. Relative expression levels (ddCq) were calculated according to Haimes & Kelley (2010), and expression in DE exposed animals was compared with that in same-sex FA control animals.

5.2.4 Immunohistochemistry Analysis of Cortical Lamina Organization

OCT-embedded P60 mouse brains were cut sagittally at 10-12 µm starting 2000 µm away from midline, and the somatosensory cortex region was sampled 200 µm apart for five serial sets. The sections were direct mounted on glass slides and air dried before being stored at -80°C.

Immunohistochemistry was performed as previously described (Englund et al., 2005) with the following primary antibodies at the indicated dilutions: rabbit anti-Tbr1 (1:2,000; kindly provided by Dr. from Robert Hevner, University of Washington), rat anti-Tbr2 (1:200; ebioscience, 14-4875-82), rabbit anti-CUX1 (1:200; Santa Cruz, sc-13024), rat anti- Ctip2 (1:1,000; Abcam, 18465), mouse anti- Calb (1:3,000; Sigma, c9848), and rabbit anti- Parvalbumin (PV) (1:1,000; Swant, pv 27); secondary antibodies Alexa Fluor 488-conjugated goat anti-rabbit (1:600, Thermo Fisher Scientific), 568-conjugated goat anti-mouse (1:600, Thermo Fisher Scientific), and 568-conjugated goat anti-mouse (1:600, Thermo Fisher Scientific). The chromosome counterstain DAPI (4',6-diamidino-2-phenylindole) (Sigma, St. Louis, MO) was used to label DNA after incubation with primary and secondary antibodies, following the manufacturer's instructions. Brains from five animals in each experimental group were processed and analyzed, and 3-5 sections were collected per brain. Digital immunofluorescence images were obtained on a Zeiss Axio Imager Z1. In each image cortical depth, i.e., the distance between ventricle and pia, was divided into 10 evenly spaced bins, with bin 1 nearest to the pia. Fluorescently labeled cells were counted in each bin and area of each bin was measured using Adobe Photoshop, with the researcher blinded to the experimental groups. Cell density in each bin was calculated by dividing cell count to bin area.

5.2.5 Statistical Analysis

Two-way ANOVA with Bonferroni posttest was used to assess change in mRNA levels of transcription factors due to DE exposure in whole brain samples collected at PND3.

Two-tailed T-test was used to assess differences in cell density between FA and DE brains of the same sex in each bin. F-test was also used to assess equality of variances between FA and DE brains of the same sex in each bin. In hippocampus, Tbr2+ cells in the DG were counted in 3-5 tissue sections from each of the five mice sampled per experiment group. Averaged Tbr2+ cell counts for each animal were normalized to same sex FA controls. Unpaired T-test with Welch's

correction was conducted to compare differences in Tbr2+ cell counts in hippocampus between FA- and DE- exposed brains of same sex mice.

5.3. Results

5.3.1 Developmental DE exposure is associated with increased expression of Pax6, Tbr2, and Tbr1 at PND3

mRNA levels of transcription factors known to modulate neurogenesis and neurodifferentiation were measured by qRT-PCR analysis with RNA samples isolated from PND3 whole brains. Relative expression of the target genes Pax6, Tbr2, Tbr1, Sp1, Crb1 were normalized to the housekeeping gene GAPDH. Expression of all five transcription factors tested increased significantly in brains of DE- exposed male mice, as compared to FA-exposed controls (Fig. 4.1A-E). In female mice, Tbr1 and Crb1 also showed trends of increasing expression due to DE exposure when compared to same-sex control animals, but the differences werenot statistically significant. There were no differences in GAPDH expression between DE- and FA-exposed animals of either sex (not shown).

5.3.2 Developmental DE exposure is associated with decreased adult neurogenesis.

T-box brain 2 (Tbr2) has been used as a marker for neurogenesis since it is only expressed by intermediate neurons (Englund et al., 2005; Hodge et al., 2008; Liu and Crews, 2017; Mouihate, 2016). In the adult brain, neurogenesis occurs in two discrete areas, the subventricular zone (SVZ) and dentate gyrus (DG) (Abrous et al., 2005; Toda and Gage, 2017). In the DG of mice developmentally exposed to DE, significantly decreased adult neurogenesis, as marked by a decreased number of Tbr2-positive cells, was found in both males and females (Fig. 5.2).

5.3.3 Developmental DE exposure is associated with disorganization of cortical lamina in adult mice.

Disrupted cerebral cortex development has been found in mice genetically modified to over express PAX6 as well as in mice prenatally exposed to PM2.5 (Imamura and Greer, 2013; Zhang et al., 2018). To assess potential effects on lamina organization due to PAX6 up-regulation associated with developmental DE exposure,, immunohistochemical analysis was performed with the lamina-specific markers T-box brain 1 (Tbr1), COUP-TF-interacting protein 2 (CTIP2), CUT-like homeobox 1 (CUX1), calbindin (CALB), parvalbumin (PV) on tissue sections from P60 mouse brains. Statistically significant differences were found in the cortical distribution of Tbr1-, CALB-, and PV-positive cells (Fig. 5.3-5.5). Tbr1 is a transcription factor protein known for its role in glutamatergic neuron differentiation (Englund et al., 2005; Mihalas and Hevner, 2017). Developmental DE exposure affected the localization pattern of Tbr1-positive cells in males only. In DE-exposed males, a statistically significant decrease in Tbr1-positive cell density in cortical layers II/III was observed, while the normal characteristically distinct, bi-layer pattern of Tbr1-positive cells localizing in layers II/II and V was observed in FA- exposed mice of both sexes and in DE- exposed female mice (Fig. 5.3C, 5.3D). CALB is a calcium binding protein known to be expressed by interneurons localized in cortical layer II/III (Beguin et al., 2013). In DE- exposed female mice, a statistically significant increase in CALB-positive cell density was found in cortical layer VI as compared to FA- exposed females. In contrast, no significant difference in CALB-positive cell density was found between FA- and DE- exposed male mice (Fig. 5.4C, 5.4D). PV is a calcium-binding albumin protein expressed by interneurons localizing in layer II/III (Beguin et al., 2013; Gonchar, 2008). In DE-exposed male mice, a statistically significant increase in PV-positive cell density was found in cortical layers IV and VI compared to FA- exposed males, whereas no significant difference in PV-positive cell density was found between FA- and DE-exposed female mice (Fig. 5.5C, 5.5D). No significant difference was found in distribution of Ctip2- and CUX1- positive cells following DE exposure (Supplemental Figures 5.1 and 5.2).

5.4. Discussion

5.4.1 Upregulation of PAX6 from developmental DE exposure positively regulates neurogenic pathways during CNS development.

We examined mRNA levels of five different transcription factors (PAX6, Tbr2, Tbr1, Sp1, and Creb1) known to modulate neurogenic pathways (Dworkin & Mantamadiotis, 2010; Englund et al., 2005; Sansom et al., 2009; Ström et al., 1996) and found statistically significant increases for all five transcription factors in DE- exposed males at PND3 (Fig. 5.1). Temporal expression of PAX6, Tbr2, and Tbr1 has been shown to control the process of neurogenesis and neurodifferentiation, as these genes are expressed sequentially by radial glia, intermediate progenitor cells, and postmitotic neurons, respectively, during neurogenic events in both fetal and adult brains (Brill et al., 2009; Englund et al., 2005; Hodge et al., 2008; Roybon et al., 2009a, 2009b). In addition, PAX6 has been shown to play an essential role in controlling the balance between neural stem cell self-renewal and neurogenesis in both *in vivo* and *in vitro* models (Gan et al., 2014; Sansom et al., 2009). In transgenic mice over-expressing PAX6, expression of Tbr2 and Tbr1 were found to be positively regulated in fetal brain (Sansom et al., 2009). Our findings of increased PAX6, Tbr2, and Tbr1 mRNA levels in brains of PND3 male mice developmentally exposed to DE (Fig. 5.1A- C) are consistent with the reported findings that PAX6 upregulates expression of Tbr2 and Tbr1, leading to the promotion of neurogenesis over neural stem cell self-renewal (Imamura and Greer, 2013; Manuel et al., 2006).

5.4.2 Neurodegenerative consequences caused by developmental DE exposure.

Immunohistochemical analysis in the DG of P60 mice developmentally exposed to DE demonstrated a significant decrease in the number of Tbr2+ cells in DE-exposed mice of both sexes, as compared to FA-exposed controls (Fig. 5.2). Tbr2 has been used as a marker for adult neurogenesis in many animal studies (Brill et al., 2009; Hodge et al., 2008; Liu & Crews, 2017;

Mihalas & Hevner, 2017; Mouihate, 2016), as Tbr2 is only expressed by newly divided intermediate neural progenitor cells (Englund et al., 2005; Hodge et al., 2008). Our findings show that developmental DE exposure decreases adult neurogenesis in the DG as late as PND60. Other animal studies have shown decreased adult neurogenesis due to acute and subacute exposure to traffic related air pollution in adult mice (Cheng et al., 2017; Coburn et al., 2018). A study conducted in PAX77 mice, a transgenic mouse strain over-expressing PAX6, provides a possible explanation for the decreased adult neurogenesis in DE- exposed mice. In PAX77 mice, an increased number of Tbr2-positive cells was observed in the neocortex at E12.5 followed by reports of microcephaly at E14.5, with no increase in apoptosis (Sansom et al., 2009). These results suggest that over-promotion of neurogenesis early in CNS development depletes neural progenitor cells' self-renewal potential, which leads to decreased neurogenesis during later stages of corticogenesis, as well as decreased adult neurogenesis (Fig. 5.2).

We also found increased mRNA levels of transcription factor Sp1 in brains of PND3 male mice developmentally exposed to DE (Fig 5.1D). This is of interest because Sp1 has been found to upregulate β -amyloid precursor protein (APP) as a result of environmental influences occurring during brain development, leading to amyloidogenesis and cognitive decline at later age (Basha et al., 2005; Bihaqi et al., 2014). These studies focused on developmental exposure to lead, a metal which was not present in the DE used in the present study (Fox et al., 2014); however the DE mixture does include other metals in the same valence group, such as zinc (Zn) and tin (Sn), which could exert similar modes of toxicity on the developing CNS.

We also found increased mRNA levels of transcription factor Creb1 in brains of PND3 male mice developmentally exposed to DE (Fig 5.1E). Since Creb1 is reported to play a role in neuronal survival during adult neurogenesis (Herold et al., 2011; Zhu et al., 2004), further assessments of whether the sex-dependent Creb1 upregulation due to DE exposure persisted in adult mice would

definitely be of interest to elucidate key mechanistic events contributing to developmental origin of neurodegenerative disorders.

5.4.3 Developmental DE exposure leads to disrupted cortical lamina organization.

In PAX77 transgenic mice overexpressing PAX 6, cell cycle length and cell cycle exit were found to be increased, resulting in reduced neurogenesis at late stages of corticogenesis. In the cortex of PAX77 mice, a decreased number of Tbr1-positive cells was found in the superficial layers, while Tbr1-positive cell numbers were unaffected in deeper cortical layers (Georgala et al., 2011; Manuel et al., 2006). We have found increased Pax6 expression levels by RT-qPCR in whole brain samples from PND3 male mice exposed to DE (Fig 5.1A), as well as a significantly decreased number of Tbr1-positive cells in cortical layers II/III from PND60 male mice developmentally exposed to DE (Fig. 5.3C). Thus, our findings mirror those reported for the PAX77 mouse model, as cortical layers are generated with the “inside-out” pattern: neurons in deeper-layers were born during early stages of corticogenesis (Kadoshima et al., 2013; Rakic, 1974; Shen et al., 2006). The sex-specific finding from Tbr1 immunohistochemistry analysis was expected, since the effects of developmental DE exposure on PAX6, Tbr2, Tbr1 expression levels are also male specific (Fig 5.1 A-C), and because expression of Tbr2 and Tbr1 has been shown to be modulated by PAX6 (Englund et al., 2005; Imamura and Greer, 2013; Sansom et al., 2009)

In PAX77 transgenic mice, overexpression of Pax6 does not seem to affect cortical lamina organization (Georgala et al., 2011); however, we have previously reported downregulation of reelin expression levels in brains of PND3 mice developmentally exposed to DE (Chang et al., 2018b). Since reelin has been known to play a critical role in guiding the process of neuronal migration (D’Arcangelo, 2014; Michetti et al., 2014), we performed immunohistochemistry analysis with four additional cortical laminar specific markers (CALB , PV, Ctip2, and CUX1) to further evaluate the extent of potential effects on cortical organizational associated with developmental DE exposure. We found mild changes in distribution of CALB+ and PV+ cells in

deeper layers of the cortex (Suppl. Fig. 5.1, 5.2), while no significant changes in cell distribution were found with the markers Ctip2 or CUX1 (Fig. 5.6, Fig. 5.7). Although the level of cortical disorganization found in DE- exposed mice is mild compared to findings in other models, i.e. the reelin knockout mice (Boyle et al., 2011), our results parallel reports of small patches of disorganization found in prefrontal cortex of adolescent ASD patients (Stoner et al., 2014b). Considering that disruption of developmental events elicited by a pervasive environmental toxicant such as air pollution would have long-lasting effects in organizational structure of the brain, the public health implications suggested by our finding are rather striking.

5.5 Figures

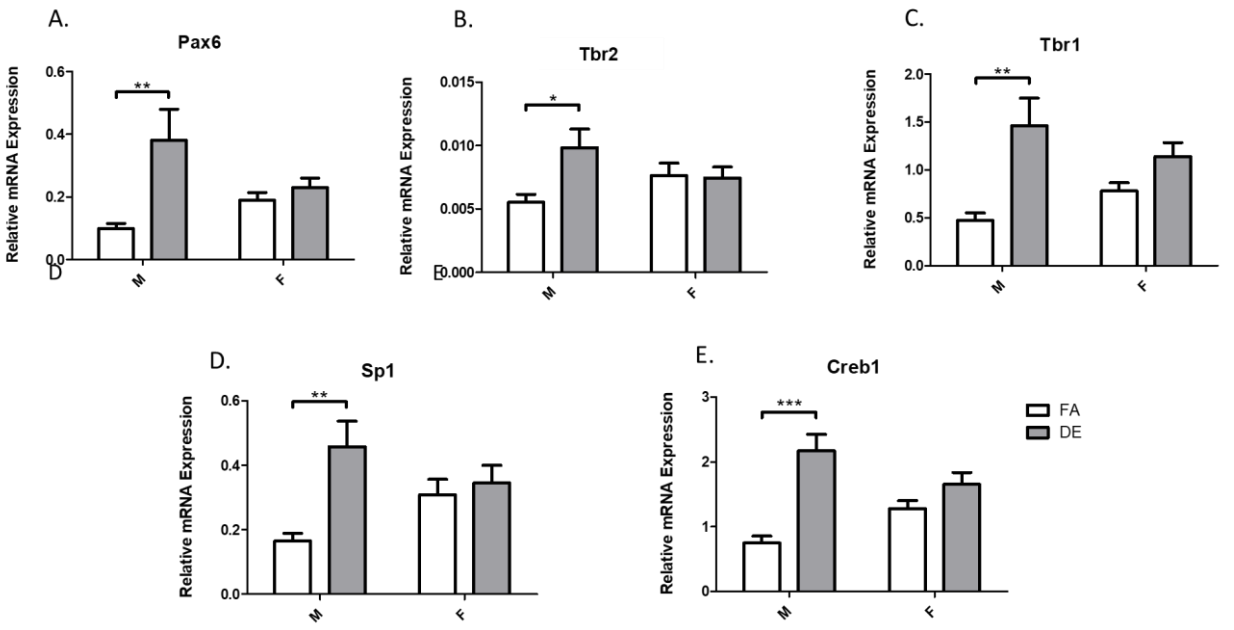

Fig. 5.1 mRNA Levels of Neurogenic Transcription Factors at PND3

mRNA levels of transcription factors Pax6 (A), Tbr2 (B) , Tbr1 (C), Sp1 (D), and Creb1 (E) were measured in whole brain samples from PND3 pups exposed to either DE or FA from E0 to PND3. mRNA levels were normalized to the housekeeping gene GAPDH. Results represent the mean (± SE) of 5 mice taken from different litters for each experimental group. For all five transcription factors measured, mRNA levels were found to be significantly increased in DE-exposed males when compared to FA- exposed males(* $p<0.05$; ** $p<0.01$; *** $p<0.001$; two-way ANOVA with Bonferroni posttest).

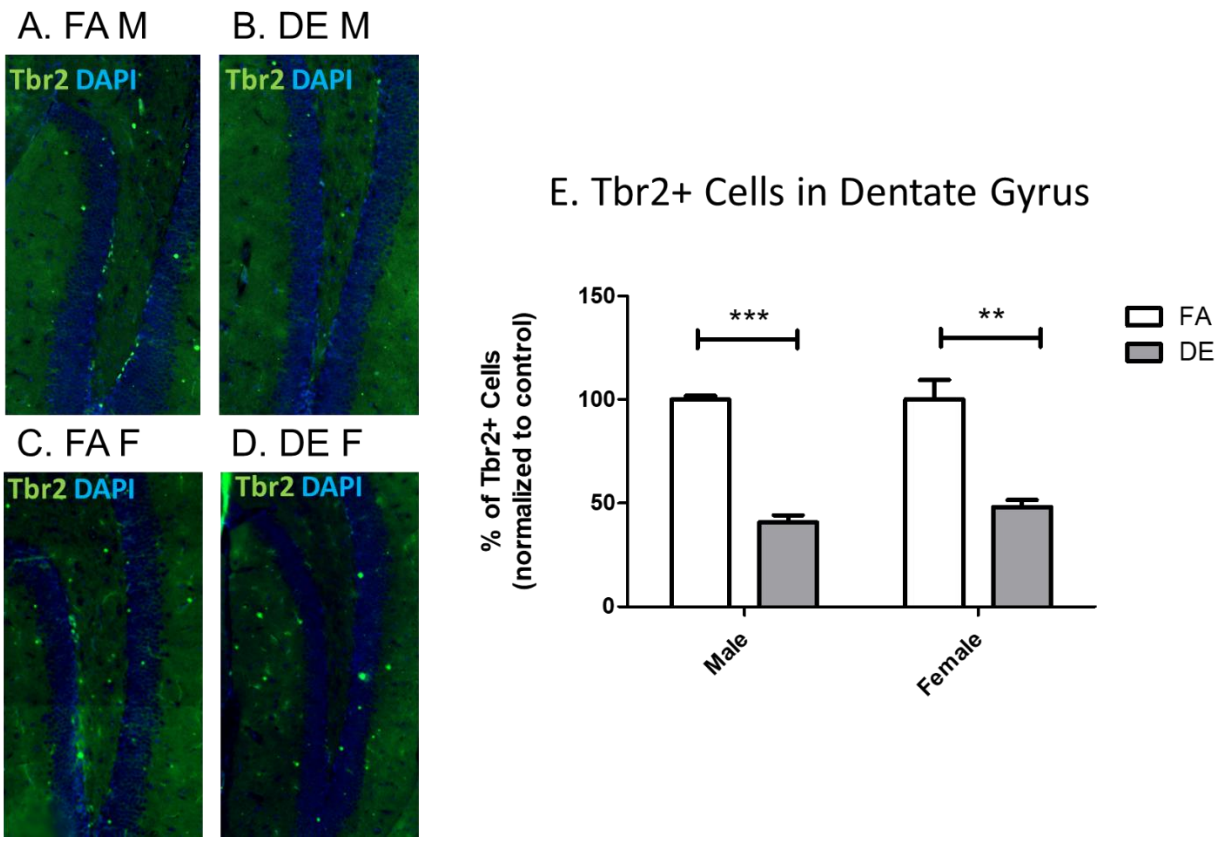

Fig. 5.2 Adult Neurogenesis in PND60 Dentate Gyrus.

Representative image from a FA- exposed male (A), DE- exposed male (B), FA- exposed female (C), and DE- exposed female (D) are shown with Tbr2+ cells (in green) and nuclei counter stain DAPI (in blue). A significant decrease in number of Tbr2+ cells was found in mice exposed to DE in both sexes (E). Results represent the mean (± SE) of 5 mice from different litters for each experimental group (**p<0.01; ***p<0.001; Unpaired t-test with Welch's correction)

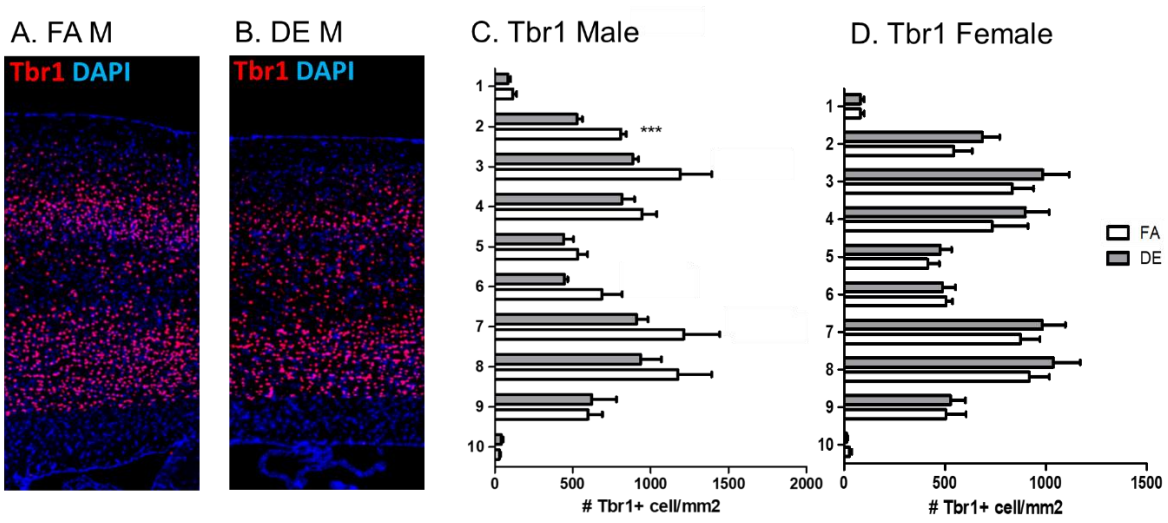

Fig. 5.3 Tbr1 in PND60 Cortex.

In cortex of control mice, Tbr1 is mostly localized in layers II/II and V as shown in the Allen Brain Atlas (Sunkin et al., 2013). (A, B) Representative image of Tbr1+ cells (red) with nuclei counterstain DAPI (blue) from FA- and DE- exposed males. DE-exposed males showed a statistically significant decrease in Tbr1-positive cell density in cortical layer II/III compared to FA- exposed males (C). No difference in Tbr1+ cell distribution was observed with DE exposure in female mice (D). Results represent the mean (± SE) of 5 mice from different litters for each experimental group; 3-5 sections/ mouse were examined (***p<0.001; unpaired T-test with Welch's correction;)

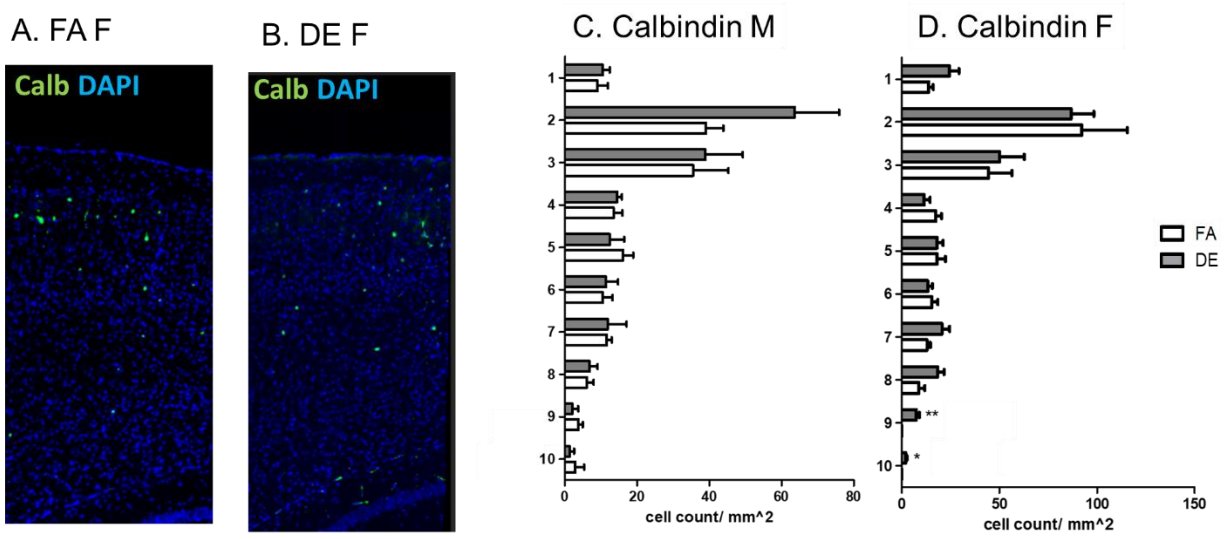

Fig. 5.4 Calbindin in PND60 Cortex.

Calbindin (CALB) is a calcium binding protein, Calb expressing interneurons have been shown to localize in cortical layer II/III (Beguin et al., 2013). (A, B) Representative image of Calb+ cells (green) with nuclei counterstain DAPI (blue) from FA- and DE- exposed females. In DE-exposed females, a statistically significant increase in CALB-positive cell density was found in cortical layer VI when compared to FA- exposed females, while no significant difference in CALB-positive cell density was found between FA- and DE- exposed male mice (C, D). Results represent the mean (± SE) of 5 mice from different litters for each experimental group; 3-5 sections/ mouse were examined (*$p<0.05$, **$p<0.01$; unpaired T-test with Welch's correction;)

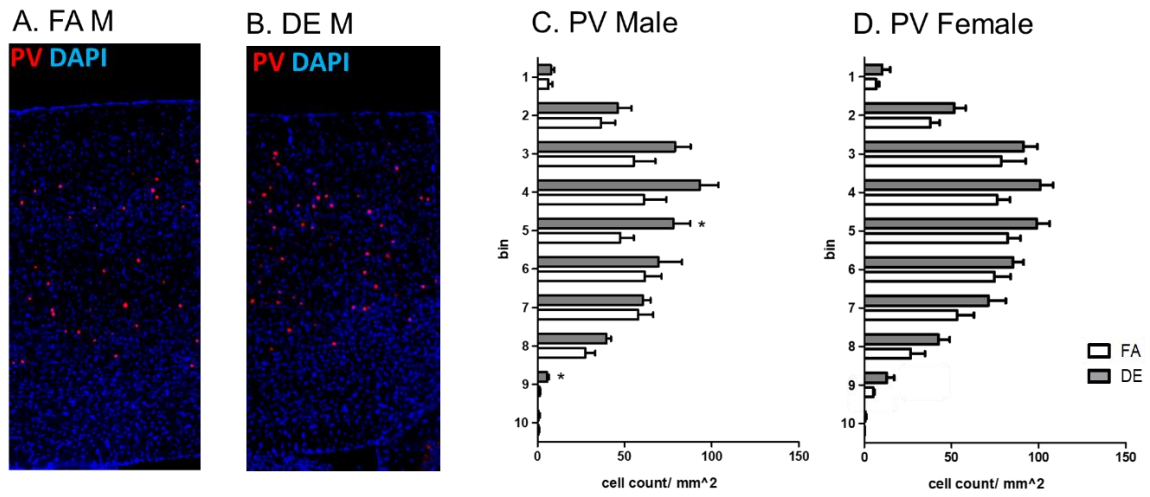

Fig. 5.5 Parvalbumin in PND60 Cortex.

Parvalbumin (PV) is a calcium-binding albumin protein expressed by interneurons localizing in layer II/III (Beguin et al., 2013; Gonchar, 2008). (A, B) Representative image of PV+ cells (red) with nuclei counterstain DAPI (blue) from FA- and DE- exposed males. In DE- exposed males a statistically significant increase in PV-positive cell density was found in cortical layers IV and VI when compared to FA- exposed males (C), while no significant difference in PV-positive cell were found between FA- and DE- exposed female mice (D). Results represent the mean (± SE) of 5 mice from different litters for each experimental group; 3-5 sections/ mouse were examined (*$p<0.05$; unpaired T-test with Welch's correction;)

5.6 Appendix

Supplemental Table 5.1. Sequences of primers for qRT-PCR

	Forward Primer Sequence (5' -> 3')	Reverse primer Sequence (5' -> 3')
PAX6	ACTTTAACCAAGGGCGGTGAG	TTCACTCCGCTGTGACTGTTC
Tbr1	CCGGAGACTCAGTTCATCGC	GCCCGTGTAGATCGTGTCAT
Tbr2	GTGACGGCCTACCAAAACAC	CCACCTCTTCGCTGAATCGT
Sp1	AGGCCTCCAGACCATTAACC	TCCATGATCACCTGGGGTGT
Creb1	ACTCAGCCGGGTACTACCAT	GAGGCAGCTTGAACAACAACT
GAPDH	TGACCTCAACTACATGGTCTACA	CTTCCCATTCTCGGCCTTG

Sequences of primer sets used in the present study are shown; both forward and reverse primers are listed from 5’ to 3’.

Supplemental Figure 5.1 Ctip2 in PND60 Cortex.

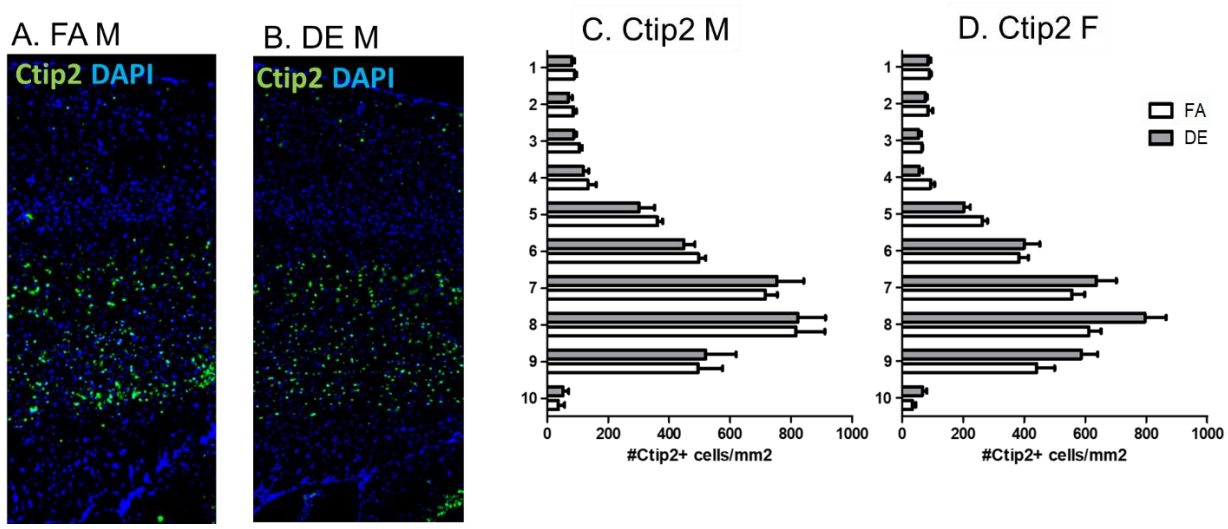

COUP-TF-interacting protein 2 (Ctip2) is expressed in cortical layer V as shown in the Allen Brain Atlas (Sunkin et al., 2013). (A, B) Representative image of Ctip2+ cells (green) with nuclei counterstain DAPI (blue) from FA- and DE- exposed males. Developmental DE exposure did not cause any statistically significant difference in Ctip2+ cell distribution in mice of either sex (C, D). Results represent the mean (± SE) of 5 mice from different litters for each experimental group; 3-5 sections/ mouse were examined (unpaired T-test with Welch's correction;)

Supplemental Figure 5.2 CUX1 in PND60 Cortex.

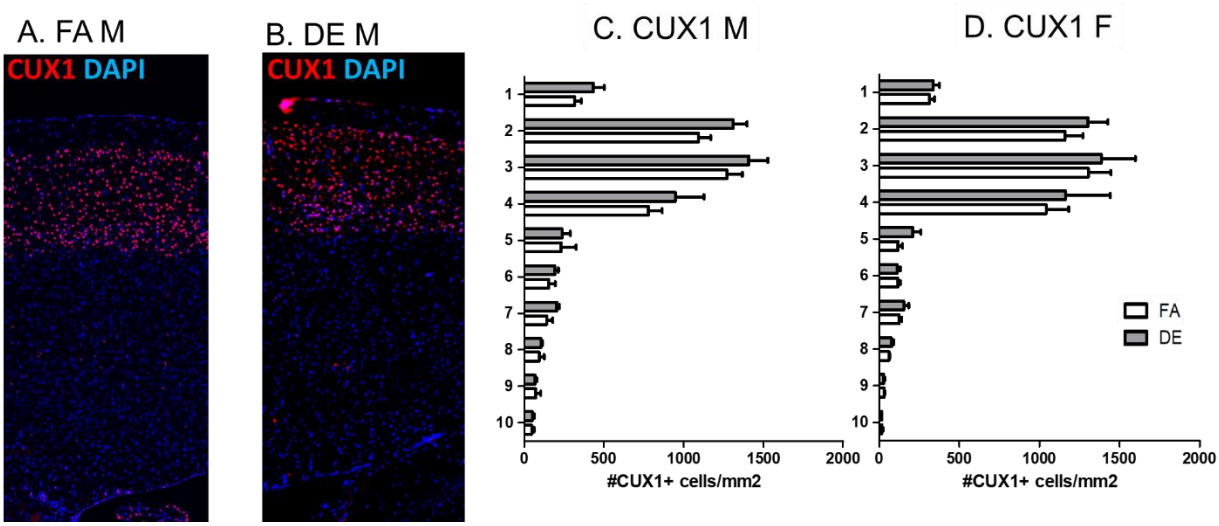

CUT-like homeobox 1 (CUX1) is expressed in cortical layers II/III and IV as shown in the Allen Brain Atlas (Sunkin et al., 2013). (A, B) Representative image of CUX1+ cells (red) with nuclei counterstain DAPI (blue) from FA- and DE- exposed males. Developmental DE exposure did not cause any statistically significant difference in CUX1+ cell distribution in mice of either sex (C, D). Results represent the mean (± SE) of 5 mice from different litters for each experimental group; 3-5 sections/ mouse were examined (unpaired T-test with Welch's correction;)

Chapter 6

CONCLUSIONS AND FUTURE DIRECTIONS

Autism spectrum disorder (ASD) represent a heterogeneous group of disorders characterized by difficulties in social interactions, impaired verbal and nonverbal communication, and repetitive behaviors. In 2014, the CDC National Health Interview Survey estimated ASD prevalence to be 1 in 45 for American children. Prompted by the escalating prevalence of ASD, emerging epidemiological studies provided evidence associating developmental traffic-related air pollution (TRAP) exposure with increased ASD risk. Given the pervasive nature of TRAP and the sizeable global population facing potentially high levels of exposure, in this thesis project we investigated the neurotoxic effects of developmental exposure to DE in mice, to contribute to knowledge of this emerging public health concern.

Following a series of preliminary studies involving only pre-natal exposure to DE (Chapter 2), we carried out a comprehensive assessment of autism-related behavioral effects following prenatal and early life exposure (E0-PND21) to DE (Chapter 3). In DE-exposed mice, we found altered behavioral phenotypes consistent with all three characteristic domains of autism, i.e. increased repetitive behavior, altered vocal and olfactory communication, decreased social sniffing, and inability to differentiate social novelty. Results from this study support epidemiological findings of an association between TRAP and ASD (Becerra et al., 2013; Guxens et al., 2016; Morales-Suárez-Varela et al., 2017; Raz et al., 2017; Volk et al., 2011, 2013). Our findings are also in agreement with reports from recently published rodent studies showing exposure to ambient PM2.5 leads to decreased number of neonatal USV calls, inability to differentiate social novelty,

decreased interactive sniffing response, and increased repetitive grooming (Church et al., 2017; Li et al., 2017a).

We next hypothesized a mechanistic pathway potentially affected by developmental DE exposure that may be relevant to ASD. We found that developmental exposure to DE elicited neuroinflammation; specifically, it was associated with upregulated expression of IL-6 and downstream activation of the JAK2/ STAT3 pathway, which was previously shown to play a key role in modulating ASD-like behavior in mice with maternal immune activation (Choi et al., 2016; Hsiao and Patterson, 2011; Smith et al., 2007). Since STAT3 has been shown to upregulate DNMT1 expression and DNMT1 has been shown to modulate RELN expression (Dong et al., 2015; Huang et al., 2016; Kundakovic et al., 2009; Zhang et al., 2006, 2005), we further investigated this relationship with respect to developmental DE exposure, and found increased DNMT1 expression and decreased expression of RELN in brains of PND3 mice exposed to DE. These findings suggest that developmental exposure to DE upregulated the key inflammatory cytokine IL-6, which activated the JAK2/STAT3 pathway and promoted upregulation of DNMT1, which in turn down regulated RELN expression at an early developmental age. Grounded on RELN's critical role in guiding the process of neuronal migration (D'Arcangelo, 2014; Jossin & Cooper, 2011; Lee & D'Arcangelo, 2016), our findings further showed signs of cortical lamina disorganization in the somatosensory cortex of DE-exposed adult mice. A recent study showing that activation of neurons in the S1DZ region in the somatosensory cortex induces ASD-like behavior in mice (Shin Yim et al., 2017) suggests a possible connection between the cortical disorganization found in DE-exposed mice and the ASD-like behavioral phenotypes that were found in the current study. To my knowledge, this is the first time that a mechanistic pathway connecting air pollution-induced neuroinflammation todownstream molecular changes in brain structural morphology similar to those found in ASD patients, in an exposure model causing an ASD-like behavioral phenotype.

Additional studies suggest that developmental exposure to DE causes up-regulation of the PAX6, Tbr2, and Tbr1, factors involved in theneurogenic pathway, thusdisrupting the temporal balance between neurogenesis and progenitor cell self-renewal, and causing decreased neurogenesis during late corticogenesis, as well as decreased adult neurogenesis. In addition, we have shown that developmental DE exposure causes increased mRNA levels of Sp1, a transcription factor known to upregulate β -amyloid precursor protein (APP). Overall, these findings suggest that developmental air pollution exposure may increase risk for later onset neurodegenerative diseases by altering expression levels of key transcription factors known to modulate neurodegenerative risk, leading to decreased adult neurogenesis. However, a detailed mechanistic explanation for such changes remains unclear. Given the pervasive nature of traffic related air pollution and the size of population exposed globally, future studies are much warranted to carefully evaluate both the potential hazard and the exact mode of toxicity. Additionally, further studies aimed at investigating potential gene-environment interactions could help identify sensitive populations and further inform future air quality policy.

Bibliography

Abrous, D.N., Koehl, M., M.L., M., 2005. Adult Neurogenesis: From Precursers to Network and Physiology. Physiol. Rev. 85, 523–569.

Allen, J. L., Oberdorster, G., Morris-Schaffer, K., Wong, C., Klocke, C., Sobolewski, M., Conrad, K., Mayer-Proschel, M., Cory-Slechta, D.A., 2016. Developmental neurotoxicity of inhaled ambient ultrafine particle air pollution: Parallels with neuropathological and behavioral features of autism and other neurodevelopmental disorders. Neurotoxicol. 59, 140-154.

Allen, J., Liu, X., Pelkowski, S., Palmer, B., Conrad, K., Oberdörster, G., Weston, D., Mayer-pröschel, M., Cory-slechta, D., 2014. Early Postnatal Exposure to Ultrafine Particulate Matter Air Pollution: Persistent Ventriculomegaly, Neurochemical Disruption, and Glial Activation Preferentially in Male Mice. Environ. Health Perspect. 122, 939–945.

Amodeo, D.A., Jones, J.H., Sweeney, J.A., Ragozzino, M.E., 2012. Differences in BTBR T+ tf/J and C57BL/6J mice on probabilistic reversal learning and stereotyped behaviors. Behav. Brain Res. 227, 64–72.

Angoa-Pérez, M., Kane, M.J., Briggs, D.I., Francescutti, D.M., Kuhn, D.M., 2013. Marble burying and nestlet shredding as tests of repetitive, compulsive-like behaviors in mice. J. Vis. Exp. 82, e50978.

Auten, R.L., Gilmour, M.I., Krantz, Q.T., Potts, E.N., Mason, S.N., Foster, W.M., 2012. Maternal diesel inhalation increases airway hyperreactivity in ozone-exposed offspring. Am. J. Respir. Cell Mol. Biol. 46, 454–460.

Autism Speaks Webpage, 2013. DSM-5 Diagnostic Criteria. Autism Speak. Inc. URL https://www.autismspeaks.org/what-autism/diagnosis/dsm-5-diagnostic-criteria

Basha, M.R., Wei, W., Bakheet, S. a, Benitez, N., Siddiqi, H.K., Ge, Y.-W., Lahiri, D.K., Zawia,

N.H., 2005. The fetal basis of amyloidogenesis: exposure to lead and latent overexpression of amyloid precursor protein and beta-amyloid in the aging brain. J. Neurosci. 25, 823–829.

Becerra, T.A., Wilhelm, M., Olsen, J., Cockburn, M., Ritz, B., 2013. Children ' s Health Ambient Air Pollution and Autism in Los Angeles County , California. Environ. Health Perspect. 380, 380–386.

Beguin, S., Crépel, V., Aniksztejn, L., Becq, H., Pelosi, B., Pallesi-Pocachard, E., Bouamrane, L., Pasqualetti, M., Kitamura, K., Cardoso, C., Represa, A., 2013. An epilepsy-related ARX polyalanine expansion modifies glutamatergic neurons excitability and morphology without affecting gabaergic neurons development. Cereb. Cortex. 23, 1484–1494.

Bihaqi, S.W., Bahmani, A., Subaiea, G.M., Zawia, N.H., 2014. Infantile exposure to lead and late-age cognitive decline: relevance to AD. Alzheimers. Dement. 10, 187–195.

Blick, M.G., Puchalski, B.H., Bolanos, V.J., Wolfe, K.M., Green, M.C., Ryan, B.C., 2015. Novel object exploration in the C58/J mouse model of autistic-like behavior. Behav. Brain Res. 282, 54–60.

Block, M.L., Calderón-Garcidueñas, L., 2009. Air pollution: mechanisms of neuroinflammation and CNS disease. Trends Neurosci. 32, 506–516.

Boksa, P., 2010. Effects of prenatal infection on brain development and behavior: a review of findings from animal models. Brain. Behav. Immun. 24, 881–897.

Bolton, J., Marinero, S., Hassanzadeh, T., Le, D., Belliveau, C., Mason, S. N., Auten, R. L., Bilbo, S.D., 2017. Gestational exposure to air pollution alters cortical volume, microglial morphology, and microglia-neuron interactions in a sex-specific manner. Front. Synaptic Neurosci. 9, 1–16.

Bolton, J.L., Auten, R.L., Bilbo, S.D., 2014. Prenatal air pollution exposure induces sexually

dimorphic fetal programming of metabolic and neuroinflammatory outcomes in adult offspring. Brain. Behav. Immun. 37, 30–44.

Bolton, J.L., Smith, S.H., Huff, N.C., Gilmour, M.I., Foster, W.M., Auten, R.L., Bilbo, S.D., 2012. Prenatal air pollution exposure induces neuroinflammation and predisposes offspring to weight gain in adulthood in a sex-specific manner. FASEB J. 26, 4743–4754.

Bonthius, D.J., Pantazis, N.J., Karacay, B., Bonthius, N.E., Taggard And, D. a, Lothman, E.W., 2001. Alcohol exposure during the brain growth spurt promotes hippocampal seizures, rapid kindling, and spreading depression. Alcohol. Clin. Exp. Res. 25, 734–745.

Boyle, M.P., Bernard, A., Thompson, C.L., Ng, L., Boe, A., Mortrud, M., Hawrylycz, M.J., Jones, A.R., Hevner, R.F., Lein, E.S., 2011. Cell-type-specific consequences of Reelin deficiency in the mouse neocortex, hippocampus, and amygdala. J. Comp. Neurol. 519, 2061–2089.

Bozdagi, O., Sakurai, T., Papapetrou, D., Wang, Xi., Dickstein, D., Takahashi, N., Kajiwara, Y., Yang, M., Katz, A., Scattoni, M. L., Harris, M., Saxena, R., Silverman, J., Crawley, J., Zhou, Q., Hof, P., Buxbaum, J., 2010. Haploinsufficiency of the autism-associated Shank3 gene leads to deficits in synaptic function, social interaction, and social communication. Mol. Autism 1, 15.

Branchi, I., Santucci, D., Alleva, E., 2006. Analysis of Ultrasonic Vocalizations Emitted by Infant Rodents. Curr. Protoc. Toxicol. 30, 13.12.1–13.12.14.

Brill, M.S., Ninkovic, J., Winpenny, E., Hodge, R.D., Ozen, I., Yang, R., Lepier, A., Gascón, S., Erdelyi, F., Szabo, G., Parras, C., Guillemot, F., Frotscher, M., Berninger, B., Hevner, R.F., Raineteau, O., Götz, M., 2009. Adult generation of glutamatergic olfactory bulb interneurons. Nat. Neurosci. 12, 1524–1533.

Brook, R.D., Rajagopalan, S., Pope, C.A., Brook, J.R., Bhatnagar, A., Diez-Roux, A. V.,

Holguin, F., Hong, Y., Luepker, R. V., Mittleman, M.A., Peters, A., Siscovick, D., Smith, S.C., Whitsel, L., Kaufman, J.D., 2010. Particulate matter air pollution and cardiovascular disease: An update to the scientific statement from the american heart association. Circulation. 121, 2331–2378.

Brudzynski, S.M., Kehoe, P., Callahan, M., 1999. Sonographic Structure of Isolation-Induced Ultrasonic Calls of Rat Pups. Dev. Psychobiol. 34, 195–204.

Calderón-Garcidueñas, L., Cross, J. V., Franco-Lira, M., Aragón-Flores, M., Kavanaugh, M., Torres-Jardón, R., Chao, C. k., Thompson, C., Chang, J., Zhu, H., D'Angiulli, A., 2013a. Brain immune interactions and air pollution: macrophage inhibitory factor (MIF), prion cellular protein (PrPC), Interleukin-6 (IL-6), interleukin 1 receptor antagonist (IL-1Ra), and interleukin-2 (IL-2) in cerebrospinal fluid and MIF in serum differentiat. Front. Neurosci. 7, 1–11.

Calderón-Garcidueñas, L., Franco-Lira, M., Mora-Tiscareño, A., Medina-Cortina, H., Torres-Jardón, R., Kavanaugh, M., 2013b. Early Alzheimer's and Parkinson's Disease Pathology in Urban Children: Friend versus Foe Responses—It Is Time to Face the Evidence. Biomed Res. Int. 2013, 1–16.

Calderón-Garcidueñas, L., Kulesza, R.J., Doty, R.L., D'Angiulli, A., Torres-Jardón, R., 2015. Megacities air pollution problems: Mexico City Metropolitan Area critical issues on the central nervous system pediatric impact. Environ. Res. 137, 157–169.

Calderón-Garcidueñas, L., Leray, E., Heydarpour, P., Torres-Jardón, R., Reis, J., 2016. Air pollution, a rising environmental risk factor for cognition, neuroinflammation and neurodegeneration: The clinical impact on children and beyond. Rev. Neurol. 172, 69–80.

Calderón-Garcidueñas, L., Mora- Tiscareño, A., Styner, M., Gómez-Garza, G., Zhu, H., Torres-Jardón, R., Medina-Cortinaa, M. Kavanaugh, M., D'Angiulli, A., 2012. White matter

hyperintensities, systemic inflammation, brain growth, and cognitive functions in children exposed to air pollution. J. Alzheimer's Dis. 31, 183–191.

Calderón-Garcidueñas, L., Mora-Tiscareño, A., Ontiveros, E., Gómez-Garza, G., Barragán-Mejía, G., Broadway, J., Chapman, S., Valencia-Salazar, G., Jewells, V., Maronpot, R.R., Henríquez-Roldán, C., Pérez-Guillé, B., Torres-Jardón, R., Herrit, L., Brooks, D., Osnaya-Brizuela, N., Monroy, M.E., González-Maciel, A., Reynoso-Robles, R., Villarreal-Calderon, R., Solt, A.C., Engle, R.W., 2008. Air pollution, cognitive deficits and brain abnormalities: A pilot study with children and dogs. Brain Cogn. 68, 117–127.

Calderón-Garcidueñas, L., Reynoso-Robles, R., Vargas- Martínez, J., Gómez-Maqueo-Chew, A., Pérez-Guillé, B., Mukherjee, P.S., Torres-Jardón, R., Perry, G., Gónzalez-Maciel, A., 2016. Prefrontal white matter pathology in air pollution exposed Mexico City young urbanites and their potential impact on neurovascular unit dysfunction and the development of Alzheimer's disease. Environ. Res. 146, 404–417.

Careaga, M., Murai, T., Bauman, M.D., 2017. Maternal Immune Activation and Autism Spectrum Disorder: From Rodents to Nonhuman and Human Primates. Biol. Psychiatry 81, 391–401.

Chang, K., Tsai, C., Chiou, Y., Chiu, C., Jeng, K., Huang, C.F., 2005. IL-6 induces neuroendocrine dedifferentiation and cell proliferation in non-small cell lung cancer cells. Am. J. Physiol. Lung Cell Mol. Physiol . 446–453.

Chang, Y.-C., Cole, T.B., Costa, L.G., 2017. Behavioral Phenotyping for Autism Spectrum Disorders in Mice. Curr. Protoc. Toxicol. 72, 11.22.1–11.22.21

Chang, Y., Cole, T.B., Costa, L.G., Costa, L.G., 2018a. Prenatal and early-life diesel exhaust exposure causes autism-like behavioral changes in mice. Part. Fibre Toxicol. (in press)

Chang, Y., Daza, R., Cole, T.B., Hevner, R., Costa, L.G., Cole, T.B., Costa, L.G., 2018b.

Prenatal and Early Life Diesel Exhaust Exposure Disrupts Cortical Lamina Organization : Evidence for a Reelin-Related Pathogenic Pathway Induced by Interleukin-6 . (in preparation)

Cheng, L., Lau, W.K.W., Fung, T.K.H., Lau, B.W.M., Chau, B.K.H., Liang, Y., Wang, Z., So, K.F., Wang, T., Chan, C.C.H., Lee, T.M.C., 2017. PM2.5 Exposure Suppresses Dendritic Maturation in Subgranular Zone in Aged Rats. Neurotox. Res. 32, 50–57.

Choi, G.B., Yim, Y.S., Wong, H., Kim, S., Kim, H., Kim, S. V, Charles, A., Littman, D.R., Huh, J.R., Choi, G.B., Yim, Y.S., Wong, H., Kim, S., Kim, H., Kim, S. V, Charles, A., 2016. The maternal interleukin-17a pathway in mice promotes autismlike phenotypes in offspring. Science. 351(6276): 933–939.

Christensen, D.L., Baio, J., Braun, K.V.N., Bilder, D., Charles, J., Constantino, J.N., Daniels, J., Durkin, M.S., Fitzgerald, R.T., Kurzius-Spencer, M., Lee, L.-C., Pettygrove, S., Robinson, C., Schulz, E., Wells, C., Wingate, M.S., Zahorodny, W., Yeargin-Allsopp, M., 2016. Prevalence and Characteristics of Autism Spectrum Disorder Among Children Aged 8 Years - Autism and Developmental Disabilities Monitoring Network, 11 Sites, United States, 2012. Morb. Mortal. Wkly. report. Surveill. Summ. 65, 1–23.

Church, J.S., Tijerina, P.B., Emerson, F.J., Coburn, M.A., Blum, J.L., Zelikoff, J.T., Schwartzer, J.J., 2017. Perinatal exposure to concentrated ambient particulates results in autism-like behavioral deficits in adult mice. Neurotoxicology. 65, 231-240.

Coburn, J.L., Cole, T.B., Dao, K.T., Costa, L.G., 2018. Acute exposure to diesel exhaust impairs adult neurogenesis in mice: prominence in males and protective effect of pioglitazone. Arch. Toxicol. (in press)

Cole, T.B., Coburn, J., Dao, K., Roqué, P., Chang, Y., Kalia, V., Guilarte, T.R., Dziedzic, J., Costa, L.G., 2016. Sex and genetic differences in the effects of acute diesel exhaust

exposure on inflammation and oxidative stress in mouse brain. Toxicology. 374, 1–9.

Costa, L.G., Chang, Y.-C., Cole, T.B., 2017. Developmental Neurotoxicity of Traffic-Related Air Pollution: Focus on Autism. Curr. Environ. Heal. Reports. 4, 156–165.

Costa, L.G., Cole, T.B., Coburn, J., Chang, Y., Dao, K., Roque, P.J., 2017. Neurotoxicity of traffic-related air pollution. Neurotoxicology 59, 133–139.

Costa, L.G., Cole, T.B., Coburn, J., Chang, Y.C., Dao, K., Roque, P., 2014. Neurotoxicants are in the air: Convergence of human, animal, and in vitro studies on the effects of air pollution on the brain. Biomed Res. Int. 2014, 736385.

Crawley, J.N., 2012. Translational animal models of autism and neurodevelopmental disorders. Dialogues Clin. Neurosci. 14, 293–305.

D'Arcangelo, G., 2014. Reelin in the Years: Controlling Neuronal Migration and Maturation in the Mammalian Brain. Adv. Neurosci. 2014, 1–19.

Deacon, R.M.J., 2006. Digging and marble burying in mice : simple methods for in vivo identification of biological impacts. Nat. Protoc. 1, 122–124.

Deacon, R.M.J., Rawlins, J.N.P., 2006. T-maze alternation in the rodent. Nat. Protoc. 1, 7–12.

De Felice, A., Scattoni, M.L., Ricceri, L., Calamandrei, G., 2015. Prenatal exposure to a common organophosphate insecticide delays motor development in a mouse model of idiopathic autism. PLoS One 10, e0121663.

DeFranco, E., Moravec, W., Xu, F., Hall, E., Hossain, M., Haynes, E.N., Muglia, L., Chen, A., 2016. Exposure to airborne particulate matter during pregnancy is associated with preterm birth: A population-based cohort study. Environ. Heal. A Glob. Access Sci. Source 15, 1–8.

Ding, L., Zhu, D., Peng, D., Zhao, Y., 2017. Air pollution and asthma attacks in children: A

case–crossover analysis in the city of Chongqing, China. Environ. Pollut. 220, 348–353.

Dong, E., Ruzicka, W.B., Grayson, D.R., Guidotti, A., 2015. DNA-methyltransferase1 (DNMT1) binding to CpG rich GABAergic and BDNF promoters is increased in the brain of schizophrenia and bipolar disorder patients. Schizophr. Res. 167, 35–41.

Dworkin, S., Mantamadiotis, T., 2010. Targeting CREB signalling in neurogenesis. Expert Opin. Ther. Targets. 14, 869–879.

Englund, C., Fink, A., Charmaine, L., Pham, D., Ray, D.A.M., Bulfone, A., Kowalczyk, T., Hevner, R.F., 2005. Pax6, Tbr2, and Tbr1 Are Expressed Sequentially by Radial Glia, Intermediate Progenitor Cells, and Postmitotic Neurons in Developing Neocortex. J. Neurosci. 25, 247–251.

Erta, M., Quintana, A., Hidalgo, J., 2012. Interleukin-6, a major cytokine in the central nervous system. Int. J. Biol. Sci. 8, 1254–66.

Ey, El., Torquet, N., Le Sourd, A. M., Leblond, C. S., Boeckers, T. M., Faure, P., Bourgeron, T., 2013. The Autism ProSAP1/Shank2 mouse model displays quantitative and structural abnormalities in ultrasonic vocalisations. Behav. Brain Res. 256, 677–689.

Favre, M.R., La Mendola, D., Meystre, J., Christodoulou, D., Cochrane, M., Markram, H., Markram, K., 2015. Predictable enriched environment prevents development of hyperemotionality in the VPA rat model of autism. Front. Neurosci. 9, 1–14.

Feng, J., Yu, H., Mi, K., Su, X., Li, Y., Li, Q., Sun, J., 2018. One year study of PM 2.5 in Xinxiang city, North China: Seasonal characteristics, climate impact and source. Ecotoxicol. Environ. Saf. 154, 75–83.

Fox, J.R., Cox, D.P., Drury, B.E., Gould, T.R., Kavanagh, T.J., Paulsen, M.H., Sheppard, L., Simpson, C.D., Stewart, J.A., Larson, T. V., Kaufman, J.D., 2015. Chemical

characterization and in vitro toxicity of diesel exhaust particulate matter generated under varying conditions. Air Qual. Atmos. Health. 8, 507–519.

Franco, S.J., Martinez-Garay, I., Gil-Sanz, C., Harkins-Perry, S.R., Müller, U., 2011. Reelin Regulates Cadherin Function via Dab1/Rap1 to Control Neuronal Migration and Lamination in the Neocortex. Neuron 69, 482–497.

Fuertes, E., Standl, M., Forns, J., Berdel, D., Garcia-Aymerich, J., Markevych, I., Schulte-Koerne, G., Sugiri, D., Schikowski, T., Tiesler, C.M.T., Heinrich, J., 2016. Traffic-related air pollution and hyperactivity/inattention, dyslexia and dyscalculia in adolescents of the German GINIplus and LISAplus birth cohorts. Environ. Int. 97, 85–92.

Fujimoto, A., Tsukue, N., Watanabe, M., Sugawara, I., Yanagisawa, R., Takano, H., Yoshida, S., Takeda, K., 2005. Diesel exhaust affects immunological action in the placentas of mice. Environ. Toxicol. 20, 431–440.

Furutachi, S., Miya, H., Watanabe, T., Kawai, H., Yamasaki, N., Harada, Y., Imayoshi, I., Nelson, M., Nakayama, K.I., Hirabayashi, Y., Gotoh, Y., 2015. Slowly dividing neural progenitors are an embryonic origin of adult neural stem cells. Nat. Neurosci. 18, 657–665.

Fuster-Matanzo, A., Llorens-Martín, M., Jurado-Arjona, J., Avila, J., Hernández, F., 2012. Tau protein and adult hippocampal neurogenesis. Front. Neurosci. 6, 1–6.

Gan, Q., Lee, A., Suzuki, R., Yamagami, T., Stokes, A., Nguyen, B., Pleasure, D., Wang, J., Chen, H.-W., Zhou, C.J., 2014. Pax6 Mediates β-Catenin Signaling for Self-Renewal and Neurogenesis by Neocortical Radial Glial Stem Cells. Stem Cells. 32, 45–58.

Georgala, P.A., Manuel, M., Price, D.J., 2011. The generation of superficial cortical layers is regulated by levels of the transcription factor Pax6. Cereb. Cortex 21, 81–94.

George, E.D., Bordner, K.A., Elwafi, H.M., Simen, A.A., 2010. Maternal separation with early

weaning: a novel mouse model of early life neglect. BMC Neurosci. 11: 123.

Glad, J.A., Brink, L.L., Talbott, E.O., Lee, P.C., Xu, X., Saul, M., Rager, J., 2012. The relationship of ambient ozone and PM2.5 levels and asthma emergency department visits: Possible influence of gender and ethnicity. Arch. Environ. Occup. Heal. 67, 103–108.

Gleason, J.A., Bielory, L., Fagliano, J.A., 2014. Associations between ozone, PM2.5, and four pollen types on emergency department pediatric asthma events during the warm season in New Jersey: A case-crossover study. Environ. Res. 132, 421–429.

Gonchar, Y., 2008. Multiple distinct subtypes of GABAergic neurons in mouse visual cortex identified by triple immunostaining. Front. Neuroanat. 1: 3.

Gould, T., Larson, T., Stewart, J., Kaufman, J.D., Slater, D., McEwen, N., 2008. A controlled inhalation diesel exhaust exposure facility with dynamic feedback control of PM concentration. Inhal. Toxicol. 20, 49–52.

Grayson, D.R., Chen, Y., Costa, E., Dong, E., Guidotti, A., Kundakovic, M., Sharma, R.P., 2006. The human reelin gene: Transcription factors (+), repressors (-) and the methylation switch (+/-) in schizophrenia. Pharmacol. Ther. 111, 272–286.

Guxens, M., Ghassabian, A., Gong, T., Garcia-Esteban, R., Porta, D., Giorgis-Allemand, L., Almqvist, C., Aranbarri, A., Beelen, R., Badaloni, C., Cesaroni, G., De Nazelle, A., Estarlich, M., Forastiere, F., Forns, J., Gehring, U., Ibarluzea, J., Jaddoe, V, J., 2016. Air pollution exposure during pregnancy and childhood autistic traits in four European population-based cohort studies: The ESCAPE project. Environ. Health Perspect. 124, 133–140.

Guxens, M., Garcia-Esteban, R., Giorgis-Allemand, L., Forns, J., Badaloni, C., Ballester, F., Beelen, R., Cesaroni, G., Chatzi, L., de Agostini, M., de Nazelle, A., Eeftens, M.,

Fernandez, M.F., Fernández-Somoano, A., Forastiere, F., Gehring, U., Ghassabian, A., Heude, B., Jaddoe, V.W. V, Klümper, C., Kogevinas, M., Krämer, U., Larroque, B., Lertxundi, A., Lertxuni, N., Murcia, M., Navel, V., Nieuwenhuijsen, M., Porta, D., Ramos, R., Roumeliotaki, T., Slama, R., Sørensen, M., Stephanou, E.G., Sugiri, D., Tardón, A., Tiemeier, H., Tiesler, C.M.T., Verhulst, F.C., Vrijkotte, T., Wilhelm, M., Brunekreef, B., Pershagen, G., Sunyer, J., 2014. Air pollution during pregnancy and childhood cognitive and psychomotor development: six European birth cohorts. Epidemiol. 25, 636–647.

Haimes, J., Kelley, M., 2010. Demonstration of a ΔΔ C q Calculation Method to Compute Relative Gene Expression from qPCR Data. GE Heal. Tech Note 1–4.

Hallmayer, J., Cleveland, S., Torres, a., Phillips, J., Cohen, B., Torigoe, T., Miller, J., Fedele, a., Collins, J., Smith, K., Lotspeich, L., Croen, L. a., Ozonoff, S., Lajonchere, C., Grether, J.K., Risch, N., 2011. Genetic Heritability and Shared Environmental Factors Among Twin Pairs With Autism. Arch. Gen. Psychiatry 68, 1095–1102.

Hartz, A.M.S., Bauer, B., Block, M.L., Hong, J.-S., Miller, D.S., 2008. Diesel exhaust particles induce oxidative stress, proinflammatory signaling, and P-glycoprotein up-regulation at the blood-brain barrier. FASEB J. 22, 2723–2733.

Health Effects Institute, 2010. Traffic-Related Air Pollution: A Critical Review of the Literature on Emissions, Exposure, and Health Effects. Heal. Eff. Inst. URL https://www.healtheffects.org/ publication/traffic-related-air-pollution-critical-review-literature- emissions-exposure-and-health

Herold, S., Jagasia, R., Merz, K., Wassmer, K., Lie, D.C., 2011. CREB signalling regulates early survival, neuronal gene expression and morphological development in adult subventricular zone neurogenesis. Mol. Cell. Neurosci. 46, 79–88.

Hodge, R.D., Kowalczyk, T.D., Wolf, S. a, Encinas, J.M., Rippey, C., Enikolopov, G.,

Kempermann, G., Hevner, R.F., 2008. Intermediate progenitors in adult hippocampal neurogenesis: Tbr2 expression and coordinate regulation of neuronal output. J. Neurosci. 28, 3707–3717.

Hsiao, E.Y., Patterson, P.H., 2011. Activation of the maternal immune system induces endocrine changes in the placenta via IL-6. Brain. Behav. Immun. 25, 604–615.

Huang, L., Hu, B., Ni, J., Wu, J., Jiang, W., Chen, C., Yang, L., Zeng, Y., Wan, R., Hu, G., Wang, X., 2016. Transcriptional repression of SOCS3 mediated by IL-6/STAT3 signaling via DNMT1 promotes pancreatic cancer growth and metastasis. J. Exp. Clin. Cancer Res. 35:27.

Hulst, A. Van, Barnett, T.A., Gauvin, L., Daniel, M., Kestens, Y., Bird, M., Gray-donald, K., Lambert, M., Hulst, A. Van, Barnett, T.A., Gauvin, L., Daniel, M., 2014. Emergency department visits for asthma in relation to the Air Quality Health Index: A case-crossover study in Windsor, Canada. Can. J. Public Heal. 105, 336–341.

Ikonomidou, C., 2010. Prenatal effects of antiepileptic drugs. Epilepsy Curr. 10, 42–46.

Imamura, F., Greer, C.A., 2013. Pax6 regulates Tbr1 and Tbr2 expressions in olfactory bulb mitral cells. Mol. Cell. Neurosci. 54, 58–70.

Impagnatiello, F., Guidotti, A.R., Pesold, C., Dwivedi, Y., Caruncho, H., Pisu, M.G., Uzunov, D.P., Smalheiser, N.R., Davis, J.M., Pandey, G.N., Pappas, G.D., Tueting, P., Sharma, R.P., Costa, E., 1998. A decrease of reelin expression as a putative vulnerability factor in schizophrenia. Proc Natl Acad Sci. 95,15718-1523.

Inano, K., Suetake, I., Ueda, T., Miyake, Y., Nakamura, M., Okada, M., Tajima, S., 2000. Maintenance-Type DNA Methyltransferase Is Highly Expressed in Post-Mitotic Neurons and Localized in the Cytoplasmic Compartment. J Biochem 128, 315–321.

Jossin, Y., Cooper, J.A., 2011. Reelin, Rap1 and N-cadherin orient the migration of multipolar neurons in the developing neocortex. Nat. Neurosci. 14, 697–703.

Ju, A., Hammerschmidt, K., Tantra, M., Krueger, Di., Brose, N., Ehrenreich, H., 2014. Juvenile manifestation of ultrasound communication deficits in the neuroligin-4 null mutant mouse model of autism. Behav. Brain Res. 270, 159–164.

Jung, C.-R., Lin, Y.-T., Hwang, B.-F., 2013. Air Pollution and Newly Diagnostic Autism Spectrum Disorders: A Population-Based Cohort Study in Taiwan. PLoS One 8, e75510.

Kadoshima, T., Sakaguchi, H., Nakano, T., Soen, M., Ando, S., Eiraku, M., Sasai, Y., 2013. Self-organization of axial polarity, inside-out layer pattern, and species-specific progenitor dynamics in human ES cell-derived neocortex. Proc. Natl. Acad. Sci. 110, 20284–20289.

Kalkbrenner, A.E., Schmidt, R.J., Penlesky, A.C., 2014. Environmental chemical exposures and autism spectrum disorders: a review of the epidemiological evidence. Curr. Probl. Pediatr. Adolesc. Health Care 44, 277–318.

Kent, B.A., Mistlberger, R.E., 2017. Sleep and hippocampal neurogenesis: Implications for Alzheimer's disease. Front. Neuroendocrinol. 45, 35–52.

Khan, S., Gregory, M., 2014. Sub-national Road Transport Fuel Consumption Statistics. Dep. Energy Clim. Chang. https://www.gov.uk/government/uploads/system/uploads/attachment_data/file/322458/sub_national_road_transport_consumption_factsheet_2012.pdf

Kicinski, M., Vermeir, G., Van Larebeke, N., Den Hond, E., Schoeters, G., Bruckers, L., Sioen, I., Bijnens, E., Roels, H.A., Baeyens, W., Viaene, M.K., Nawrot, T.S., 2015. Neurobehavioral performance in adolescents is inversely associated with traffic exposure. Environ. Int. 75, 136–143.

Kim, H.J., Jeon, S. J., Han, S., Bahn, G. H., Shin, C. Y., Kim, K.C., Cho, K. S., Yang, S. M., Gonzales, E. L., Valencia, S., Eun, P. H., Choi, C. S., Mabunga, D. F., Kim, J., Noh, J.K., 2017. Sex Differences in Autism-Like Behavioral Phenotypes and Postsynaptic Receptors Expression in the Prefrontal Cortex of TERT Transgenic Mice. Biomol Ther. 10, 1–10.

King, M., Bearman, P., 2009. Diagnostic change and the increased prevalence of autism. Int. J. Epidemiol. 38, 1224–1234.

Kirsten, T., Chaves-Kirsten, G., Chaible, L., Silva, A., Martins, D., Britto, L., Dagli, M., Torrão, A., Palermo-Neto, J., Bernardi, M., 2012. Hypoactivity of the central dopaminergic system and autistic-like behavior induced by a single early prenatal exposure to lipopolysaccharide. J. Neurosci. Res. 90, 1903–1912.

Kundakovic, M., Chen, Y., Costa, E., Grayson, D., 2007. DNA methyltransferase inhibitors coordinately induce expression of the human reelin and glutamic acid decarboxylase 67 genes. Mol. Pharmacol. 71, 644–653.

Kundakovic, M., Chen, Y., Guidotti, A., Grayson, D.R., 2009. The reelin and GAD67 promoters are activated by epigenetic drugs that facilitate the disruption of local repressor complexes. Mol. Pharmacol. 75, 342–354.

Lainiola, M., Procaccini, C., Linden, A.M., 2014. MGluR3 knockout mice show a working memory defect and an enhanced response to MK-801 in the T- and Y-maze cognitive tests. Behav. Brain Res. 266, 94–103.

Langley, E. a, Krykbaeva, M., Blusztajn, J.K., Mellott, T.J., 2014. High maternal choline consumption during pregnancy and nursing alleviates deficits in social interaction and improves anxiety-like behaviors in the BTBR T+Itpr3tf/J mouse model of autism. Behav. Brain Res. 278C, 210–220.

Langrish, J.P., Li, X., Wang, S., Lee, M.M.Y., Barnes, G.D., Miller, M.R., Cassee, F.R., Boon, N.A., Donaldson, K., Li, J., Li, L., Mills, N.L., Newby, D.E., Jiang, L., 2012. Reducing personal exposure to particulate air pollution improves cardiovascular health in patients with coronary heart disease. Environ. Health Perspect. 120, 367–372.

Larner, S.F., Wang, J., Goodman, J., O'Donoghue Altman, M.B., Xin, M., Wang, K.K.W., 2017. In vitro neurotoxicity resulting from exposure of cultured neural cells to several types of nanoparticles. J. Cell Death 10, 8–14.

Lee, G.H., D'Arcangelo, G., 2016. New Insights into Reelin-Mediated Signaling Pathways. Front. Cell. Neurosci. 10, 1–8.

Lee, P.C., Raaschou-Nielsen, O., Lill, C.M., Bertram, L., Sinsheimer, J.S., Hansen, J., Ritz, B., 2016. Gene-environment interactions linking air pollution and inflammation in Parkinson's disease. Environ. Res. 151, 713–720.

Levenson, J.M., Qiu, S., Weeber, E.J., 2008. The role of reelin in adult synaptic function and the genetic and epigenetic regulation of the reelin gene. Biochim. Biophys. Acta 1779, 422–431.

Li, K., Li, L., Cui, B., Gai, Z., Li, Q., Wang, S., Yan, J., Lin, B., Tian, L., Liu, H., Liu, X., Xi, Z., 2017. Early Postnatal Exposure to Airborne Fine Particulate Matter Induces Autism-like Phenotypes in Male Rats. Toxicol. Sci. 13;13(2):e0192614

Lim, C.S., Kim, H., Yu, N.K., Kang, S.J., Kim, T.H., Ko, H.G., Lee, J., Yang, J. eun, Ryu, H.H., Park, T., Gim, J., Nam, H.J., Baek, S.H., Wegener, S., Schmitz, D., Boeckers, T.M., Lee, M.G., Kim, E., Lee, J.H., Lee, Y.S., Kaang, B.K., 2017. Enhancing inhibitory synaptic function reverses spatial memory deficits in Shank2 mutant mice. Neuropharmacology 112, 104–112.

Lintas, C., Sacco, R., Persico, A.M., 2016. Differential methylation at the RELN gene promoter in temporal cortex from autistic and typically developing post-puberal subjects. J. Neurodev. Disord. 8: 18.

Liu, F., Huang, Y., Zhang, F., Chen, Q., Wu, B., Rui, W., Zheng, J.C., Ding, W., 2015. Macrophages treated with particulate matter PM2.5 induce selective neurotoxicity through glutaminase-mediated glutamate generation. J. Neurochem. 134, 315–326.

Liu, J., Li, W., Wu, J., Liu, Y., 2018. Visualizing the intercity correlation of PM 2 . 5 time series in the Beijing-Tianjin-Hebei region using ground-based air quality monitoring data . Plos One. 1–14.

Liu, W., Crews, F.T., 2017. Persistent Decreases in Adult Subventricular and Hippocampal Neurogenesis Following Adolescent Intermittent Ethanol Exposure. Front. Behav. Neurosci. 11, 1–15.

Liu, Y., Chien, W.-M., Medvedev, I.O., Weldy, C.S., Luchtel, D.L., Rosenfeld, M.E., Chin, M.T., 2013. Inhalation of diesel exhaust does not exacerbate cardiac hypertrophy or heart failure in two mouse models of cardiac hypertrophy. Part. Fibre Toxicol. 10, 49.

Ma, Wayne and Chen, T.-P., 2014. Beijing's Bad-Air Days, Finally Counted. Wall Str. J. Apr 14, 2014

Manuel, M., Georgala, P.A., Carr, C.B., Chanas, S., Kleinjan, D.A., Martynoga, B., Mason, J.O., Molinek, M., Pinson, J., Pratt, T., Quinn, J.C., Simpson, T.I., Tyas, D.A., van Heyningen, V., West, J.D., Price, D.J., 2006. Controlled overexpression of Pax6 in vivo negatively autoregulates the Pax6 locus, causing cell-autonomous defects of late cortical progenitor proliferation with little effect on cortical arealization. Development 134, 545–555.

Maruszak, A., Pilarski, A., Murphy, T., Branch, N., Thuret, S., 2014. Hippocampal neurogenesis

in Alzheimer's disease: Is there a role for dietary modulation? J. Alzheimer's Dis. 38, 11–38.

Michetti, C., Romano, E., Altabella, L., Caruso, A., Castelluccio, P., Bedse, G., Gaetani, S., Canese, R., Laviola, G., Scattoni, M.L., 2014. Mapping pathological phenotypes in reelin mutant mice. Front. Pediatr. 2: 95.

Mihalas, A.B., Elsen, G.E., Bedogni, F., Daza, R.A.M., Ramos-laguna, K.A., Arnold, S.J., Hevner, R.F., Mihalas, A.B., Elsen, G.E., Bedogni, F., Daza, R.A.M., Ramos-laguna, K.A., 2016. Intermediate Progenitor Cohorts Differentially Generate Cortical Layers and Require Tbr2 for Timely Acquisition of Neuronal Subtype Identity. Cell Reports. 16(1):92-105.

Mihalas, A.B., Hevner, R.F., 2017. Control of Neuronal Development by T-Box Genes in the Brain. Curr. Top. Dev. Biol. 122, 279-312

Min, J. young, Min, K. bok, 2017. Exposure to ambient PM10and NO2and the incidence of attention-deficit hyperactivity disorder in childhood. Environ. Int. 99, 221–227.

MohanKumar, S.M.J., Campbell, A., Block, M., Veronesi, B., 2008. Particulate matter, oxidative stress and neurotoxicity. Neurotoxicology 29, 479–88.

Monteiro, P., Feng, G., 2017. SHANK proteins: roles at the synapse and in autism spectrum disorder. Nat. Rev. Neurosci. 18,147-157

Morales-Suárez-Varela, M., Peraita-Costa, I., Llopis- González, A., 2017. Systematic review of the association between particulate matter exposure and autism spectrum disorders. Environ. Res. 153, 150–160.

Morton-Bermea, O., Garza-Galindo, R., Hernández-Álvarez, E., Ordoñez-Godínez, S.L., Amador-Muñoz, O., Beramendi-Orosco, L., Miranda, J., Rosas-Pérez, I., 2018. Atmospheric PM2.5 Mercury in the Metropolitan Area of Mexico City. Bull. Environ.

Contam. Toxicol. (in press)

Mouihate, A., 2016. Prenatal Activation of Toll-Like Receptor-4 Dampens Adult Hippocampal Neurogenesis in An IL-6 Dependent Manner. Front. Cell. Neurosci. 10:173.

Moy, S., Riddick, N., Nikolova, Vi., Teng, B., Agster, K., Nonneman, R., Young, N., Baker, L., Nadler, J., Bodfish, J., 2014. Repetitive behavior profile and supersensitivity to amphetamine in the C58/J mouse model of autism. Behav. Brain Res. 259, 200–214.

Moy, S.S., Nadler, J. J., Young, N. B., Perez, A., Holloway, L. P., Barbaro, R. P., Barbaro, J. R., Wilson, L. M., Threadgill, D. W., Lauder, J. M., Magnuson, T. R., Crawley, J.N., 2007. Mouse behavioral tasks relevant to autism: Phenotypes of 10 inbred strains. Behav. Brain Res. 176, 4–20.

MuhChyi, C., Juliandi, B., Matsuda, T., Nakashima, K., 2013. Epigenetic regulation of neural stem cell fate during corticogenesis. Int. J. Dev. Neurosci. 31, 424–433.

Noh, J.S., Sharma, R.P., Veldic, M., Salvacion, A. a, Jia, X., Chen, Y., Costa, E., Guidotti, A., Grayson, D.R., 2005. DNA methyltransferase 1 regulates reelin mRNA expression in mouse primary cortical cultures. Proc. Natl. Acad. Sci. 102, 1749–1754.

Onore, C.E., Schwartzer, J.J., Careaga, M., Berman, R.F., Ashwood, P., 2014. Maternal Immune Activation Leads to Activated Inflammatory Macrophages in Offspring. Brain. Behav. Immun. 35, 220–226.

Orellano, P., Quaranta, N., Reynoso, J., Balbi, B., Vasquez, J., 2017. Association of outdoor air pollution with the prevalence of asthma in children of Latin America and the Caribbean: A systematic review and meta-analysis. J. Asthma. 6:1-13 .

Pan, H.H., Chen, C.T., Sun, H.L., Ku, M.S., Liao, P.F., Lu, K.H., Sheu, J.N., Huang, J.Y., Pai, J.Y., Lue, K.H., 2014. Comparison of the effects of air pollution on outpatient and inpatient

visits for asthma: A population-based study in Taiwan. PLoS One 9;e9619

Pandis, S. N., Skyllakou, K., Florou, K., Kostenidou, E., Kaltsonoudis, C., Hasa, E., Presto, A., 2016. Urban particulate matter pollution: a tale of five cities. Faraday Discuss. 189, 277-290

Parker-Athill, E.C., Tan, J., 2010. Maternal immune activation and autism spectrum disorder: interleukin-6 signaling as a key mechanistic pathway. Neurosignals. 18, 113–28.

Pesold, C., Impagnatiello, F., Pisu, M.G., Uzunov, D.P., Costa, E., Guidotti, A., Caruncho, H.J., 1998. Reelin is preferentially expressed in neurons synthesizing gamma-aminobutyric acid in cortex and hippocampus of adult rats. Proc. Natl. Acad. Sci. U. S. A. 95, 3221–3226.

Rakic, 1974. Neurons in Rhesus Monkey Visual Cortex : Systematic Relation between Time of Origin and Eventual Disposition. Science. 183, 425–427.

Raz, Raanan, Roberts, Andrea L, Lyall, Kristen, Hart, Jaime E, Just, Allan C, Laden, Francine, Weisskopf, M.G., 2014. Autism Spectrum Disorder and Particulate Matter Air Pollution before, during, and after Pregnancy: A Nested-Case-Control Analysis within the Nurses' Health Study II Cohort. Environ. Health Perspect. 123, 264–70.

Raz, R., Levine, H., Pinto, O., Broday, D.M., Weisskopf, Y., Weisskopf, M.G., 2017. Traffic Related Air Pollution and Autism Spectrum Disorder: A Population Based Nested Case-Control Study in Israel. Am J Epidemiol. 17, e31093

Reiner, O., Karzburn, E., Kshirsagar, A., Kaibuchi, K., 2016. Regulation of Neuronal Migration, an Emerging Topic in Autism Spectrum Disorders (ASD). J. Neurochem. 136, 440–56.

Riley, E.A., Schaal, L., Sasakura, M., Crampton, R., Gould, T.R., Hartin, K., Sheppard, L., Larson, T., Simpson, C.D., Yost, G., 2016. Correlations between short-term mobile monitoring and long- term passive sampler measurements of traffic-related air pollution.

Atmos Env. May, 229–239.

Roberts, A., Lyall, K., Hart, J., Laden, F., Just, A., Bobb, J., 2013. Children ' s Health Perinatal Air Pollutant Exposures and Autism Spectrum Disorder in the Children of Nurses ' Health Study II Participants. Environ. Health Perspect. 978, 978–984.

Robertson, K.D., Uzvolgyi, E., Liang, G., Talmadge, C., Sumegi, J., Gonzales, F.A., Jones, P.A., 1999. The human DNA methyltransferases (DNMTs) 1, 3a and 3b: Coordinate mRNA expression in normal tissues and overexpression in tumors. Nucleic Acids Res. 27, 2291–2298.

Romano, E., Michetti, C., Caruso, A., Laviola, G., Scattoni, M.L., 2013. Characterization of neonatal vocal and motor repertoire of reelin mutant mice. PLoS One 8, e64407.

Roqué, P.J., Dao, K., Costa, L.G., 2016. Microglia mediate diesel exhaust particle-induced cerebellar neuronal toxicity through neuroinflammatory mechanisms. Neurotoxicology 56, 204–214.

Rossignol, D., Genuis, S., Frye, R., 2014. Environmental toxicants and autism spectrum disorders: a systematic review. Transl. Psychiatry 4, e360.

Roybon, L., Deierborg, T., Brundin, P., Li, J.Y., 2009a. Involvement of Ngn2, Tbr and NeuroD proteins during postnatal olfactory bulb neurogenesis. Eur. J. Neurosci. 29, 232–243.

Roybon, L., Hjalt, T., Stott, S., Guillemot, F., Li, J.Y., Brundin, P., 2009b. Neurogenin2 directs granule neuroblast production and amplification while neuroD1 specifies neuronal fate during hippocampal neurogenesis. PLoS One 4, e4779

Samuelsson, A., Jennische, E., Hansson, H., Holma, A., 2006. Prenatal exposure to interleukin-6 results in inflammatory neurodegeneration in hippocampus with NMDA / GABA A dysregulation and impaired spatial learning. Am J Physiol Regul Integr Comp Physiol. 290,

1345–1356.

Sansom, S.N., Griffiths, D.S., Faedo, A., Kleinjan, D.J., Ruan, Y., Smith, J., Van Heyningen, V., Rubenstein, J.L., Livesey, F.J., 2009. The level of the transcription factor Pax6 is essential for controlling the balance between neural stem cell self-renewal and neurogenesis. PLoS Genet. 5, 20–23.

Scattoni, Maria L. ; Ricceri, Laura; and Crawley, J., 2011. Unusual Repertoire of Vocalizations in Adult BTBR T+tf/J Mice Genes Brain Behav . Genes Brain Behav. 10, 44–56.

Scattoni, M.L., Crawley, J., Ricceri, L., 2009. Ultrasonic vocalizations: a tool for behavioural phenotyping of mouse models of neurodevelopmental disorders. Neurosci Biobehav Rev. 33, 508–515.

Scattoni, M.L., Gandhy, S.U., Ricceri, L., Crawley, J.N., 2008. Unusual repertoire of vocalizations in the BTBR T+tf/J mouse model of autism. PLoS One 3, e3067.

Scattoni, M.L., Martire, A., Cartocci, G., Ferrante, A., Ricceri, L., 2013. Reduced social interaction, behavioural flexibility and BDNF signalling in the BTBR T+tf/J strain, a mouse model of autism. Behav. Brain Res. 251, 35–40.

Semplea, B. D., Blomgrenb, K., Gimlina, K., Ferrieroe, D. M., Noble-Haeussleina, L.J., 2013. Brain development in rodents and humans: Identifying benchmarks of maturation and vulnerability to injury across species. Prog Neurobiol. 7, 1–16.

Shelton, J.F., Hertz-Picciotto, I., Pessah, I.N., 2012. Tipping the balance of autism risk: Potential mechanisms linking pesticides and Autism. Environ. Health Perspect. 120, 944–951.

Shen, Q., Wang, Y., Dimos, J.T., Fasano, C.A., Phoenix, T.N., Lemischka, I.R., Ivanova, N.B., Stifani, S., Morrisey, E.E., Temple, S., 2006. The timing of cortical neurogenesis is encoded within lineages of individual progenitor cells. Nat. Neurosci. 9, 743–751.

Shi, Yusheng, T.M., Yamaguchi, Y., Li, Z., Gu, X., Chen, X., 2018. Long-term trends and spatial patterns of satellite-retrieved PM2.5 concentrations in South and Southeast Asia from 1999 to 2014. Sci. Total Environ. 15, 177–86.

Shin Yim, Y., Park, A., Berrios, J., Lafourcade, M., Pascual, L.M., Soares, N., Yeon Kim, J., Kim, S., Kim, H., Waisman, A., Littman, D.R., Wickersham, I.R., Harnett, M.T., Huh, J.R., Choi, G.B., 2017. Reversing behavioural abnormalities in mice exposed to maternal inflammation. Nature 549, 482–487.

Silverman, J., Turner, S., Barkan, C., Tolu, S., Saxena, R., Hung, A., Sheng, M., Crawley, J., 2011. Sociability and motor functions in Shank1 mutant mice. Brain Res. 1380, 120–137.

Silverman, J.L., Pride, M.C., Hayes, J.E., Puhger, K.R., Butler-Struben, H.M., Baker, S., Crawley, J.N., 2015. GABAB Receptor Agonist R-Baclofen Reverses Social Deficits and Reduces Repetitive Behavior in Two Mouse Models of Autism. Neuropsychopharmacology 40, 2228–2239.

Silverman, J.L., Yang, M., Lord, C., Crawley, J.N., 2010. Behavioural phenotyping assays for mouse models of autism. Nat. Rev. Neurosci. 11, 490–502.

Singh, S., Solecki, D.J., 2015. Polarity transitions during neurogenesis and germinal zone exit in the developing central nervous system. Front. Cell. Neurosci. 9, 1–8.

Smith, R.B., Fecht, D., Gulliver, J., Beevers, S.D., Dajnak, D., Blangiardo, M., Ghosh, R.E., Hansell, A.L., Kelly, F.J., Anderson, H.R., Toledano, M.B., 2017. Impact of London's road traffic air and noise pollution on birth weight: retrospective population based cohort study. 359, j5299

Smith, S.E.P., Li, J., Garbett, K., Mirnics, K., Patterson, P.H., 2007. Maternal immune activation alters fetal brain development through interleukin-6. J. Neurosci. 27, 10695–10702.

Soberanes, S., Gonzalez, A., Urich, D., Chiarella, S.E., Radigan, K. a, Osornio-Vargas, A., Joseph, J., Kalyanaraman, B., Ridge, K.M., Chandel, N.S., Mutlu, G.M., De Vizcaya-Ruiz, A., Budinger, G.R.S., 2012. Particulate matter Air Pollution induces hypermethylation of the p16 promoter Via a mitochondrial ROS-JNK-DNMT1 pathway. Sci. Rep. 2, 275.

Stoner, R., Chow, M.L., Boyle, M.P., Sunkin, S.M., Mouton, P.R., Roy, S., Wynshaw-Boris, A., Colamarino, S.A., Lein, E.S., Courchesne, E., 2014. Patches of disorganization in the neocortex of children with autism. N. Engl. J. Med. 370, 1209–1219.

Ström, A.C., Forsberg, M., Lillhager, P., Westin, G., 1996. The transcription factors Sp1 and Oct-1 interact physically to regulate human U2 snRNA gene expression. Nucleic Acids Res. 24, 1981–1986.

Suades-González, E., Gascon, M., Guxens, M., Sunyer, J., 2015. Air Pollution and Neuropsychological Development: A Review of the Latest Evidence. Endocrinol. 156, en20151403.

Suglia, S.F., Gryparis, A., Wright, R.O., Schwartz, J., Wright, R.J., 2008. Association of black carbon with cognition among children in a prospective birth cohort study. Am. J. Epidemiol. 167, 280–286.

Sunyer, J., Esnaola, M., Alvarez-Pedrerol, M., Forns, J., Rivas, I., Lopez-Vicente, M., Suades-Gonzalez, E., Foraster, M., Garcia-Esteban, R., Basagana, X., Viana, M., Cirach, M., Moreno, T., Alastuey, A., Sebastian-Galles, N., Nieuwenhuijsen, M., Querol, X., 2015. Association between Traffic-Related Air Pollution in Schools and Cognitive Development in Primary School Children: A Prospective Cohort Study. PLoS Med. 12, 1–24.

Suzuki, T., Oshio, S., Iwata, M., Saburi, H., Odagiri, T., Udagawa, T., Sugawara, I., Umezawa, M., Takeda, K., 2010. In utero exposure to a low concentration of diesel exhaust affects spontaneous locomotor activity and monoaminergic system in male mice. Part. Fibre

Toxicol. 7, 7.

Tachibana, K., Takayanagi, K., Akimoto, A., Ueda, K., Shinkai, Y., 2015. Prenatal diesel exhaust exposure disrupts the DNA methylation pro fi le in the brain of mouse offspring. J. Toxicol. Sci. 40, 1–11.

Talbott, Evelyn O., Arena, Vincent C., Rager, Judith R., Clougherty, Jane E., Michanowicz, Drew R., Sharma, Ravi K., Stacy, S.L., 2015. Fine particulate matter and the risk of autism spectrum disorder. Environ. Res. 140, 414–420.

Tang, W., Huang, S., Du, L., Sun, W., Yu, Z., Zhou, Y., Chen, J., Li, X., Li, X., Yu, B., Chen, D., 2018. Expression of HMGB1 in maternal exposure to fine particulate air pollution induces lung injury in rat offspring assessed with micro-CT. Chem. Biol. Interact. 280, 64–69.

Tanner, C.M., Goldman, S.M., Ross, G.W., Grate, S.J., 2014. The disease intersection of susceptibility and exposure: chemical exposures and neurodegenerative disease risk. Alzheimers. Dement. 10, S213-25.

Tanwar, V., Gorr, M.W., Velten, M., Eichenseer, C.M., Long, V.P., Bonilla, I.M., Shettigar, V., Ziolo, M.T., Davis, J.P., Baine, S.H., Carnes, C.A., Wold, L.E., Wold, L.E., 2017. In Utero Particulate Matter Exposure Produces Heart Failure, Electrical Remodeling, and Epigenetic Changes at Adulthood. J. Am. Heart Assoc. 6(4). pii: e005796

Tessum, M.W., Larson, T., Gould, T.R., Simpson, C.D., Yost, M.G., Vedal, S., 2018. Mobile and Fixed-Site Measurements To Identify Spatial Distributions of Traffic-Related Pollution Sources in Los Angeles. Environ. Sci. Technol. 52, 2844–2853

Thirtamara R., Keerthi, Doherty-Lyons, S., Bolden, C. Willis, D., Hoffman, C., Zelikoff, J., Chen, L.-C., Gu, H., 2013. Prenatal and early-life exposure to high-level diesel exhaust particles leads to increased locomotor activity and repetitive behaviors in mice. Autism Res. 6, 248–

257.

Toda, T., Gage, F.H., 2017. Review: adult neurogenesis contributes to hippocampal plasticity. Cell Tissue Res. 10 (1007) ,s00441

Torre-Ubieta, Luis; Won, Hyejung; Stein, J., Geschwind, D., 2016. Advancing the understanding of autism disease mechanisms through genetics. Nat. Med. 116, 1477–1490.

Tronnes, A.A., Koschnitzky, J., Daza, R., Hitti, J., Ramirez, J.M., Hevner, R., 2015. Effects of Lipopolysaccharide and Progesterone Exposures on Embryonic Cerebral Cortex Development in Mice. Reprod. Sci. 23, 771–778.

Tsukada, T., Simamura, E., Shimada, H., Arai, T., Higashi, N., Akai, T., Iizuka, H., Hatta, T., 2015. The suppression of maternal-fetal leukemia inhibitory factor signal relay pathway by maternal immune activation impairs brain development in mice. PLoS One 10, e0129011.

U.S. Environmental Protection Agency, 2015. Air Quality Index (AQI) Basics. AirNow. URL https://airnow.gov/index.cfm?action=aqibasics.aqi

van Donkelaar, A., Martin, R. V., Brauer, M., Boys, B.L., 2014. Use of satellite observations for long-term exposure assessment of global concentrations of fine particulate matter. Environ. Health Perspect. 110, 135–143.

van Kempen, E., Fischer, P., Janssen, N., Houthuijs, D., van Kamp, I., Stansfeld, S., Cassee, F., 2012. Neurobehavioral effects of exposure to traffic-related air pollution and transportation noise in primary schoolchildren. Environ. Res. 115, 18–25.

Veldic, M., Caruncho, H.J., Liu, W.S., Davis, J., Satta, R., Grayson, D.R., Guidotti, a, Costa, E., 2004. DNA-methyltransferase 1 mRNA is selectively overexpressed in telencephalic GABAergic interneurons of schizophrenia brains. Proc. Natl. Acad. Sci. U. S. A. 101, 348–353.

Volk, H.E., Hertz-Picciotto, I., Delwiche, L., Lurmann, F., McConnell, R., 2011. Residential proximity to freeways and autism in the CHARGE study. Environ. Health Perspect. 119, 873–877.

Volk, H.E., Lurmann, F., Penfold, B., Hertz-Picciotto, I., McConnell, R., 2013. Traffic-related air pollution, particulate matter, and autism. JAMA Psych. 70, 71–7.

Wang, Q., Zhang, H., Liang, Q., Knibbs, L.D., Ren, M., Li, C., Bao, J., Wang, S., He, Y., Zhu, L., Wang, X., Zhao, Q., Huang, C., 2018. Effects of prenatal exposure to air pollution on preeclampsia in Shenzhen, China. Environ. Pollut. 237, 18–27.

Weber-Stadlbauer, U., 2017. Epigenetic and transgenerational mechanisms in infection-mediated neurodevelopmental disorders. Transl. Psychiatry 7, e1113.

Weldy, C.S., Liu, Y., Chang, Y.-C., Medvedev, I.O., Fox, J.R., Larson, T. V, Chien, W.-M., Chin, M.T., 2013. In utero and early life exposure to diesel exhaust air pollution increases adult susceptibility to heart failure in mice. Part. Fibre Toxicol. 10:59.

WHO, 2016. WHO | Exposure to ambient air pollution. Who. URL http://www.who.int/gho/phe/outdoor_air_pollution/exposure/en/

Win-Shwe, T.-T., Fujimaki, H., 2011. Nanoparticles and neurotoxicity. Int. J. Mol. Sci. 12, 6267–6280.

Wöhra, Markus; Scattoni, M.L., 2013. Behavioural methods used in rodent models of autism spectrum disorders: Current standards and new developments. Behav. Brain Res. 251, 5–17.

Won, H., Lee, H.R., Gee, H.Y., Mah, W., Kim, J.I., Lee, J., Ha, S., Chung, C., Jung, E.S., Cho, Y.S., Park, S.G., Lee, J.S., Lee, K., Kim, D., Bae, Y.C., Kaang, B.K., Lee, M.G., Kim, E., 2012. Autistic-like social behaviour in Shank2-mutant mice improved by restoring NMDA

receptor function. Nature 486, 261–265.

Wrenn, C.C., Harris, A.P., Saavedra, M.C., Crawley, J.N., 2003. Social transmission of food preference in mice: Methodology and application to galanin-overexpressing transgenic mice. Behav. Neurosci. 117, 21–31.

Wurzman, R., Forcelli, P. a, Griffey, C.J., Kromer, L.F., 2015. Repetitive grooming and sensorimotor abnormalities in an ephrin-A knockout model for Autism Spectrum Disorders. Behav. Brain Res. 278, 115–128.

Xu, W., Hawkey, A.B., Li, H., Dai, L., Brim, H.H., Frank, J.A., Luo, J., Barron, S., Chen, G., 2018. Neonatal Ethanol Exposure Causes Behavioral Deficits in Young Mice. Alcohol. Clin. Exp. Res. (in press)

Yamazaki, S., Shima, M., Yoda, Y., Oka, K., Kurosaka, F., Shimizu, S., Takahashi, H., Nakatani, Y., Nishikawa, J., Fujiwara, K., Mizumori, Y., Mogami, A., Yamada, T., Yamamoto, N., 2015. Exposure to air pollution and meteorological factors associated with children's primary care visits at night due to asthma attack: case-crossover design for 3-year pooled patients. BMJ Open. 5:e005736.

Yang, M., Abrams, D., Zhang, J., Weber, M., Katz, A., Clarke, A., Silverman, J., Crawley, J., 2012. Low sociability in BTBR T+tf/J mice is independent of partner strain. Physiol. Behav. 107, 649–662.

Yang, M., Scattoni, M.L., Zhodzishsky, V., Chen, T., Caldwell, H., Young, W.S., Mcfarlane, H.G., Jacqueline, N., 2007. Social approach behaviors are similar on conventional versus reverse lighting cycles , and in replications across cohorts , in BTBR T + tf / J , C57BL / 6J , and vasopressin receptor 1B mutant mice. Front Behav Neurosci. 1, 1–9.

Yin, F., Lawal, A., Ricks, J., Fox, J.R., Larson, T., Navab, M., Fogelman, A.M., Rosenfeld, M.E.,

Araujo, J.A., 2013. Diesel exhaust induces systemic lipid peroxidation and development of dysfunctional pro-oxidant and pro-inflammatory high-density lipoprotein. Arterioscler. Thromb. Vasc. Biol. 33, 1153–1161.

Yokota, S., Moriya, N., Iwata, M., Umezawa, M., Oshio, S., Takeda, K., 2013. Exposure to diesel exhaust during fetal period affects behavior and neurotransmitters in male offspring mice. J. Toxicol. Sci. 38, 13–23.

Yorifuji, T., Kashima, S., Higa Diez, M., Kado, Y., Sanada, S., Doi, H., 2016. Prenatal Exposure to Traffic-related Air Pollution and Child Behavioral Development Milestone Delays in Japan. Epidemiology 27, 57–65.

Zhang, Q., Wang, H.Y., Marzec, M., Raghunath, P.N., Nagasawa, T., Wasik, M.A., 2005. STAT3- and DNA methyltransferase 1-mediated epigenetic silencing of SHP-1 tyrosine phosphatase tumor suppressor gene in malignant T lymphocytes. Proc. Natl. Acad. Sci. U. S. A. 102, 6948–53.

Zhang, Q., Wang, H.Y., Woetmann, A., Raghunath, P.N., Odum, N., Wasik, M.A., 2006. STAT3 induces transcription of the DNA methyltransferase 1 gene (DNMT1) in malignant T lymphocytes. Blood. 108(3): 1058–1064.

Zhang, T., Zheng, X., Wang, X., Zhao, H., Wang, T., Zhang, H., Li, W., Shen, H., Yu, L., 2018. Maternal Exposure to PM2.5 during Pregnancy Induces Impaired Development of Cerebral Cortex in Mice Offspring. Int. J. Mol. Sci. 19, 257.

Zheng, J. yu, Liang, K. shan, Wang, X. jun, Zhou, X. ying, Sun, J., Zhou, S. nian, 2016. Chronic Estradiol Administration During the Early Stage of Alzheimer's Disease Pathology Rescues Adult Hippocampal Neurogenesis and Ameliorates Cognitive Deficits in Aβ1-42 Mice. Mol. Neurobiol. 54, 1–14.

Zhu, D.Y., Lau, L., Liu, S.H., Wei, J.S., Lu, Y.M., 2004. Activation of cAMP-response-element-binding protein (CREB) after focal cerebral ischemia stimulates neurogenesis in the adult dentate gyrus. Proc. Natl. Acad. Sci. U. S. A. 101, 9453–9457.